FINAL REPORT

An Electrocoagulation and Electrooxidation Treatment Train to Degrade Perfluoroalkyl Substances and Other Persistent Organic Contaminants in Groundwater

SERDP Project ER18-1278

AUGUST 2021

Dora Chiang, PhD., P.E.
Wood

Qingguo Huang, Ph.D.
University of Georgia

Shangtao Liang, Ph.D.
Jing Zhou, Ph.D., P.E.
AECOM

SERDP
DOD ▪ EPA ▪ DOE

REPORT DOCUMENTATION PAGE

Form Approved
OMB No. 0704-0188

1. REPORT DATE *(DD-MM-YYYY)*	**2. REPORT TYPE**	**3. DATES COVERED** *(From - To)*
25/08/2021	SERDP Final Report	3/13/2018 - 3/12/2022

4. TITLE AND SUBTITLE

An Electrocoagulation and Electrooxidation Treatment Train to Degrade Perfluoroalkyl Substances and Other Persistent Organic Contaminants in Groundwater

5a. CONTRACT NUMBER
18-C-0009

5b. GRANT NUMBER

5c. PROGRAM ELEMENT NUMBER

6. AUTHOR(S)
Dora Chiang: Wood

Qingguo Huang: University of Georgia

Shangtao Liang and Jing Zhou: AECOM

5d. PROJECT NUMBER
ER18-1278

5e. TASK NUMBER

5f. WORK UNIT NUMBER

7. PERFORMING ORGANIZATION NAME(S) AND ADDRESS(ES)
Wood
https://www.woodplc.com/

8. PERFORMING ORGANIZATION REPORT NUMBER
ER18-1278

9. SPONSORING/MONITORING AGENCY NAME(S) AND ADDRESS(ES)
Strategic Environmental Research and Development Program (SERDP)
4800 Mark Center Drive, Suite 16F16
Alexandria, VA 22350-3605

10. SPONSOR/MONITOR'S ACRONYM(S)
SERDP

11. SPONSOR/MONITOR'S REPORT NUMBER(S)
ER18-1278

12. DISTRIBUTION/AVAILABILITY STATEMENT
DISTRIBUTION STATEMENT A. Approved for public release: distribution unlimited.

13. SUPPLEMENTARY NOTES

14. ABSTRACT
This study aims at developing a novel treatment train that combines electrocoagulation (EC) with electrochemical oxidation (EO) treatment to remove and degrade per- and polyfluoroalkyl substances (PFAS) including perfluoroalkyl acids (PFAAs) and their organic co-contaminants in contaminated groundwater. PFAS are extremely persistent because of their unique molecular structures, and currently, there is no cost-effective technology that is applicable for on-site PFAA destruction. This study is of great societal and environmental significance by providing a technology potentially practical for eliminating and destructing PFAS in groundwater. Although PFAS are evaluated as the target contaminants in this study, the EC and EO technologies can be used individually or in combination to address a wide range of different co-contaminants.

15. SUBJECT TERMS
Poly- and perfluoroalkyl substances, Electrocoagulation, Electrochemical oxidation, Treatment train, Groundwater

16. SECURITY CLASSIFICATION OF:			**17. LIMITATION OF ABSTRACT**	**18. NUMBER OF PAGES**	**19a. NAME OF RESPONSIBLE PERSON**
a. REPORT	**b. ABSTRACT**	**c. THIS PAGE**			Dora Chiang
UNCLASS	UNCLASS	UNCLASS	UNCLASS	81	**19b. TELEPHONE NUMBER** *(Include area code)* 404-720-1343

Table of Contents

List of Tables

List of Figures

List of Acronyms

ºC	Degrees Celsius
4:2 FtS	Fluorotelomer sulfonic acid 4:2
6:2 FtS	Fluorotelomer sulfonic acid 6:2
8:2 FtS	Fluorotelomer sulfonic acid 8:2
AFFF	Aqueous Film Forming Foam
AIX	Anion ion exchange resin
AOP	Advanced oxidation process
BDD	Boron-doped diamond
BET	Brunauer–Emmett–Teller
cc	Cubic centimeters
cm	Centimeters
DC	Direct current
DET	Direct electron transfer
DI	Deionized
DOC	Dissolved organic carbon
DoD	United States Department of Defense
EC	Electrocoagulation
EO	Electrochemical oxidation
ESTCP	Environmental Security Technology Certification Program
Fe	Iron
FOSA	Perfluorinated sulfonamide
FTSA	Fluorotelomer sulfonic acid
GAC	Granular activated carbon
ICP-MS	Inductively coupled plasma mass spectrometer
ISR	Internal standard recovery
L	Liters
$m^2 g^{-1}$	Square meters per gram
mA/cm^2	Milliamperes per square centimeter
mg	Milligrams
mg L^{-1}	Milligrams per liter
min	Minutes
µL	Microliters
mL	Milliliters
mL min^{-1}	Milliliter per minute
µm	Microns
µM	Micromoles
mm	Millimeters

List of Acronyms (Continued)

mM	Millimoles
mol L^{-1}	moles per liter
mS cm^{-1}	Millisiemens per centimeter
ng L-1	Nanograms per liter
OH	Hydroxyl radical
PFAA	Perfluoroalkyl acid
PFAS	Per- and polyfluoroalkyl substances
PFBS	Perfluorobutanesulfonic acid
PFCA	Perfluoroalkyl carboxylate
PFHpA	Perfluoroheptanoic acid
PFHxA	Perfluorohexanoic acid
PFHxS	Perfluorohexanesulfonic acid
PFNA	Perfluorononanoic acid
PFOA	Perfluorooctanoic acid
PFOS	Perfluorooctanesulfonic acid
PFSA	Perfluorosulfonic acid
PI	Principal Investigator
PP	Polypropylene
ppm	Parts per million
ppt	Parts per trillion
QA/QC	Quality assurance/quality control
RPD	Relative percent difference
rpm	Revolutions per minute
SERDP	Strategic Environmental Research and Development Program
SPE	Solid phase extraction
TOC	Total organic carbon
UGA	University of Georgia
USEPA	United States Environmental Protection Agency
WAFB	Wurtsmith Air Force Base

Keywords

Poly- and perfluoroalkyl substances, Electrocoagulation, Electrochemical oxidation, Treatment train, Groundwater

Acknowledgements

This study was supported in part by U.S. Department of Defense SERDP ER-1278. We thank Beibei Wang and Lu Wang for help with laboratory work, Dr. Sayed Hassan from the Center for Applied Isotope Studies for help with the ICP-MS measurement and analysis, and Mr. Dirk Pohlmann from Bay West LLC for supporting the groundwater sampling effort at Wurtsmith Air Force Base (WAFB).

ABSTRACT

Introduction and Objectives

This study aims at developing a novel treatment train that combines electrocoagulation (EC) with electrochemical oxidation (EO) treatment to remove and degrade per- and polyfluoroalkyl substances (PFAS) including perfluoroalkyl acids (PFAAs) and their organic co-contaminants in contaminated groundwater. PFAS are extremely persistent because of their unique molecular structures, and currently, there is no cost-effective technology that is applicable for on-site PFAA destruction. This study is of great societal and environmental significance by providing a technology potentially practical for eliminating and destructing PFAS in groundwater. Although PFAS are evaluated as the target contaminants in this study, the EC and EO technologies can be used individually or in combination to address a wide range of different co-contaminants.

Technical Approach

In this study, PFAS and co-contaminants were sorbed and concentrated on the flocs formed through EC. The flocs were then dissolved in a low volume of acidic solution releasing PFAS into the same acidic solution. PFAS were then destroyed effectively with the EO process. The study contains two tasks. Task 1 is a laboratory bench study to verify and optimize the performance of EC and separation of PFAS and co-contaminants from flocs. Task 2 is a laboratory bench study to combine the individual treatment processes in an integral train and evaluate its performance. Both the spiked water system and the United States Department of Defense (DoD) site groundwater were evaluated in Task 1 and Task 2. Task 3 includes project management, reporting, preparation of peer-reviewed technical journal manuscripts, and technology transfer.

Results

Under the optimized EC treatment conditions, the removal rates for most long-chain PFAS compounds (carbon number 6-10) in spiked water, such as PFNA, PFOA, PFOS, PFHxS, 8:2 FtS, 6:2 FtS, and FOSA, were above 90%. The PFAS removal efficiency follows the order of FOSA≈ 8:2 FTS≈PFNA > PFOS > PFOA > 6:2 FTS > PFHxS > PFHpA > PFHxA ≈ PFBS. For groundwater samples, under a high current density (5 milliampere per square centimeter [mA/cm^2]), the removal for PFOA, PFNA, PFHxS, PFOS, 6:2 FtS, and 8:2 FtS were above 90%. It was observed that EC-derived foam was generated when a relatively high current density (> 1 mA/cm^2) was applied to a relatively high PFAS concentration (> 0.1 micromolar [µM]) during EC. The floc and foam could be completely dissolved by a small amount of H_2SO_4, and the recovery rate was about 100%. Preliminary EO tests indicated that PFAS in all three EC-derived solutions were removed efficiently during EO. Except for PFBS, PFHxA, and 4:2 FtS, the concentrations of all other PFAS were removed nearly completely.

Benefits

This research supports the Strategic Environmental Research and Development Program (SERDP) mission to reduce the DoD's liabilities by developing sustainable, cost-effective technologies for expedited site cleanup and closure by proposing a treatment train that can remove and degrade PFAS and co-contaminants in groundwater. This coupling approach allows for the treatment of

contaminant concentrations from parts per trillion (ppt) to parts per million (ppm) levels and requires low energy consumption with no sorbent regeneration and PFAA waste generation. The project demonstrates the treatment effectiveness of the individual processes and the coupled processes. It is also important to note that this treatment train involves EO destruction on site, therefore it avoids off-site transportation and disposal of PFAS-laden wastes.

EXECUTIVE SUMMARY

1. Introduction

Per- and polyfluoroalkyl substances (PFAS) are a class of synthetic chemicals composed of a carbon chain that are fully or partially fluorinated (Buck et al., 2011; Ghisi et al., 2019), which includes perfluoroalkyl acids (PFAAs) and the precursor chemicals that can potentially transform to PFAAs under natural and/or treatment conditions (Gonzalez et al., 2021; Ahrens and Bundschuh 2014; Arvaniti and Stasinakis, 2015; Liu and Avendano, 2013). The unique molecular structures make PFAS possess high thermal and chemical stability, partially due to the high energy carbon-fluorine bond (Hudlicky, 1979; Zhang et al., 2013; Vecitis et al., 2009; Torres et al., 2009). Having been used extensively in a wide variety of industrial and commercial applications, including surfactants, fire retardants, and oil-repellent coatings (Paul et al., 2009; Rahman et al., 2014), PFAS entered natural aquatic environments during manufacturing, transport, product use, and disposal (Davis et al., 2007). PFAS are mobile with aqueous phase and recalcitrant, and have been detected in the groundwater at concentrations from nanograms per liter (ng L^{-1}) to several milligrams per liter (mg L^{-1}) at sites where PFAS were involved in firefighting practices (Andersen et al., 2008; Corsini et al., 2012). The occurrence of PFAS in the environment has drawn public concern because of their global distribution, environmental persistence, bioaccumulation, and potential toxicity (Pistocchi and Loos, 2009; Guelfo and Adamson, 2018; Gomis et al., 2018; Conder et al., 2008). Thus, it is of great importance to develop effective techniques to remove and degrade PFAS from contaminated water.

The treatment technologies currently used to remove PFAS are primarily separation technologies without destruction of PFAS. Sorption by activated carbon or ion exchange resin have been used to remove PFAS from water (Du et al., 2014; Lampert et al., 2007; Xiao et al., 2017; Zhang et al., 2019), but have various limitations such as limited capacity, rapid breakthrough, and difficult regeneration of used sorbent. In addition, the sorption technologies only transfer the contaminants without destruction of molecular structure, and the spent sorbent still needs off-site incineration that may cause secondary hazards. In addition, the application of these technologies to treat large volumes of diluted PFAS wastewaters is not technically and economically favorable. Public concern and scrutiny of PFAS containing water and wastes will continue to grow, and off-site PFAS waste disposal and incineration options will soon become more restricted and less available.

Electrocoagulation (EC) is an alternative to conventional chemical coagulation for municipal and industrial wastewater treatment as well as drinking water purification. EC has multiple advantages including the ability to be configured into drinking water treatment systems, commercial availability of energy optimized modules, the reduced usage of corrosive chemicals, and the lower labor costs because of the higher degree of automation and low maintenance. Additionally, in some instances it appeals as a pretreatment step reducing mass loading onto downstream processes such as media or membrane filtration. Small-scale electrocoagulation units are already being extensively used for industrial wastewater treatment. EC has shown some potential to remove PFAS from water by some recent studies (Lin et al., 2015; Yang et al., 2016; Wang et al., 2016). The dissolution of charged cations (e.g., Zn^{2+}, Al^{3+}, Fe^{3+}) from the sacrificial anode simultaneously forms monomeric and polymeric hydroxyl complex species, which can strongly sorb certain pollutants and remove them from contaminated water (Mollah et al., 2004).

Lin et al. evaluated PFAS removal using various sacrificial anodes, including aluminum, iron, zinc, and magnesium (Lin et al., 2015), suggesting that PFAS can be quickly sorbed on the surface of the zinc hydroxide flocs in situ generated during the EC process, mainly via hydrophobic interaction. Yang et al. found that the EC process with Fe anode rapidly removed PFAS from contaminated waters (Yang et al., 2016). The electrolytic generation of gases (H_2, O_2) in an EC-based treatment process can cause the formation of foams when surface-active PFAS are present in water (Ebersbach et al., 2016). This will significantly increase air-water interfaces and allow PFAS to be concentrated in the foam, which itself is an effective method to separate PFAS from contaminated water (i.e., foam fractionation) (Ebersbach et al., 2016; Meng et al., 2018). While PFAS are adsorbed on flocs and separated from waters, PFAS are not destroyed. We proposed the PFAS-laden flocs can be collected and easily dissolved in a controlled volume of acid solution (i.e., PFAS concentrate), and the PFAS concentrate can be ready for destruction.

A number of technologies have been examined for PFAS destruction, including electrooxidation (EO) (Niu et al., 2016), sonochemical oxidation (Moriwaki et al., 2005; Cheng et al., 2008), thermolysis (Krusic and Roe, 2004), plasma oxidation (Yasuoka et al., 2011; Singh et al., 2019), hydrated electron reduction (Bentel et al., 2019), and photochemical oxidation and laccase-mediator reaction (Sun et al., 2017; Luo et al., 2018). As extremely recalcitrant chemicals, destruction of PFAS for treatment purposes is challenging for the conventional treatment technologies or advanced oxidation processes (AOPs) based on hydroxyl radical ($^{\bullet}OH$) (Carter and Farrell, 2008). EO exhibits stronger degradation ability than conventional AOPs due to the combination of direct electron transfer (DET) reaction on the anode and the oxidation by $^{\bullet}OH$ produced by anodic oxidation of water (Zhi et al., 2003), which has been proven effective to destruct PFAS using "non-active" anodes, including boron-doped diamond (BDD), PbO_2, SnO_2-Sb, and Magnéli phase titanium suboxides (Carter and Farrell, 2008; Lin et al., 2012; Niu et al., 2012; Shi et al., 2019; Wang et al., 2020). Especially, Magnéli phase titanium suboxides, with the general formula of Ti_nO_{2n-1} ($4 < n < 10$), have recently been explored as a promising electrode due to their wide electrochemical window for water oxidation, chemical inertness, and low production cost (Walsh and Wills, 2010; Hui et al., 2018; Radjenovic and Sedlak, 2015). The degradation of organic contaminant occurs only near or at the anode surface, which is usually limited by mass transfer from bulk solution to the anode surface (Trellu et al., 2018). Enhancement of target concentration in the bulk solution is an effective way to improve the EO treatment efficiency (Soriano et al., 2019), and it appears that the EC process may serve such a purpose well, as described above (Lin et al., 2015; Martinezhuitle et al., 2015). In addition, the acid dissolution of EC flocs generates an acidic solution which contains abundant metal ions and acid anions. This acidic solution with high electrical conductivity is ideal for the subsequent EO process by promoting the anodic reaction of PFAS.

The objective of this study was thus to examine the feasibility of a novel treatment train that combines EC and EO to remove and degrade PFAS in an aqueous solution. The EC performance was evaluated with a mixture of PFAS at different concentrations under different current densities. The PFAS thus transferred to floc and foam by EC were recovered and concentrated by acid dissolution and then destroyed by the EO treatment.

2. Objectives

This DoD SERDP project ER18-1278 is funded with the technical objectives of developing a novel and cost-effective treatment train that concentrates PFAS on flocs generated by EC then subsequently destroys PFAS through the EO process. The identified treatment scheme includes (1) EC to remove PFAS and co-contaminants from groundwater; (2) formation of PFAS and co-contaminant-enriched flocs; (3) a recovery process to dissolve flocs and release PFAS and co-contaminants into a small volume of aqueous solution; and (4) EO degradation of concentrated PFAS and co-contaminants in the small-volume aqueous solution.

This project has the objectives to examine the EC technology for PFAS removal and the degree of destruction for PFAS in the EC PFAS concentrate.

3. Technical Approach

The overarching goal of this project is to develop a practical and cost-effective treatment train coupling EC and EO for treatment of groundwater containing low concentrations of PFAS and co-contaminants. The project is organized in three interrelated research tasks. Task 1 is a laboratory bench-scale study to verify PFAS and co-contaminant removal by EC and the separation of PFAS and co-contaminants from flocs. Task 2 is a laboratory bench-scale study to combine individual treatment processes and evaluate the sequential treatment processes and performance. Task 3 includes project management, reporting, and preparation of journal manuscripts.

This project report summarizes the completed Task 1 activities and the Task 1 results only. This project report also summarizes the preliminary assessment of coupling EC with EO; however, the full Task 2 scope and Task 3 were not implemented.

Task 1 Bench-Scale Evaluation of Electrocoagulation

Task 1 focuses on the EC process for optimized PFAS sorption and the evaluation of PFAS-laden floc dissolution and re-precipitation of dissolved zinc. Specifically, Subtask 1 systematically evaluated the efficiency of PFAS sorption on EC-generated zinc hydroxide flocs in response to important water conditions and EC operation variables. In Subtask 2, different methods were explored and compared to release PFAS from the sludge of the zinc hydroxide flocs to form concentrated solutions amenable for subsequent EO. The mass balance during the PFAS recovery process was evaluated. Task 1 started with spiked water systems to understand the mass balance, mechanisms, and kinetics of each individual process on PFAS and co-contaminants. The treatment performance evaluation using site groundwater (containing PFAAs and precursors) was conducted in Subtask 3. Dr. Huang and his research team at University of Georgia (UGA) are the key performers of this task. This task was completed in the fourth quarter of 2019. A go/no-go report and a whitepaper summarizing Task 1 results were submitted in the first quarter of 2020.

Task 2 Evaluation of Bench-Scale Treatment Train

Task 2 is a laboratory bench study to combine the individual unit operations into a sequential treatment train and evaluate its performance. The EC treatment conditions were selected based on the Task 1 results, and the EO conditions were selected based on the EO optimization studies conducted under a different SERDP project at UGA for which Dr. Huang is the Principal Investigator (PI), and adjusted, as necessary. Task 2 involves using bench-scale EC-EO to treat

PFAS in spiked water and groundwater from a DoD site. The schematic treatment diagram is presented in **Figure 1**.

Preliminary tests on EO treatment of waste solution from EC process for treating spiked water were completed at co-PI Dr. Jack Huang's laboratory, before the project was terminated in 2Q21.

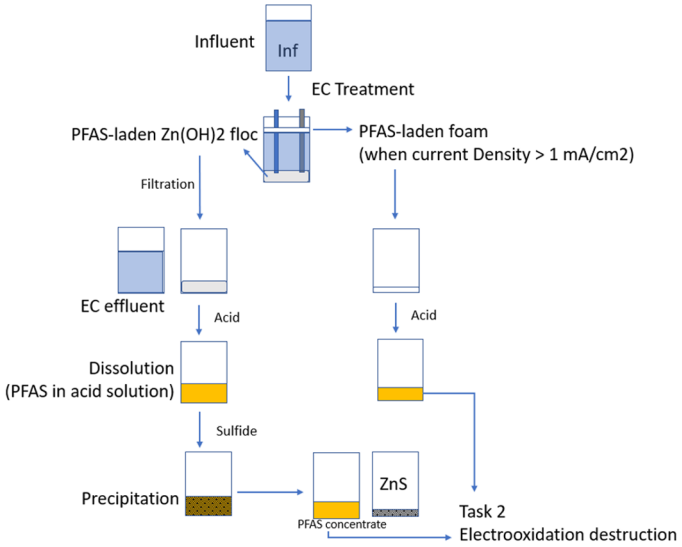

Figure 1. Illustration of Task 1 and Task 2 EC-EO processes.

4. Results and Discussion

PFAS Removal by EC using High Current Density

EC performance was first evaluated at 5 mA cm^{-2} for 60 minutes (min) in a solution of 10 PFAS (each concentration at 0.5 µM) with 20 millimolar (mM) Na_2SO_4 as supporting electrolyte. The PFAS removal efficiency is shown in **Figure 2A**. After 60 min of EC treatment, the concentrations of all PFAS in the aqueous phase decreased but to varying degrees. The removal of PFOS, PFOA, PFNA, and 8:2 FtS was greater than 99%, while that of PFHxS and 6:2 FtS was greater than 90%. The PFAS removal efficiency generally followed the chain length of the PFAS with better removal for the longer-chain PFAS. This difference of removal efficiency between long- and short-chain PFAS through the EC process was similar to what was observed in our previous study (Lin et al., 2015), because longer-chain PFAS have higher hydrophobicity and surface activity, which was primarily responsible for the PFAS sorption (Kissa, 2001).

Here, it was found that EC-derived foam was generated when a current density greater than 1 mA cm^{-2} was applied and when PFAS concentration was high (individual concentration greater than 0.1 µM) during electrocoagulation. The PFAS fractionation into foam would impact the distribution of PFAS in different phases. The generation of foam apparently resulted from the gases formed on electrodes (H_2 on cathode and O_2 on anode) in combination with the surfactant properties of PFAS, and it is also related to the concentration of the PFAS. Thus, longer-chain PFAS were rapidly removed at the beginning time, then slower concentration change occurred since less foam was generated with the reduction of PFAS in solution.

PFAS distribution among different phases (floc, aqueous, and foam) after EC treatment was examined, as shown in **Figure 2B**. It appeared that a considerable fraction of the removed PFAS distributed into the foam. The contribution of zinc hydroxide adsorption was relatively minor probably because of (1) competition from foam fractionation and (2) the relative high concentration of PFAS had saturated the sorption sites on zinc hydroxide flocs. The preferential distribution of PFAS into the foam phase could have speeded up and enhanced PFAS removal from the aqueous phase, and the foam could have then been readily and rapidly recovered for subsequent EO treatment. The foam generation was not observed in the low current density EC experiment with low PFAS concentration (e.g., 0.005 μM each PFAS).

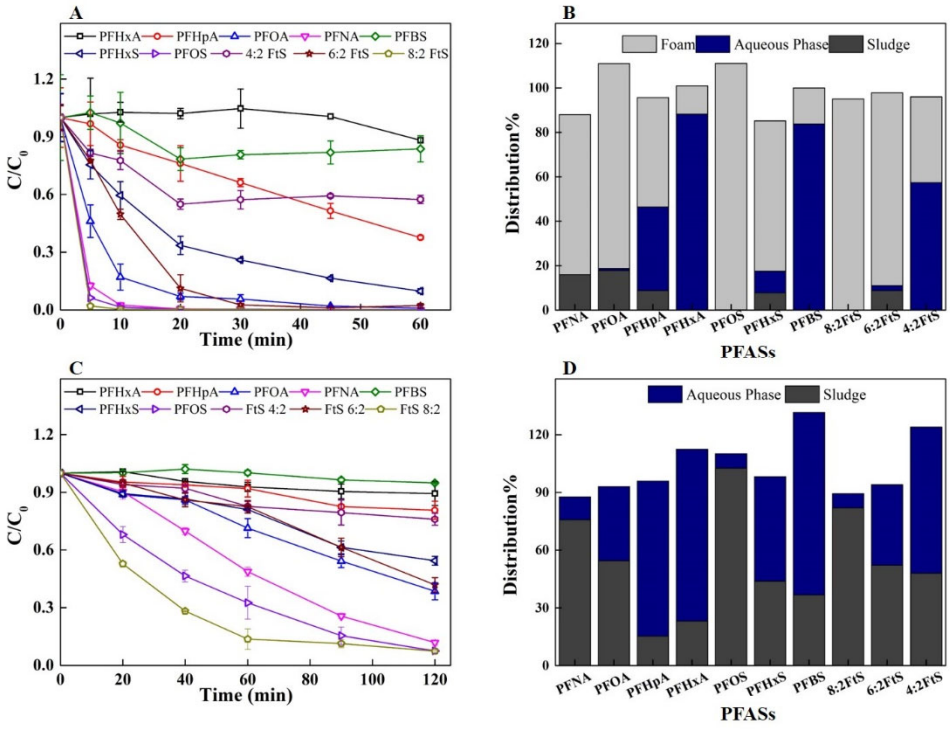

Figure 2. (A) Removal of 10 PFAS (high concentration) over time during EC process by zinc anode; (B) The mass distribution of 10 PFAS in different phases after EC treatment (C0 = 0.5 μM, current density = 5.0 mA cm^{-2}, 20 mM Na_2SO_4, EC reaction time = 120 min); (C) Removal of PFAS (low concentration) from aqueous phase over time in EC process; (D) The distribution of 10 PFAS after EC treatment. (C0 = 0.005 μM, current density = 0.3 mA cm^{-2}, 20 mM Na_2SO_4, EC reaction time = 120 min).

PFAS Removal by EC using Low Current Density

The EC treatment using a very low current density of 0.3 mA cm^{-2} was performed on a spiked solution comprising a mixture of 10 PFAS (0.005 μM each) and 20 mM Na_2SO_4 as supporting electrolyte. This solution was treated using EC for 120 min. The experimental results indicate that PFAS were removed from the aqueous phase to varying degrees by the EC process (**Figure 2C**). After 120 min of reaction time, the removal efficiency generally corresponded to the chain lengths of the PFAS, and the long-chain PFAS were better removed than the short-chain PFAS. Greater than 90% removal was achieved for PFOS and 8:2 FtS after a 120-min reaction time. PFAS

removal efficiency was below 24% when the carbon chain length was C6 or shorter. The PFAS removal at low current density was generally less than the EC at a higher current density. The foam formation was not observed under this condition. The mass recoveries of all PFAS ranged from 87.6% (PFNA) to 131.6% (PFBS), that is, removed PFAS were transformed in floc generated in the EC process.

EC Treatment of Groundwater

A groundwater sample was collected from a fire training area at Wurtsmith Air Force Base. The groundwater sample was analyzed for the 10 PFAS monitored in this study. Nine out of the 10 PFAS were detected in the contaminated groundwater. 4:2 FTS was below its detection limit of 3.7 ng L^{-1}. The groundwater sample with a supplement of 20 mM Na_2SO_4 was adjusted to pH of 3.8, and then was subjected to EC treatment at the current density of 0.3 mA cm^{-2} for 120 min; the results are shown in **Figure 3A**. The concentrations of all PFAS in the aqueous phase decreased during the EC treatment. The removal of PFOS and PFOA was greater than other PFAS. The PFAS removal ratio generally followed the chain length of the PFAS with better removal for the longer-chain PFAS (**Figure 3A**), which is consistent with the results of the spiked solution.

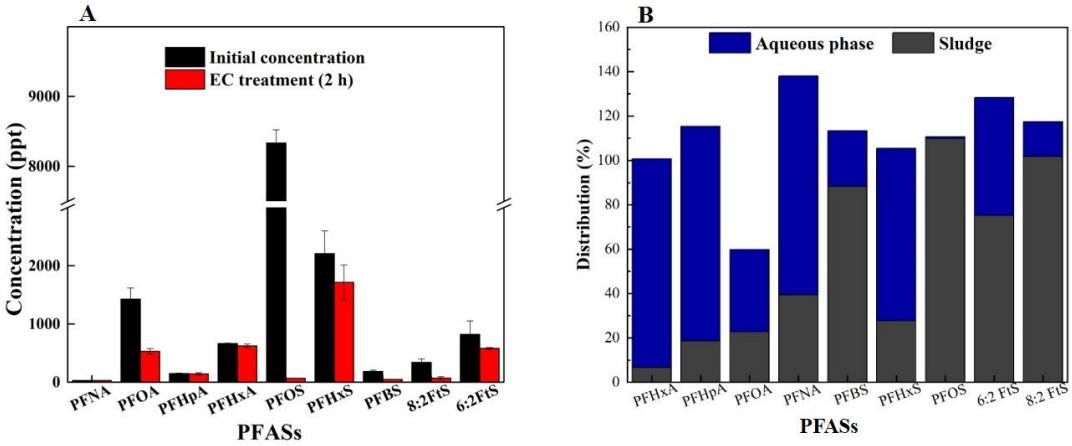

Figure 3. (A) EC treatment of PFAS in contaminated groundwater; and (B) the distribution of 9 PFAS in different phases after EC treatment using current density of 0.3 mA cm^{-2} and 20 mM Na_2SO_4 for 120 min.

The PFAS mass distribution in different phases for all 9 PFAS are presented in **Figure 3B**. The operation conditions of this study were identical to those shown in **Figure 2C** (spiked solution), except that the PFAS concentrations in groundwater are different from the spiked solution. The PFAS mass distribution are generally consistent except that PFNA had lower sorption on the floc in groundwater sample that might be from its low concentration relative to other PFAS, and PFBS on the other hand had higher sorption on sludge in the groundwater sample than the spiked water sample that might be from the influence of other constituent in real groundwater. The relatively low recovery of PFOA (60%) in the groundwater sample was not seen in the spiked water sample (93%) (**Figure 2D**). These may reflect an analytic issue or other causes remained to be examined.

EO Treatment of Concentrated Solution

Three concentrated solutions prepared through EC process were subjected to EO treatment using a Magnéli phase Ti_4O_7 anode at the current density of 10 mA cm^{-2}. Solution I was the dissolved solution of PFAS-laden floc generated using low current density condition after 120 min (0.3 mA cm^{-2}, 0.005 μM each of 10 PFAS). Solution II was the acid dissolved PFAS-laden floc solution obtained through EC treatment under the high current density condition after 60 min (5 mA cm^{-2}, 0.5 μM each of 10 PFAS), and the conductivity of Solution I and Solution II were 208.6 millisiemens per centimeter (mS cm^{-1}) and 15.1 mS cm^{-1}, respectively. The foam collected during this EC process was supplemented with 20 mM Na_2SO_4 to a final volume of 10 mL as Solution III.

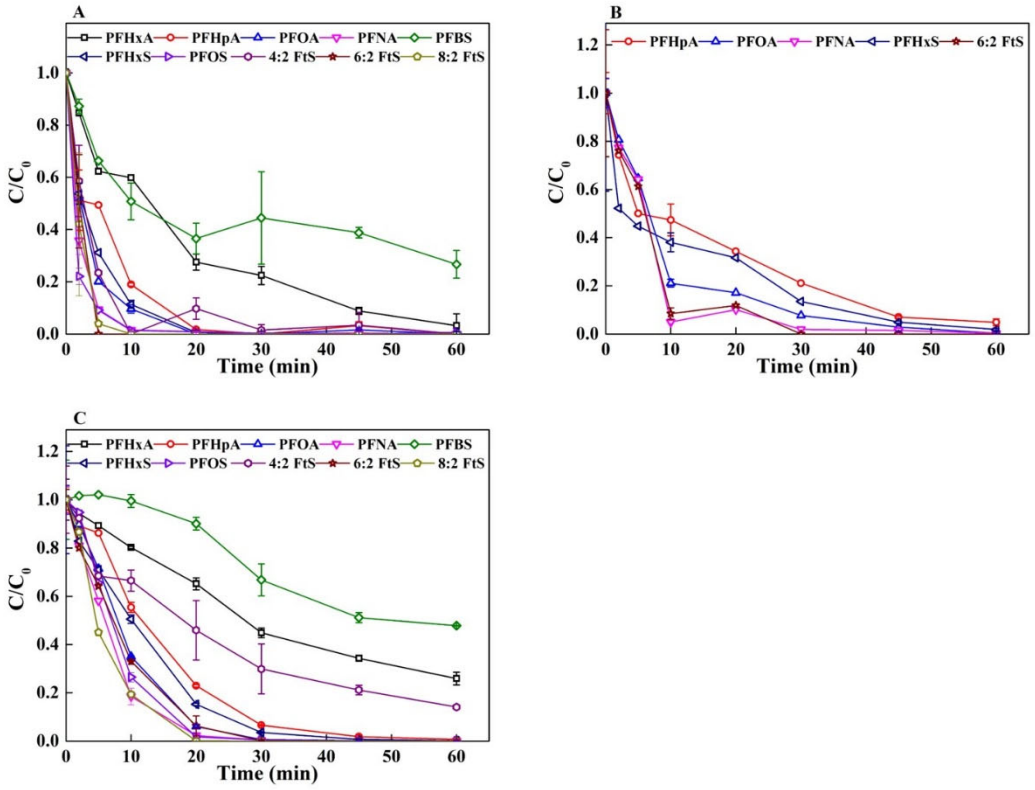

Figure 4. PFAS concentration during EO treatment (current density = 10 mA cm^{-2}) of three solutions prepared by EC. (A) Solution I: acid dissolved solution of the PFAS-laden flocs produced by EC at 0.3 mA cm^{-2}; (B) Solution II: acid dissolved solution of PFAS-laden flocs produced by EC at 5 mA cm^{-2}; (C) Solution III: foam solution produced during EC at 5 mA cm^{-2}.

Figure 4 shows the concentration profiles of each PFAS in Solution I (**Figure 4A**), Solution II (**Figure 4B**) and Solution III (**Figure 4C**) during the EO treatments. PFAS removal in all three EC-derived solutions was evident during EO. Over 95% degradation of all PFAS was achieved within 60 min in Solution I except for PFBS (73.4%). The degradation of PFAS at 60 min in Solution III was over 90% except for PFBS (52.3%), PFHxA (74.2%), and 4:2 FtS (85.9%). This is consistent with other studies showing shorter-chain PFAS more recalcitrant to EO (Zhuo et al., 2012). All five PFAS in Solution II were removed over 90% within 60 min. Similar degradation profiles were also found in our earlier study (Wang et al., 2020), which has verified that rapid mineralization to CO_2 and F^- was the main degradation pathway due to the DET reaction and surface-bound hydroxyl radical working in concert (Shi et al., 2019). Moreover, it should be noted

that Solution I and Solution II had high conductivity because of the presence of zinc and sulfate ions, and therefore, no supplement of electrolyte addition was needed, while 20 mM Na_2SO_4 was supplemented to Solution III for the EO treatment.

The concentration of Zn^{2+} in the EO process was also monitored. It was found that Zn^{2+} concentration in all three solutions decreased after 60 min; the removal rates were 63.5% (Solution I), 34.5% (Solution II) and 63.4% (Solution III), respectively. Considering distinct precipitates on the surface of the cathode and the electrochemical mechanism, it was speculated that the Zn^{2+} was removed through electro-reduction occurring on the cathode. Therefore, the EC-EO treatment train developed herein could be used to remove and degrade PFAS from water without residual zinc in the final effluent.

5. Implications for Future Research and Benefits

This study showed that EC with zinc anode can efficiently remove 10 PFAS, particularly for longer-chain PFAS. Due to special surfactants properties of PFAS, EC-derived foam was generated when a relatively high current density (> 1 mA cm^{-2}) was applied to a relatively high PFAS concentration (each PFAS > 0.1 μM) during the EC process; however, no foam appeared to be formed when a lower PFAS concentration mixture was treated by EC, regardless of a low or high current density being applied. Significant amounts of removed PFAS were fractionated into foam at EC treatment conditions facilitating foam formation, which will be applicable to separate PFAS from wastewater with high PFAS concentration, such as electroplating wastewater and reverse osmosis retentate (Ebersbach et al., 2016). For the low PFAS concentration solution such as groundwater, PFAS was quickly adsorbed on the floc in situ generated in EC process. Moreover, acid dissolution methods were developed, and successfully recovered PFAS from floc and foam in a controlled volume acid solution for the final destruction by EO treatment. The EC-EO treatment train developed in this study allows for the treatment of PFAS from wastewater at the concentrations ranging from several ppt to ppm levels, with no sorbent regeneration or PFAS waste generation. Given the limitation associated with EO in cost, strength, and scale, the EC-EO treatment train might provide an effective alternative scheme to destruct PFAS on site. Nevertheless, the coupling approach showed a relatively poor removal efficiency for short-chain PFAS, mainly limited by the EC process. Further study is warranted to enhance the EC removal efficiency of short-chain PFAS using other metal or mixed-metal anodes.

1. OBJECTIVE

This study directly responds to the Strategic Environmental Research and Development Program (SERDP) FY18 Statement of Need (SON), **SON Number ERSON-18-C2: In-Situ and Ex-Situ Remediation of Per- and Polyfluoroalkyl Substance (PFAS) Contaminated Groundwater**.

PFAS are a class of emerging contaminants that are stable and persistent. The criteria considered safe and protective of human health and the environment are extremely low at parts per trillion (ppt). The only demonstrated technology available to remove PFAS in groundwater is filtration that separates PFAS from water by adsorbing them onto filtration media (e.g., granular activated carbon [GAC], anion ion exchange resin [AIX]). These technologies have many advantages, including acceptable installation and operation costs, along with proven effectiveness for removing the regulated perfluorooctane sulfonate (PFOS) and perfluorooctanoic acid (PFOA). The spent filtration media, if not incinerated or disposed of after single use of the media, need reactivation or regeneration for reuse, and the reactivation or regeneration processes do not completely destroy PFAS. Public concern and scrutiny of PFAS containing water and wastes continue to grow, and off-site PFAS waste disposal and incineration options will soon become more restricted and less available. The total engineering solution hypothesized for managing PFAS and their comingled plumes at Department of Defense (DoD) sites should include both separation (e.g., filtration, precipitation, stabilization) and destruction mechanisms that leave minimum or no residual PFAS waste for off-site disposal or incineration. The ideal treatment train approach should be cost-competitive compared to the GAC or AIX treatment followed by incineration, and should be technically proven of being able to mineralize PFAS with no or minimum byproduct accumulations as secondary pollution.

This project evaluates an ex-situ treatment train that combines electrocoagulation (EC) and electrochemical oxidation (EO) to address PFAS and their co-contaminants in groundwater. Through this treatment train approach, PFAS and co-contaminants, including petroleum compounds, and chlorinated solvents, will be first effectively removed from impacted water and concentrated on EC-generated flocs, and then subsequently destroyed through the EO process. The EC process is a proven and commercialized technology for treating large volumes of wastewater with low cost, but EC technology has not been fully evaluated for treating a wider range of PFAS or under different operation conditions. Many studies have documented the effectiveness and extent of PFAS treatment using EO. The coupling of EC and EO is innovative and synergetic in that the destruction of PFAS by EO is much more efficient when they are concentrated by EC. Therefore, this innovative approach attempts to couple these two electrochemical-based treatment technologies into one treatment train in a synergetic manner for PFAS treatment.

The overarching objective of this project is to verify an effective treatment scheme coupling EC and EO to effectively manage groundwater impacted by PFAS. The identified treatment scheme includes (1) EC to remove PFAS from groundwater; (2) formation of PFAS enriched flocs; (3) a process to dissolve flocs and form PFAS concentrate; and (4) EO degradation of PFAS concentrate.

2. BACKGROUND

2.1 PFAS Treatment

Waste fuels and extinguishing agents, such as Aqueous Film Forming Foam (AFFF) formulations, were employed and released into the environment without treatment for several decades. These releases often occurred repeatedly over many years, leading to large amounts of contaminants (fuels and AFFF) infiltrating into the subsurface. Many DoD sites with such contamination have undergone groundwater treatment for fuels, but characterization, understanding of fate and transport, and treatment of mixed contaminants, including AFFF, are not clear. While PFAS include per- and polyfluoroalkyl substances, perfluoroalkyl acids (PFAAs) are the major components in the historically used AFFF and are very persistent and relatively soluble in groundwater while having very low criteria for protection of human health and the environment. Most PFAS have surfactant characteristics that also complicate the fate and transport of PFAS at a site.

Due to the persistent and bio-accumulative nature of certain PFAS, PFAS exposure is associated with an increased risk of adverse effects for human health (Anderko and Pennea, 2020). Perfluorooctanoic acid (PFOA) and perfluorooctanesulfonic acid (PFOS), two of the most studied PFAS, are reported to bind to tissue proteins, accumulate in the blood, and at much lower levels in the liver, kidney, and brain (Ehresman et al., 2007). Human studies have found associations between exposure to PFAS and several diseases, such as high cholesterol, thyroid toxicity, and cancer (Eriksen et al., 2010; Chang et al., 2014). To mitigate human exposure, the United States Environmental Protection Agency (USEPA) established a Lifetime Health Advisory of 70 parts per trillion (ppt) for combined PFOA and PFOS concentration in drinking water (USEPA, 2019). More recently, the USEPA unveiled a PFAS Action Plan to address the public health concerns of PFAS chemicals and initiated the process to develop a national primary drinking water regulation for PFOA and PFOS (USEPA, 2019).

The treatment technologies currently under investigation to remove PFAS are primarily separation technologies without destruction of PFAS. Sorption by activated carbon or ion exchange resin have been demonstrated to remove PFAS from water, but they have various limitations such as limited capacity and rapid PFAS breakthrough. Pretreatment is also frequently needed to avoid clogging, biofouling, or for reducing media change-out frequencies. Another significant limitation of traditional media-based separation technology is that the treatment process produces PFAS-laden wastes, such as spent carbon or ion exchange media with elevated PFAS levels, which may cause secondary hazards. Hence, the long-term costs of treating PFAS-impacted water using these approaches can be substantial due to the costs associated with media replacements and disposal. Developing technologies or treatment approaches to reduce PFAS waste and achieve complete destruction of PFAS are greatly needed.

PFAS have unique stability due to the strong carbon-fluorine (C-F) bonding energy and are difficult to degrade (USEPA, 2020). The extreme chemical stability of PFAS renders them highly resistant to conventional chemical destruction technologies such as advanced oxidation processes (AOPs). AOPs rely primarily on hydroxyl radicals (OH) to destroy organic contaminants, but the relatively slow reaction rates between PFAS and aqueous OH limit their applicability (Keech et al., 2003). Hydroxyl radical alone was found to be ineffective in degrading PFAS (Javed et al.,

2020). Photolytic techniques have shown varying degrees of efficacy on high concentrations of PFAS, including direct ultraviolet (UV) photolysis, photochemical oxidation with $K_2S_2O_8$, $H_3PW_{12}O_{40}$, KI, and humic acid (HA), and photocatalysis in the presence of TiO_2 and In_2O_3 (Kirsch, 2004; Lin et al., 2012; Li et al., 2012). Ultrasonic irradiation and plasma oxidation have shown effectiveness to degrade PFAS (Holger et al., 2012). Applications of these technologies are, however, limited by their requirement on high energy input and/or special equipment.

2.2 Electrocoagulation

The electrocoagulation process involves the dissolution of metal cations from the reactor anode with simultaneous formation of hydroxyl ions and hydrogen gas at the cathode:

$$M \rightarrow M^{+} + ne^{-} \qquad (1)$$

$$2H_2O_{(l)} \rightarrow OH^{-} + H_{2(g)} \qquad (2)$$

A current is passed through a sacrificial metal electrode, oxidizing the metal (M) to its cation (M^{n+}) (Equation (1)). Simultaneously, hydrogen gas and the hydroxyl ion (OH^{-}) are produced from water (Equation (2)). Electrocoagulation thus introduces metal cations in situ, using sacrificial anodes (most commonly iron, stainless steel, or aluminum) that need to be periodically replaced. During electrocoagulation, highly charged cations (e.g., Al^{3+}, Fe^{2+}) formed at the anode destabilize colloidal particles by the formation of monomeric and polymeric hydroxyl complex species.

Electrode type. In most studies reported in the scientific literature, different electrode types can lead to different contaminant removal efficiency. Aluminum (Al), iron (Fe), mild steel, and stainless steel (SS) electrodes have been commonly used as the electrode materials. Do and Chen (1994) compared the performance of iron and aluminum electrodes for removing color from dye-containing solutions. Their conclusion was that the optimum EC operation conditions varied with the choice of anodes. Baklan and Kolesnikova (1996) investigated the relationship between 'size' of the cation introduced and treatment efficiency. The size of the cation produced (10–30μm for Fe3+ compared with 0.05–1μm for Al3+) was suggested to contribute to the higher efficiency of iron electrodes. Hulser et al. (1996) observed that electrocoagulation was strongly enhanced at aluminum surfaces in comparison with steel electrodes. This was attributed to the in-situ formation of dispersed aluminum–hydroxide complexes through hydrolysis of the aluminate ion, which does not occur when employing steel electrodes.

Coagulation. These metal hydroxyl complexes have high adsorption properties, forming strong aggregates with contaminants. The extent of metal hydrolysis via EC depends upon the total metal cation concentrations and the pH, as well as the types and concentrations of other species present in solution. For example, electrolysis in the presence of a zinc electrode produces Zn^{2+} upon anodic oxidation and zinc hydroxide, $Zn(OH)_2$. The $Zn(OH)_2$ remains in the aqueous phase as an amorphous suspension, which can remove the contaminants from the contaminated water by either complexation or electrostatic attraction followed by coagulation.

$Zn(OH)_2$ Flocs. $Zn(OH)_2$ flocs generated during the electrocoagulation process have been studied and published in numerous peer-reviewed journals (Wang et al., 2016; Hussin et al., 2017; Safwat, 2020). Wang et al. (2016) studied the use of zinc electrode for PFOA removal by generating PFAS-

laden flocs and demonstrated effective removal of PFOA from aqueous solution through formation of $Zn(OH)_2$ flocs; however, there was no research on the management of PFAS-laden flocs.

Electrocoagulation Processes for PFAS Removal and Mass Distribution. The publications of using electrocoagulation to remove PFAS are very limited. Lin et al. (2015) evaluated PFAS removal using various sacrificial anodes, including aluminum, iron, zinc, and magnesium. The tested PFAS include PFOS and PFCAs (C7-C10). Batch experiments were conducted in a cylinder EC cell with agitation to investigate the sorption kinetics and PFAA isotherms on metal hydroxide flocs. Individual PFAS concentration at 1.5 µM or 0.5 mM was spiked into deionized (DI) water together with 10 mM NaCl as electrolyte. Under the test condition of using current density at 0.5 mA/cm^2 and the starting pH at 5, zinc was identified as the best anode for PFAS removal in this electrocoagulation study (**Figure 5**). The study reports the measured surface area (48.7 square meters per gram [$m^2\ g^{-1}$]) of the freeze-dried zinc hydroxide flocs by the Brunauer–Emmett–Teller (BET) method; however, it should be noted that the measured surface area of the freeze-dried zinc hydroxide flocs by the BET method may be far less than the real surface area of the fresh zinc hydroxide flocs in aqueous solution, because the porous structure may collapse during freeze drying. The study reveals that PFAS can be quickly sorbed on the surface of the zinc hydroxide flocs generated in situ through the EC process, mainly via hydrophobic interaction.

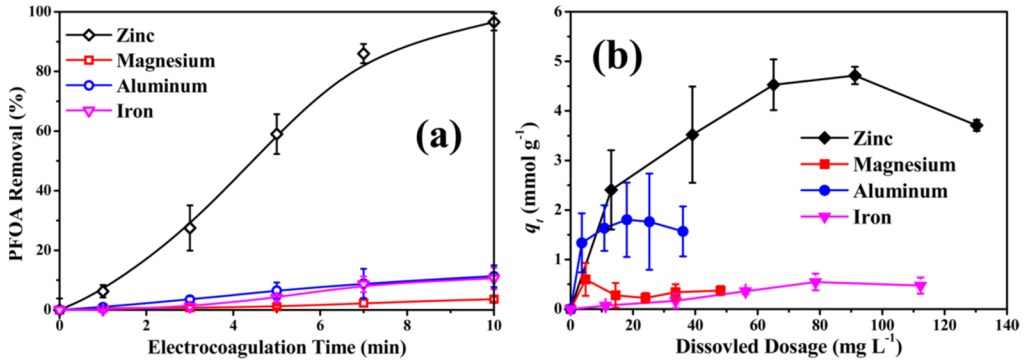

Figure 5. Removal of PFOS and PFOA during electrocoagulation process (Lin et al., 2015).

Floc-Foam. The gases (H_2, O_2) evolved at the electrodes through the water electrolysis process may be strong enough to cause flotation of the coagulated materials. Once the floc is generated, the electrolytic gas creates a flotation effect, removing the contaminants to the floc-foam layer at the liquid surface. For PFAS, the increased air-water interfaces from the evolved gases during EC may allow PFAS to partition into the air-water interface and be lifted to the liquid surface as foam.

Oxidation or Reduction. The metal hydroxide usually has high adsorption properties, thus bonding to the contaminants (bridge coagulation), or the hydroxides form larger lattice-like structures and sweep through the water (sweep coagulation), entrapping particles. However, depending on reaction conditions, electrode type, and oxygen concentration, oxidation or reduction of the contaminants may also occur (e.g., dehalogenation) (Garcia-Costa et al., 2020; Wang et al., 2020).

Commercialization and Applications. With decades of extensive research on EC technology, various commercial EC units are available on the market for treating different types of wastewater, such as water containing heavy metals and wastewater from textile, food, and paper industries.

The capacities of full-scale EC systems range from 2 to 1,000 gallons per minute (GPM). Several system design and operation parameters, including electrode arrangement, current density, concentration of anions, initial pH, and anode material, are found to have a major influence on the performance of the electrocoagulation process at scale. Based on the published literature data, the cost of using larger scale EC to treat wastewater ranges from \$0.25/m^3 to \$3.50/m^3, depending on the influent water properties and treatment goals (Moussa et al., 2017).

2.3 Electrochemical Oxidation of PFAS

Electrochemical oxidation (EO) is a technology that oxidizes organic pollutants in water by applying a current through a conductive solution between anodes and cathodes. Complete mineralization of PFAS by EO has been documented. PFAS destruction can be achieved by EO via direct electron transfer on "non-active" anodes, including boron-doped diamond (BDD), PbO_2, and SnO_2, under room temperature and atmospheric pressure at fast rates (half-lives: 5.3-21.5 min) and relatively low energy consumption (Niu et al., 2013). EO was used to effectively degrade perfluoroalkyl carboxylates (PFCAs) (C4~C8), perfluoroalkyl sulfonates (PFSAs) (C4~C8), and 6:2 fluorotelomer sulfonate in polluted groundwater even in the presence of a high dissolved organic carbon (DOC) background (DOC/PFAS ratio up to 50) (Zhuo et al., 2012). Another study reported degradation of PFAS, including PFOA and PFOS, in AFFF contaminated groundwater by EO at bench scale, and the main degradation products were F- and CO_2 (Schaefer et al., 2015). Additionally, our project team has successfully treated PFOS and PFOA in the ion-exchange regenerant waste under high total organic carbon (TOC) conditions (Liang et al., 2018). These results strongly suggest the promising potential of using EO for treatment of PFAS in groundwater or industrial wastewater.

It was also noted that the energy cost of PFAA degradation by EO is highly concentration dependent, also known as concentration effect. For example, the energy required to degrade 1 mole of PFOA for 0.5 mM PFOA solution using PbO_2 electrode was estimated as 3.1 × 105 kJ mol-1 (50% degradation) at an applied current of 10 mA cm^{-2}, while the energy consumption increases for treating a more diluted PFOA solution (an order of magnitude increased in energy consumption when PFOA concentration in the solution is two orders of magnitude lower) (Shi et al., 2019). This is because EO efficiency is often limited by mass transfer of the target chemicals from the bulk solution to the anode surfaces, in particular when the concentrations of the target chemicals are low. Relatively high energy consumption is one factor limiting the application of EO to treat large volumes of water containing low concentrations (in ppt to low ppb range) of PFAS, such as groundwater contaminated by AFFF. To overcome this limit, PFAS in low concentrations can be concentrated first for PFAS destruction using EO.

PFAS Destruction Pathway. In previous electrochemical treatment studies, short-chain PFCAs were found as the major intermediates or byproducts of PFOA and PFOS degradation (Lin et al., 2013; Charles et al., 2015; Shi et al., 2019). Our work has revealed potential pathways for electrochemical degradation of long-chain PFCAs and PFSAs, including PFOA and PFOS. At the onset, direct electron transfer occurring on the anode surface lead to the radical of PFCA or PFSA that undergoes decarboxylation or desulfurization to form $C_nF_{2n+1}\cdot$. Subsequently, $C_nF_{2n+1}\cdot$ reacts with OH, O_2, and H_2O in aqueous solution, which are abundant in an electrolysis system, and further degrades to shorter-chain PFCAs with fewer perfluorinated carbons. Finally, through a

series of CF_2-unzipping cycles, PFCAs can be mineralized to CO_2 and F^- (Le et al., 2019; Liu et al., 2019; Yang et al., 2017; Gomez-Ruiz et al., 2017).

Ti_4O_7 Electrode. Magnéli phase titanium sub-oxides, such as Ti_4O_7, have recently been explored as promising electrode materials for EO applications because of their high conductivity, and chemical inertness (Ganiyu et al., 2016; Geng et al., 2015; Kreysa et al., 2014). It has been shown that Ti_4O_7 is a typical "non-active" anode, producing hydroxyl free radicals ($HO^{\bullet}$) via water oxidation, and is also active for direct electron transfer reactions (Zaky and Chaplin, 2013). Our recent studies have demonstrated the degradation and mineralization of PFAS on Magnéli phase Ti_4O_7 electrodes (Lin et al., 2018; Liang et al., 2018; Shi et al., 2019; Wang et al., 2020).

EO Commercialization and Applications. The electrochemical technologies, especially the electrochemical advanced oxidation processes, are emergent and promising alternatives for water treatment that have shown high persistent organic pollutant removal. EO have been applied to treat actual effluents and showed noticeable results on the abatement of COD and DOC (Garcia-Segura et al., 2018). For the treatment of PFAS using EO, our team has recently completed a field demonstration for treating AFFF-impacted groundwater using combined regenerable AIX and a pilot-scale EO system. The future development of EO for PFAS destruction will be directly related to the scale-up process and electrochemical reactors design to ensure the effective and economical application of this technology.

2.4 EC and EO Treatment Train

Although the individual treatment processes (i.e., EC and EO) have been researched to treat PFAS, sequential treatment of combining EC and EO has not been studied. To the best of our knowledge, this project is the first study that evaluates EC and EO separately and sequentially as one treatment train for mixed PFAA compounds in the synthetic spiked water and in the groundwater collected from a PFAS-impacted site.

This research supports the SERDP mission to reduce DoD's liabilities by developing sustainable, cost-effective technologies for expedited site cleanup and closure by remediation of contamination in soil, sediments, and water.

3. MATERIALS AND METHODS

This section describes the experimental design and techniques used in this project.

3.1 Materials

PFAS chemicals were from Sigma Aldrich Chemical Co., Ltd (St. Louis, MO, USA), Indofine chemical company, Inc. (Hillsborough, NJ, USA), and Tokyo Chemical Industries (Tokyo, Japan). PFAS standards and the isotope labeled PFAS internal standards were from Wellington Laboratories (Ontario, Canada). **Table A1** in Supporting Information (SI) summarizes the information of all ten PFAS examined in this study and related internal standards. High performance liquid chromatography (HPLC)-grade methanol was obtained from Fisher Scientific (Pittsburgh, PA, USA). All other chemicals were from Sigma-Aldrich Chemical Co., Ltd. (St. Louis, MO, USA) at reagent grade or higher and used as received. Reaction solutions were prepared with Milli-Q water (18.2 MΩ cm^{-1} resistivity, 25 degrees Celsius [ºC]) prepared with a Nanopure Barnstead purification system (Thermo Scientific, USA). The 0.22-micron (μm) polypropylene (PP) filter was from Foxx Life Sciences (Salem, NH, USA), and the 0.22-μm acetate membrane was from Sartorius (Germany).

The EC experiments used a high purity (≥ 99.99 %) zinc anode obtained from ThyssenKrupp Online Metals LLC. A Magnéli phase Ti_4O_7 anode was used for the EO study. It was fabricated using a high-temperature sintering method as reported in our previous study (Liang et al., 2018), and the crystal structure of anode was characterized using an X'Pert PRO MRD X-ray diffractometer, confirming Ti_4O_7 being the primary component.

The project team collected AFFF-impacted groundwater samples from the Wurtsmith Air Force Base (WAFB) FT-002 groundwater treatment plant influent to evaluate the performance of treating real world samples using the EC process. Based on the PFAS characterization data, the frequently detected PFAS included 19 compounds, comprising PFCAs, PFSAs, fluorotelomer sulfonates (FtSs), and perfluoroalkane sulfonamides (FASAs).

3.2 Methods

Electrocoagulation Experiment. The EC reactor was constructed with an acrylic cylindrical EC cell (8-cm diameter and 10-cm height). A zinc sheet (0.05 × 10 × 20 cm) was placed along the circumference of the cylindrical reactor to act as the sacrificial anodes, while a 304 stainless steel rod of 3-millimeters (mm) diameter was placed in parallel to the axial center of the anode as the cathode (**Figure 6**). In each treatment, 250 milliliters (mL) of solution contained either a total of ten PFAS (shown in **S1**) with all at the same concentrations, or a single PFAS. The 20-mM Na_2SO_4 solution was used as the background electrolyte. The solution initial pH was adjusted to 3.8 using H_2SO_4 and NaOH. During the EC treatment, the solution was agitated constantly throughout the experiment using an air pump through valves equipped on the bottom of the reactor. All EC experiments were conducted in batch mode with direct current (DC) applied using a DC power source (Electro Industries Inc., Monticello, MN). A zinc anode was used for this study, because our earlier study indicated a much greater PFOA removal efficiency than other common metal anodes (iron, aluminum, and magnesium) (Lin et al., 2015) and that the residual zinc concentration was at relatively low, safe levels, and can be readily removed by precipitation.

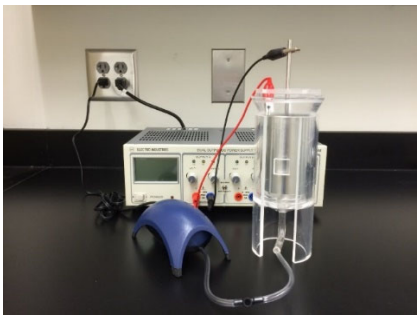

Figure 6. Bench-Scale EC Reactor

The EC experiments were performed with PFAS at different concentration levels under different current densities. It was observed that a layer of foam was formed on the aqueous phase surface when the PFAS concentrations were greater than 0.1 μM and the current density was greater than 1 mA cm^{-2}. For these conditions, the foam was collected manually by pipetting it out from the EC reactor throughout the treatment. For experiments examining the change of PFAS concentrations in the solution over time, triplicate 1-mL samples were withdrawn from the solution at pre-specified time intervals, and then centrifuged at 2,000 rpm (268 × g) for 5 min to separate the liquid and solid phases. For samples from experiments with the initial PFAS concentrations greater than 0.1 μM, 0.1 milliliter (mL) of supernatant was taken and combined with 0.1 mL of methanol-containing isotope labeled internal standards for subsequent PFAS analyses described below. For experiments with lower initial PFAS concentrations, the supernatant from centrifugation was concentrated using solid phase extraction (SPE) as described below.

For experiments examining the phase distribution of PFAS, triplicate aqueous samples were only taken at the end of the EC experiment. The remaining solution was then passed through a 0.22 μm acetate membrane (Sartorius, Germany), and the floc retained on the filter was transferred into a beaker and dissolved in 10 mL of 4.5 M H_2SO_4 solution. To eliminate the potential interference of an acidic environment to the PFAS quantification, 2 mL of concentrated solution was withdrawn and adjusted to a final pH of approximately 6.0, then injected with 40 μL of a mixed isotope labeled internal standard solution (100 ppb). The produced solution was further concentrated using SPE as described below. For the experiment with foam generation, the collected foam was mixed with 200 microliters (μL) 4.5-M H_2SO_4 solution and constant-volumed to a total volume of 10 mL, then 0.1 mL of foam solution was taken and combined with 0.1-mL of mixed isotope labeled internal standard solution for subsequent PFAS analyses. The PFAS mass distribution in all phases after an EC treatment was calculated using Equation E1:

$$\text{Phase distribution} = \frac{C_P \times V_P}{C_0 \times V_R} \times 100\% \qquad \text{E1}$$

Where, C_P (moles per liter [mol L^{-1}]) and V_P (liters [L]) are the PFAS concentration and the volume of different phases (aqueous, floc or foam), where the floc and foam phase volumes are those after acid dissolution (10 mL); C_0 (mol L^{-1}) is the initial PFAS concentration, and V_R (L) is the reaction volume. The total PFAS mass recovery was the sum of the different phase distribution.

Electrooxidation Experiment. An EC treatment was first carried out on a 250-mL solution of 10 PFAS (0.5 or 0.005 μM each) under 5 or 0.3 mA cm^{-2}. The floc recovered at the end of treatment was dissolved in 10 mL 4.5-M H_2SO_4 solution, and the collected foam was also mixed with the

acid to a total of 10 mL. The acid solution resulting from PFAS-laden flocs was directly subjected to EO treatment as described below. The acid solution from the foam dilution was supplemented with 20 mM Na_2SO_4 as the background electrolyte and then subjected to EO treatment.

EO experiments were conducted in a 25-mL electrolytic cell with a Ti_4O_7 ceramic plate (1 × 2 cm) of 3-mm thickness as the anode, and a 304 stainless steel rod (5-mm diameter) as the cathode that was placed in parallel to the central axis of the anode at a 2-cm gap. For the treatment, a 10-mL solution was placed in the cell with continuous stirring using a magnetic stirrer (IKA-RCT, Germany), while a direct current was applied to the electrodes at a constant current density (10 mA cm^{-2}). For the floc acidic solution, in pre-specified time intervals, triplicate 0.1-mL samples were withdrawn, diluted with water, and adjusted to a final pH of approximately 6.0, then injected with 40 µL of a mixed isotope labeled internal standard solution (100 ppb), and was further concentrated using SPE. For the foam solution, 0.1-mL samples were directly withdrawn and mixed with isotope labeled internal standards for subsequent analysis of PFAS concentrations. All EC and EO experiments were carried out at room temperature (25 ± 1ºC).

Solid Phase Extraction. Three different SPE cartridges, including Oasis HLB (6 cubic centimeters [cc], 200 milligrams [mg], Waters Corporation, Milford, Massachusetts), Oasis WAX for PFAS Analysis (6 cc, 150 mg, Waters Corporation, Milford, Massachusetts), and Strata™-X-AW (6 cc, 100 mg, Phenomenex, Torrance, California), were tested for a set of experiments to identify the most suitable SPE cartridge for this study (*SERDP ER18-1278 Whitepaper, 2020*). The results of the SPE cartridge evaluation tests indicated that the Oasis WAX cartridges had low recovery of internal standards, often below 10%, for both the aqueous phase and the flocs samples. In addition, the Oasis HLB provided better performance than the Strata™-X-AW cartridges in terms of quality control (QC) conformance. Therefore, the Oasis HLB cartridge was selected and used in this study as described below.

The supernatant with constant volume from centrifugation was sampled, mixed with 40 µL of a mixed isotope labeled internal standard solution (100 ppb), and then subjected to SPE using HLB cartridges (Oasis HLB SPE cartridges, 3 cc, 60 mg, Waters, Milford, USA). Briefly, the cartridge was activated using 6 mL of methanol and 6 mL of Milli-Q water in sequence, followed by loading the sample at a flow rate of approximately 0.5 milliliter per minute (mL min^{-1}), and then rinsed with 10 mL of Milli-Q water. The columns were blown dry under a vacuum, and then eluted with 1.5 mL of methanol. The eluent was then blown dry, and re-dissolved in 100 µL of methanol for subsequent UPLC-MS/MS analysis.

PFAS Analysis. The concentrations of 10 PFAS were quantified using a Waters AQCUITY I class ultra-performance liquid chromatography system coupled with a XEVO TQD triple quadrupole mass spectrometer (UPLC-MS/MS, Waters Corp., Milford, MA) in negative electrospray ionization mode (ESI-). The UPLC was equipped with an Acquity UPLC BEH C18 column (2.1 × 10 cm, 1.7 µm particle-size) operated at 40ºC. A gradient composition of solvent A (5 mM ammonium acetate in Milli-Q water) and solvent B (5 mM ammonium acetate in methanol) was used as the mobile phase at a 0.3 mL min^{-1} flow rate. The analysis was carried out in multiple reaction monitoring (MRM) mode.

For the quantification of PFAS, quality control consisted of a method blank, a laboratory control sample, sample replicate. For the method blank, the results must fall below ½ the limit of quantification. The laboratory control sample results must fall within 10% of the true value for that solution, and the relative standard deviation of triplicate is within 5%; the sample replicate recovery must be within ± 30%. The extracted internal standard recovery in all samples must be within 50 – 150% of the true value. When quality control criteria are not met, the problem is corrected, and the quality control samples and associated sample are reanalyzed. The initial calibration contains a minimum of 5 points, and linear or nonlinear calibrations must have an $R^2 \geq 0.99$ for each PFAS.

Zinc Analysis. The concentration of Zn^{2+} in the solution was determined using an ICP-MS (Perkin Elmer Elan 9000 inductively coupled plasma equipped with a mass spectrometer) (Shu et al., 2019), with a detection limit of 0.05 mg L^{-1}.

Floc Characterization. The zinc hydroxide flocs generated in selected tests were collected by membrane filtration and then freeze-dried. The floc samples were characterized for the morphology by Scanning Electron Microscope (SEM) on a Hitachi's-4800 FE-SEM system (Hitachi, Japan), and for the Brunauer–Emmett–Teller (BET) surface area using a surface area analyzer (TriStar II Plus, GA).

4. RESULTS AND DISCUSSION

4.1 EC Treatment

This project evaluates the EC technology on removing PFAS through multiple phases (**Table 1**). The subsections below describe the PFAS removal and PFAS distributions in the EC reactor for each phase of study.

Table 1. EC Study Phases.

Section	Water Matrix	PFAS	Current Density (mA cm^{-2})	pH	Objectives
4.1.1, 4.1.2	PFAS-free DI water	PFOS	1	3.8	Identify floc collection method Observe floc settlement
4.1.3	PFAS-free DI water	10 or 11 PFAS	Varied	3.8	Examine PFAS removal efficiency
4.1.4	PFAS-free DI water	10 or 11 PFAS	Varied	3.8	Floc morphology
4.1.5	PFAS-free DI water	10 PFAS	0.3 mA cm^{-2}	3.8	Isotherm-like PFAS adsorption
4.2	PFAS-free DI water	10 PFAS	0.3 mA cm^{-2} or 5 mA cm^{-2}	3.8	Zinc floc dissolution and recovery study
4.3	PFAS-free DI water	10 PFAS	0.3 mA cm^{-2} for EC; 10 mA cm^{-2} for EO	3.8 (EC)	EO treatment of PFAS in EC flocs and foams
4.4.1	PFAS-impacted groundwater	9 PFAS	0.3 mA cm^{-2}	3.8	EC treatment of PFAS in groundwater (low current)
4.4.2	PFAS-impacted groundwater	9 PFAS	5 mA cm^{-2}	3.8	EC treatment of PFAS in groundwater (high current)

4.1.1 Initial PFOS-Spiked Water Treatment

The initial EC treatment tests were conducted on PFOS-spiked PFAS-free DI water. The purpose of this study was to examine the methods for water and floc separation. Different EC reaction times and floc collection methods have been tested (**Table 2**). The PFOS removal % in water was used to direct the selection of floc collection method. During this phase of the study, the water solution contained 2.0 μM (1 mg/L) of PFOS and 20 mM of Na_2SO_4, and 1 mA/cm^2 of current density was applied, while pH was adjusted to 3.8. The EC reaction time varied from 15 min to 35 min. Both filtration and centrifugation methods were tested to determine PFOS concentrations in the filtrate vs supernatant. Speed and duration of centrifugation were also evaluated to determine the best method of separating flocs from EC-treated water for the later bench-scale studies.

Table 2. Test Conditions for PFOS-Spiked Water (initial concentration: 2 μM PFOS, 20 mM Na_2SO_4, current density: 1 mA cm^{-2}, pH 3.8).

Test Condition	Reaction Time	Sample Preparation Method (Filter or Centrifuge)	PFOS Removal (%)
1	15 min	0.22-μm polypropylene (PP) filter	90
2	30 min	Centrifugation (15,000 rpm, 20 min)	6.1
3	35 min	0.22-μm PP filter	99.4
4	35 min	Centrifugation (7,500 rpm, 5 min)	93.2

In Test 1, 90% of the PFOS was removed in 15 min by EC based on the PFOS concentrations in the filtrate (**Figure 7**). Test 2 showed no PFOS removal in the supernatant after the centrifugation under a high speed of centrifugation (15,000 rpm) for 20 min, indicating that PFOS adsorbed on the EC flocs was spun off and desorbed into the supernatant (**Figure 7**). In Test 3, 99.4% PFOS was removed in 35 min by EC based on the PFOS concentration in filtrate. In Test 4, both speed and duration of the centrifuge was decreased from Test 2; PFOS was not evidently desorbed from the floc under 7,500 rpm for 5 min. Approximately 93.2% of the PFOS was removed. The test results suggest that a high force of centrifugation (15,000 revolutions per minute [rpm]) can desorb PFOS from flocs into supernatant, thus it is not appropriate for preparing samples to track PFAS removal in the aqueous phase. Centrifugation below 7,500 rpm did not result in apparent PFAS releases from the flocs and was used in later experiments. It is possible to use a differential centrifuge for floc management during EC-EO coupling. For example, the EC solution can be centrifuged at a low speed to collect PFAS-laden flocs, then centrifuged at a high speed to release PFAS in a small volume of water for subsequent EO treatment. This approach, however, was not studied in this project.

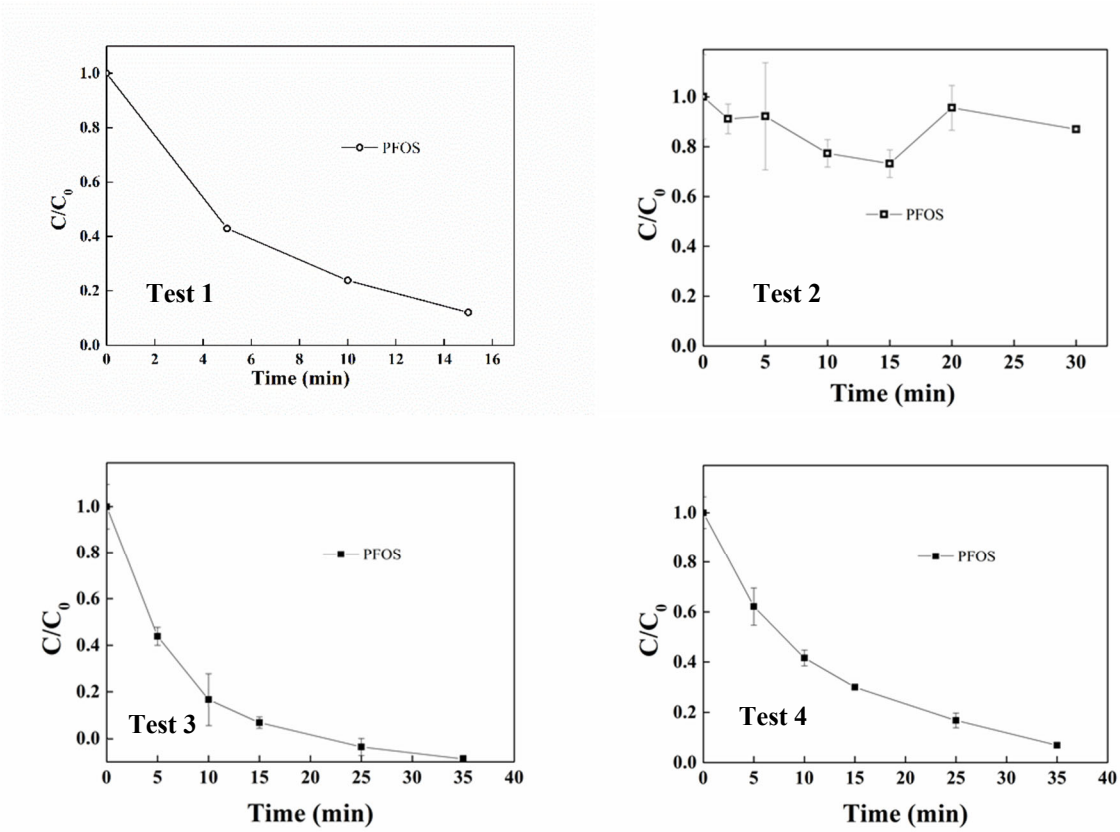

Figure 7. PFOS concentrations during EC treatment (C0 = 2 μM PFOS; Electrolyte: 20 mM Na2SO4; Current density: 1 mA cm^{-2}; pH 3.8). Test 1: Reaction time: 15 min; Treated sample preparation method: 0.22-μm PP filter; Test 2: Reaction time: 15 min; Treated sample preparation method: centrifugation 15,000 rpm, 20 min); Test 3: Reaction time: 35 min; Treated sample preparation method: 0.22-μm PP filter; Test 4: Reaction time: 35 min; Treated sample preparation method: centrifugation 7,500 rpm, 5 min. The error bars represent standard deviation of triplicate samples.

4.1.2 Initial Floc Settlement Observation

Upon completion of the EC treatment, the generated flocs were settled overnight to observe settlement of the flocs. After settling overnight, nearly all flocs deposited to the bottom of the beaker by visual observation (**Figure 8**). By decanting supernatant solution, the flocs volume reduced 16.4 times after settlement. Based on repeated observations, the flocs settled rapidly, approximately within 30 min.

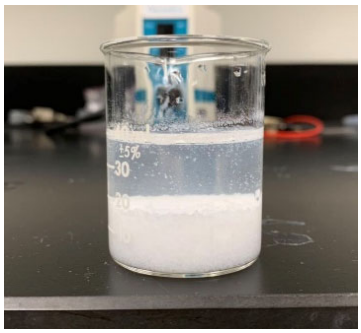

Figure 8. Floc Settlement Observation.

4.1.3 PFAS Removal in Solutions Prepared by DI Water at Different Current Density

EC performance was tested using 11 or 10 PFAS. The PFAS concentrations were 0.5, 0.01, or 0.005 µM for each PFAS (**Table 3**) under current densities of 0.3, 1, or 5 mA cm^{-2}. There were two test conditions where perfluorinated sulfonamide (FOSA) was not included because of challenges to quantify FOSA. The selection of PFAS for this project was based on the PFAS detected in the extracted groundwater collected from the WAFB FT-002 area. Under a current density of 5 mA cm^{-2}, the reaction time was 60 min. Under a lower current density (0.3 and 1 mA cm^{-2}), the reaction time was 120 min (**Table 4**). The reaction times were significantly longer than 10 min used in the Lin study (Lin et al., 2015, **Figure 5**) to verify the adsorption of a wider range of PFAS including both short-chain and long-chain PFAS. The mass distribution of PFAS in the EC reactor was also assessed. Our initial study indicates that the initial pH of a solution can impact floc formation (Lin et al., 2015), and thus the initial pH of all solutions was adjusted to 3.8 to ensure a constant starting pH.

Table 3. Tested PFAS Concentrations (µg/L).

PFAS Name	PFAS Acronym	0.005 µM	0.01 µM	0.5 µM
Perfluorononanoic acid	PFNA	2.315	4.63	231.5
Perfluorooctanoic acid	PFOA	2.065	4.13	206.5
Perfluoroheptanoic acid	PFHpA	1.815	3.63	181.5
Perfluorohexanoic acid	PFHxA	1.565	3.13	156.5
Perfluorooctanesulfonic acid	PFOS	2.495	4.99	249.5
Perfluorohexanesulfonic acid	PFHxS	1.995	3.99	199.5
Perfluorobutanesulfonic acid	PFBS	1.495	2.99	149.5
Fluorotelomer sulfonic acid 8:2	8:2 FtS	2.635	5.27	263.5
Fluorotelomer sulfonic acid 6:2	6:2 FtS	2.135	4.27	213.5
Fluorotelomer sulfonic acid 4:2	4:2 FtS	1.635	3.27	163.5
Perfluorooctanesulfonamide	FOSA	2.490	4.98	249

Table 4. Test conditions for low and high current density.

Spike	Initial Concentration (individually, µM)	Na_2SO4 (mM)	Current Density (mA cm^{-2})	pH	Reaction Time (min)
11 PFAS	0.5	20	5	3.8	60
11 PFAS	0.5	20	1	3.8	120

Spike	Initial Concentration (individually, µM)	Na_2SO4 (mM)	Current Density (mA cm^{-2})	pH	Reaction Time (min)
11 PFAS	0.01	20	5	3.8	60
10 PFAS (w/o FOSA)	0.5	20	5	3.8	60
10 PFAS (w/o FOSA)	0.005	20	0.3	3.8	120

4.1.3.1 High PFAS Concentrations, High Current Density (5 mA cm-2) for 60 Minutes – Phase 1

The EC treatment was performed at 5 mA/cm^2 for 60 min on a solution of 20 mM Na_2SO_4 as the supporting electrolyte and 11 PFAS, each at 0.5 µM. The current density of 5 mA/cm^2 was considered as upper limit applied for EC, because our previous studies suggest some PFAS degradation at this current density (Wang et al., 2020). PFAS removal efficiency is demonstrated in **Figure 9**. After 60 min of reaction time, the following PFAS achieved 90% removal: PFNA, PFOA, PFOS, 8:2 FtS, 6:2 FtS, and FOSA. PFAS removal decreased with a decrease in carbon chain length. No PFBS removal was found under this testing condition; PFBS concentrations were, in fact, increased after 60 min of reaction time. PFHxA removal efficiency was also low at 3.7%. During the EC process, a layer of foam (as shown in **Figure 10**) was formed on the top of the solution. This apparently was associated with gas generation from electrodes (H_2 on cathode and O_2 on anode) in combination with the surface activity of PFAS. It is anticipated that long-chain PFAS can fractionate into foams, particularly under high PFAS concentration conditions. The poor removal efficiency for shorter-chain PFAS can also be explained by the poor fractionation into foams and the lower interaction between short-chain PFAS and EC flocs.

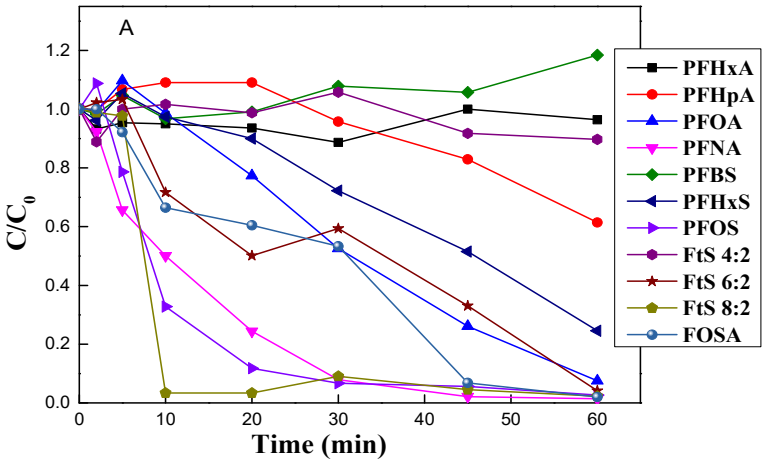

Figure 9. Removal of 11 PFAS (high concentration) over time in EC process by zinc anode (C0 = 0.5 µM, current density = 5 mA cm^{-2}, 20 mM Na_2SO_4).

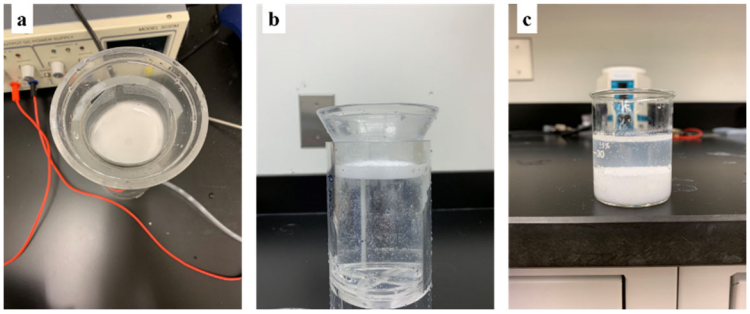

Figure 10. The (a) top view, (b) side view of foam, and (c) flocs produced in EC process under high current density.

The accountable PFAS recovery % from foam and floc are displayed in **Figure 11**. When foam and floc were co-present in the EC reactor, it appeared that a significant amount of PFAS was fractionated into foam, especially for the long-chain PFAS including FOSA, PFNA, PFOA, and PFOS, compared to PFAS adsorbed on flocs. High distribution of PFAS into foam was not previously reported (Lin et al., 2015). The PFAS mass distribution for all 11 PFAS is presented in **Table 5**. The total mass recovery ranges from 32% for PFHxS to 101% for PFBS. The mass recoveries of PFOA, PFHpA, PFOS, PFHxS, 8:2 FtS, and 6:2 FtS were below 70%. The quality assurance/quality control (QA/QC) data are listed in **Appendix A Supporting Information**. The internal standard recovery (ISR%) of most PFAS compounds in aqueous phase and sludge phase did not meet the QA/QC requirements, unlike most of the other experiments that were performed later. This reflected a challenge of the sample analysis associated with the high current density experiments, where large quantities of flocs were formed, as well as a relatively poor experiment operation during this phase of the study. The data presented in **Figure 11** thus have to be regarded as qualitative and interpreted with caution. The data quality has been improved significantly for the experiments reported in Sections 4.1.3.2 to 4.1.3.5, including the high current density tests.

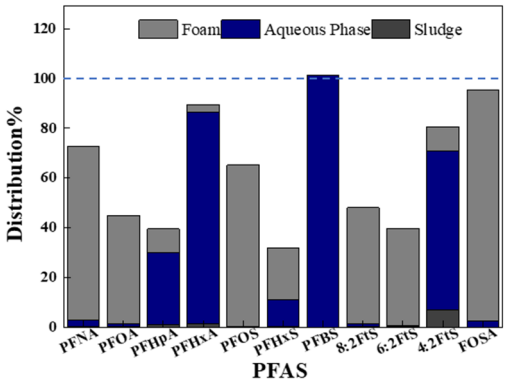

Figure 11. The distribution of 11 PFAS from different phases after EC treatment. (C0 = 0.5 μM, current density = 5 mA cm^{-2}, 20 mM Na_2SO_4).

Table 5. PFAS mass distribution (μmole) of 11 PFAS (high concentration) over time in EC process by zinc anode (C0 = 0.5 μM, current density = 5 mA cm^{-2}, 20 mM Na_2SO_4).

PFAS	PFAS Removal (%)	Aqueous Phase (%)	Foam (%)	Flocs (%)	Total Mass Recovery (%)
PFNA	98	2	70	0	72
PFOA	99	1	44	0	45
PFHpA	71	29	9	1	39
PFHxA	15	85	3	1	89
PFOS	100	0	65	0	65
PFHxS	89	11	21	0	32
PFBS	-1	101	0	0	101
8:2 FtS	99	1	46	0	47
6:2 FtS	100	0	39	0	39
4:2 FtS	36	64	9	7	80
FOSA	98	2	93	0	95

4.1.3.2 High PFAS Concentration, High Current Density (5.0 mA cm-2) for 60 Minutes-Phase 2

The Phase 1 experiment was repeated. In Phase 2, FOSA was not added into the solution. It was found that FOSA presented challenges in chemical analysis because of its low solubility. In Section 4.1.3.1, 98% of FOSA was removed.

After 60 min of EC treatment under the current density of 5 mA cm^{-2}, the concentrations of all PFAS in the aqueous phase decreased (**Figure 12**). The removal of PFOS, PFOA, PFNA, 8:2 FtS, PFHxS, and 6:2 FtS were greater than 90% (**Table 6**). The PFAS removal ratio generally followed the chain length of the PFAS with better removal for the longer-chain PFAS.

A layer of EC-derived foam was formed when the electricity was applied under this test condition. The foam was collected carefully by manually pipetting the foam out of the EC reactor throughout the treatment. After completion of the treatment, a 4.5M H_2SO_4 solution was added to the collected foam dropwise until all foam disappeared, and the solution turned into a clear aqueous phase. The "wet" foam volume was measured using a volumetric cylinder. The PFAS concentration in this solution was quantified to account for PFAS mass in the foam phase. As shown in **Table 6** and **Figure 13**, long-chain PFAS have higher interactions with EC-derived foam compared to short-chain PFAS. This can be explained by the decreased surfactant properties when carbon chain length gets shorter. Greater than 90% of PFOA, PFOS, and 8:2 FtS had incorporated into the EC-derived foam. At the completion of the EC treatment, the entire solution including flocs was collected and filtered through a 0.22-μm acetate membrane (Sartorius, Germany). Subsequently, the filtered zinc hydroxide flocs were collected and dissolved in 10 mL of 4.5-M H_2SO_4 solution, and then adjusted to pH 5.0. The PFAS concentration in this solution was then quantified to account for the PFAS quantity recovered from the floc phase. PFAS interaction with zinc hydroxide floc was relatively low compared to their interaction with the EC-derived foam.

Based on the phase 2 data, PFNA, PFOA, PFHpA, PFHxS, and 6:2 FtS had measurable interactions with flocs, but there were no measurable interactions of PFOS and 8:2 FtS with flocs. These two PFAS were completely fractionated into EC-derived foam. The PFAS mass distribution

for all 10 PFAS are presented in **Table 6**. Comparing data in Section 4.1.3.1, the mass distribution between the three phases was generally consistent but note that PFBS partitioning into foam was not observed in the phase 1 experiment.

In the phase 2 study, the techniques to account for PFAS mass in flocs and foams become more consistent; the mass recoveries of all PFAS were greater than 85%, ranging from 85.2% to 111%. One minor adjustment that was made in the analytical procedure was that the flocs were dissolved in 10 mL of acid solution instead of a smaller volume (about 4 mL) that just led to flocs dissolution prior to the SPE procedure for PFAS analysis. This might have led to a more complete PFAS release from the flocs and thus enhanced SPE recovery. The improved data quality may also reflect an improved experiment operation, and further improvement of data quality was seen in later experiments. **Appendix A** includes the QA/QC data. The data quality in terms of ISR% was significantly improved in comparison to the experiment shown in Section 4.1.3.1 (**Figure 11** and **Table 5**) under similar experiment conditions, however, the QA/QC requirements were still not met for some PFAS.

Table 6. PFAS mass distribution (%) of 10 PFAS after EC treatment (C0 = 0.5 μM, current density = 5 mA cm^{-2}, 20 mM Na_2SO_4).

Compound	PFAS Removal (%)	Aqueous Phase (%)	Foam (%)	Floc (%)	Total Mass Recovery (%)	Pseudo-First Order Rate Constant (min^{-1})
PFNA	99.9	0.1	71.9	16.0	88	0.1169
PFOA	99.1	0.9	92.2	17.8	110.9	0.0735
PFHpA	62.4	37.6	49.3	8.7	95.6	0.0161
PFHxA	11.8	88.2	12.7	0	101	0.0002
PFOS	99.8	0.2	110.8	0	111	0.0870
PFHxS	90.2	9.8	67.7	7.8	85.2	0.0378
PFBS	16.2	83.8	16.2	0	100	0.0037
8:2 FtS	100	0	95.0	0	95	0.1827
6:2 FtS	97.8	2.2	86.7	8.8	97.7	0.0774
4:2 FtS	42.6	57.4	38.5	0	95.9	0.0081

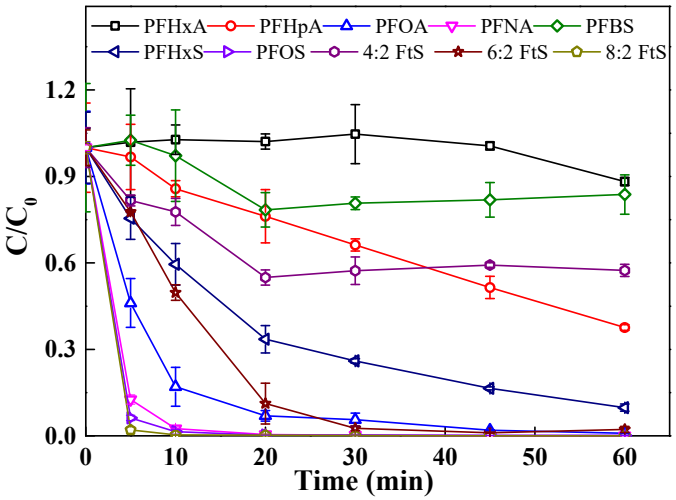

Figure 12. Removal of 10 PFAS (high concentration) over time during EC process by zinc anode (C0 = 0.5 µM, current density = 5.0 mA cm^{-2}, 20 mM Na_2SO_4).

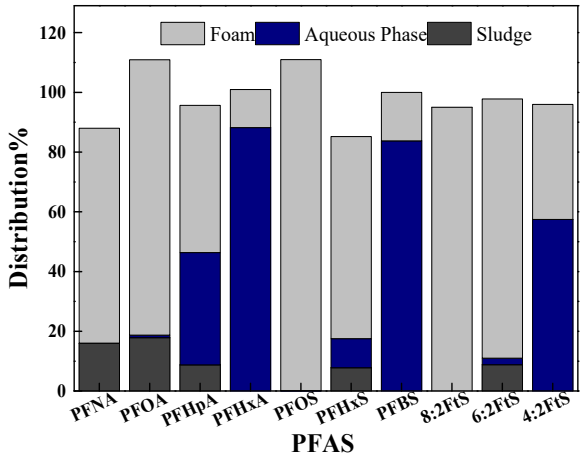

Figure 13. The mass distribution of 10 PFAS in different phases after EC treatment (C0 = 0.5 µM, current density = 5.0 mA cm^{-2}, 20 mM Na_2SO_4).

4.1.3.3 High PFAS Concentration, Low Current Density (1.0 mA cm^{-2}) for 120 Minutes

PFAS removal by EC was evaluated at 1 mA cm^{-2} in a solution containing 11 PFAS (0.5 µM each) in 20 mM Na_2SO_4. The reaction time was extended to 120 min, and samples were only collected at 120 min with no kinetic data. As shown in **Figure 14**, greater than 90% of long-chain PFNA, PFOS, and 8:2 FtS were removed after a reaction time of 120 min compared to six long-chain PFAS (PFNA, PFOA, PFOS, 8:2 FtS, 6:2 FtS, and FOSA) under high current density.

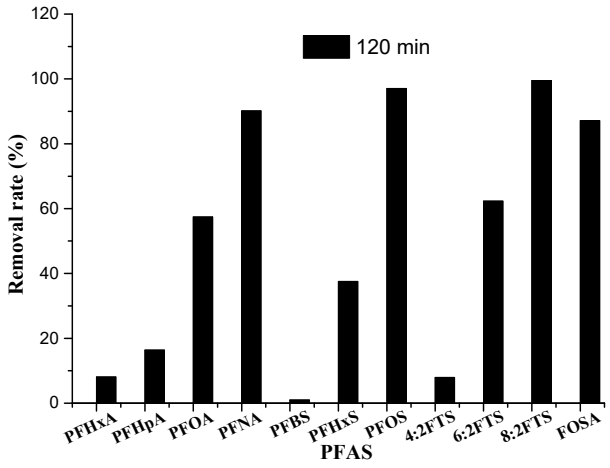

Figure 14. Removal (%) of PFAS in EC process (C0 = 0.5 μM, current density = 1 mA cm^{-2}, 20 mM Na_2SO_4, t = 120 min).

Although current density decreased from 5 to 1 mA/cm^2, foam formation was still observed. The 1 mA/cm^2 test condition was also tested to quantify the PFAS mass distribution between three different phases. In this study, the foam and flocs were collected separately, and both foam and flocs were dissolved under the pH 1.5 condition. PFAS were then analyzed to determine the distribution of PFAS in different phases (**Figure 15**). Comparing the EC treatments at 5 and 1 mA/cm^2 current density, the foam volume at 1 mA/cm^2 was less (approximately 5.0 mL) compared to 5 mA/cm^2 (total volume of approximate 30.5 mL). According to the PFAS mass distribution data (**Table 7**), the mass recoveries of PFHpA, PFHxA, PFBS, and 4:2 FtS were near or above 90%. The mass recoveries of PFOA, PFOS, 8:2 FtS, and 6:2 FtS were below 70%. PFAS mass fractionates into foam notably decreased for all PFAS at 1 mA/cm^2. Long-chain PFAS had the highest mass % fractionated into foam, between PFAS interactions with foam vs flocs, and PFAS had higher interaction with foam than flocs even for shorter-chain PFAS. The PFAS mass recovery was examined through QA/QC procedures, and the detailed data are summarized in **Appendix A**. The loss of PFAS mass not due to foam or floc interactions could be significant. In this study, such loss of PFAS had no correlation with chain lengths, and such loss may be associated with PFAS interactions with other surfaces (such as filter, apparatus of EC reactor) in the reactor and even possibly oxidation/degradation of PFAS under the tested current density condition (1 mA/cm^2).

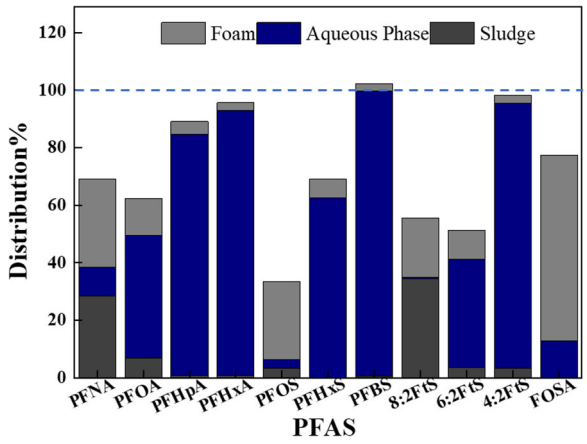

Figure 15. The distribution of 11 PFAS from flocs and foam produced in EC process (C0 = 0.5 µM, current density = 1 mA cm^{-2}, 20 mM Na_2SO_4, t = 120 min).

Table 7. PFAS Mass Distribution (µmole) of 11 PFAS (high concentration) over time in EC process by zinc anode (C0 = 0.5 µM, current density = 1 mA cm^{-2}, 20 mM Na_2SO_4).

PFAS	PFAS Removal, % *	Aqueous Phase, %	Foam, %	Flocs, %	Total Mass Recovery, %
PFNA	90.2	9.8	30.6	28.6	69.1
PFOA	57.4	42.6	12.8	6.9	62.3
PFHpA	16.4	83.6	4.5	1.0	89.1
PFHxA	8.1	91.9	2.8	0.9	95.6
PFOS	97.1	2.9	27.2	3.4	33.6
PFHxS	37.5	62.5	6.7	0.0	69.2
PFBS	1	99.0	2.6	0.6	102.2
8:2 FtS	99.5	0.5	20.6	34.5	55.7
6:2 FtS	62.3	37.7	10.0	3.7	51.3
4:2 FtS	7.9	92.1	2.7	3.4	98.2
FOSA	87.1	12.9	64.6	0.0	77.5

* PFAS removal, % = [Initial PFAS concentration (T=0)- Final PFAS concentration (T=120 min) in aqueous phase] / [Initial PFAS concentration (T=0) in aqueous phase] x 100%

4.1.3.4 Low PFAS Concentration, High Current Density (5.0 mA cm^{-2}) for 60 Minutes

The experiments were performed on a mixture of 11 PFAS (0.01 µM each) to examine their removal by EC under a high current density of 5 mA cm^{-2}. After 60 min of reaction time, the removal efficiency generally followed the chain lengths of PFAS constituents, and long-chain PFAS were better removed than short-chain PFAS (**Figure 16** and **Table 8**). Greater than 90% removal was achieved after 60-min reaction times for PFNA, PFOA, PFOS, PFHxS, 6:2 FtS, and 8:2 FtS. Current density appears to be critical on maximizing the PFAS removal based on the study that the removal efficiency was greater than the lower current density. This test condition did not observe the foam generation, and no PFAS mass distribution evaluation was conducted. The PFAS removal % (**Table 8**) was based on the PFAS concentrations detected in aqueous phase at T=0 and T=60 min. The PFAS loss could be associated with PFAS-flocs interaction or other reasons.

Table 8. PFAS removal efficiency after 60 min in EC process using zinc anode (C0 = 0.01 µM, current density = 5 mA cm^{-2}, 20 mM Na_2SO_4).

Compound	Removal Efficiency (%) at T = 60 min	Pseudo-First Order Rate Constant (min^{-1})
PFNA	96.0%	0.0578
PFOA	94.4%	0.0553
PFHpA	83.7%	0.0331
PFHxA	34.5%	0.0074
PFOS	94.9%	0.0526
PFHxS	94.6%	0.0530
PFBS	10.3%	0.0018
8:2 FtS	92.3%	0.0438
6:2 FtS	95.2%	0.0589
4:2 FtS	23.0%	0.0048
FOSA	74.1%	0.0261

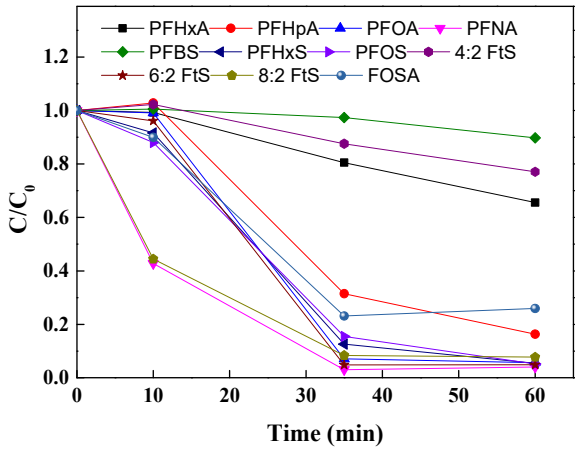

Figure 16. Removal rates of PFAS (low concentration) over time in EC process by zinc anode (C0 = 0.01 µM, current density = 5 mA cm^{-2}, 20 mM Na_2SO_4).

4.1.3.5 Low PFAS Concentration, Low Current Density (0.3 mA cm^{-2}) for 120 Minutes

The EC treatment using a very low current density of 0.3 mA cm^{-2} was performed on the PFAS-spiked water system containing 20 mM of Na_2SO_4 as a supporting electrolyte and a mixture of 10 PFAS (0.005 µM each). This solution was treated using EC for 120 min. The experimental results indicate that PFAS were removed from the aqueous phase to varying degrees by the EC process (**Figure 17**). After 120 min of reaction time, the removal efficiency generally corresponded to the chain lengths of the PFAS constituents, and the long-chain PFAS were better removed than the short-chain PFAS (**Figure 17**, **Table 9**). Greater than 90% removal was achieved after a 120-min reaction time for PFOS and 8:2 FtS only. The PFAS removal rates decreased when chain lengths got shorter for PFCAs, PFSAs, and FTS.

Table 9. PFAS mass distribution (%) of 10 PFAS (low concentration) in EC process by zinc anode (C0 = 0.005 µM, current density = 0.3 mA cm^{-2}, 20 mM Na_2SO_4).

Compound	Aqueous Phase (%)	Flocs (%)	Total Mass Recovery (%)	PFAS Removal (%)	Pseudo-First Order Rate Constant (min^{-1})
PFNA	11.8	75.8	87.6	88.2%	0.0182
PFOA	38.5	54.5	93	61.5%	0.0079
PFHpA	80.7	15.3	96	19.3%	0.0019
PFHxA	89.4	23.1	112.5	10.6%	0.0011
PFOS	7.5	102.7	110.2	92.5%	0.0215
PFHxS	54.4	43.8	98.2	45.6%	0.0052
PFBS	94.9	36.7	131.6	5.1%	0.0005
8:2 FtS	7.4	82.0	89.4	92.6%	0.0215
6:2 FtS	41.9	52.1	94	58.1%	0.0071
4:2 FtS	76.0	48.0	124	24.0%	0.0024

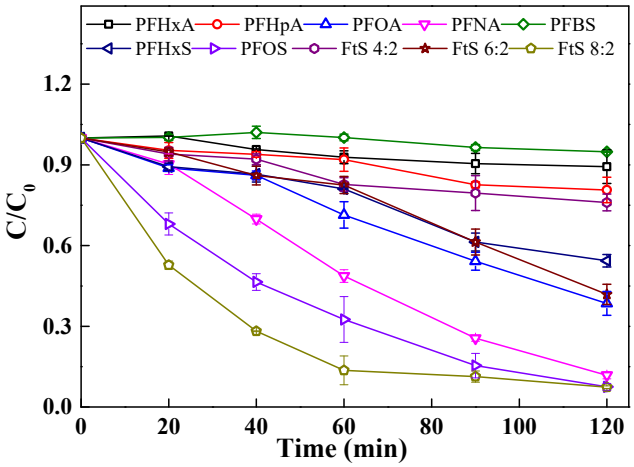

Figure 17. Removal of PFAS from aqueous phase over time in EC process (C0 = 0.005 µM, current density = 0.3 mA cm^{-2}, 20 mM Na_2SO_4).

The foam formation was not observed under this condition. The PFAS mass distribution in the aqueous and floc phases for all 10 PFAS are presented in **Figure 18** and **Table 9**. The mass recoveries of all PFAS were above 85% ranging from 87.6% (PFNA) to 131.6% (PFBS). **Appendix A** includes the QA/QC data. The QA/QC data generally meet the requirements except PFOS has a relative percent difference (RPD%) of 32.81%, greater than 30%. Oxidation or degradation of PFAS under the tested current density condition was unlikely.

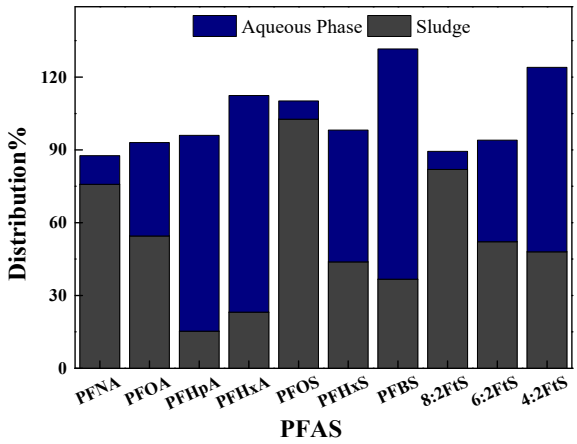

Figure 18. The distribution of 10 PFAS after EC treatment. (C0 = 0.005 μM, current density = 0.3 mA cm^{-2}, 20 mM Na_2SO_4, EC reaction time = 120 min).

4.1.4 EC Floc Morphology

The morphology of floc formed during the EC treatment varied with current density and reaction time. As shown in **Figure 19**, the flocs generated at low current density (0.3 mA cm^{-2}) showed a more crystalline flake-like structure. When a higher current density (5 mA cm^{-2}) was applied, the flocs were a more clustered amorphous or loose structure. The BET surface areas of dried flocs after degassing for 4 hours were determined at 50°C. The BET surface areas of the dried flocs generated at low current density (0.3 mA cm^{-2}) and high current density (5 mA cm^{-2}) were 101.18 and 13.36 m^2 g^{-1}, respectively. Due to a higher amount of floc generation under a higher current density, although the BET is lower, the overall sorption capability using higher current density is higher, resulting in higher PFAS removal. Additionally, the morphology of the zinc hydroxide flocs generated at 5 mA cm^{-2} observed in the first few minutes was similar to that generated at the low current density by visual observation. It appears that the structure of the flocs changed over time, with the flocs growing from a crystalline flake-like structure to a more clustered amorphous structure. This observation is important to determine the optimum reaction time under the higher current density condition.

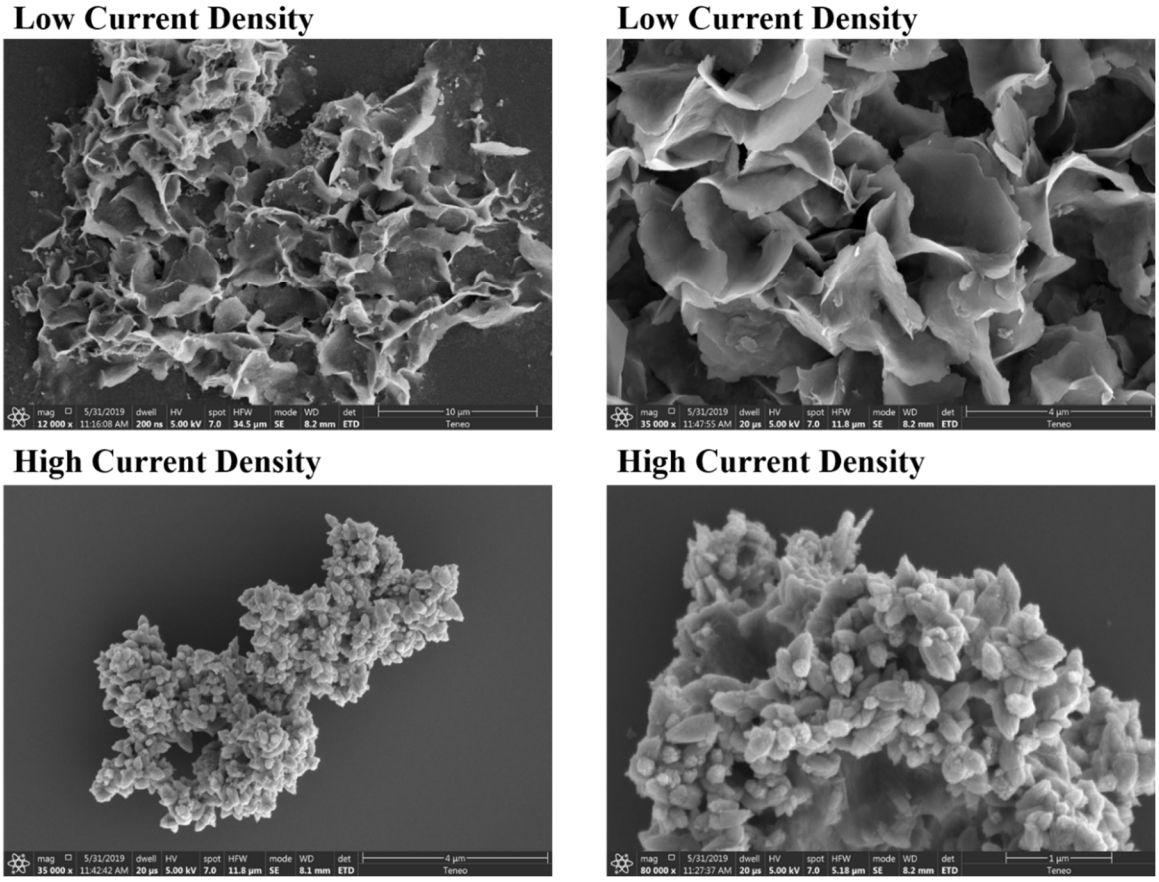

Figure 19. Field emission SEM analyses of hydroxide flocs generated in-situ in the EC process using low current density (0.3 mA cm^{-2}, 120 min) and high current density (5 mA cm^{-2}, 60 min), respectively.

4.1.5 Isotherm-Like Adsorption Study for PFAS on Flocs

A series of EC experiments were further conducted using PFAS solution comprised of 10 PFAS constituents. Initial concentrations were at different levels ranging from 0.001 to 0.1 μM (i.e., 0.001, 0.002, 0.005, 0.01, 0.02, 0.05, and 0.1 μM). The reaction time was 120 min using a low current density of 0.3 mA cm^{-2} to minimize foaming. The supernatant was collected after floc settlement from each test cell and analyzed for 10 PFAS. The data were used to evaluate the sorption capacity of each PFAS constituent and the sorbate-sorbent interactions (**Figure 20**). The sorption data of each PFAS obtained by data fitting are shown in **Table 10**. As seen, the adsorption capacity of the 10 PFAS followed the order PFOS > PFNA > 8:2 FtS > PFOA > PFHxS > 6:2 FtS > PFHpA > PFHxA > PFBS. It is in line with the order of the carbon chain length for each category, while for similar carbon chain length, PFSAs > FTSAs > PFCAs. Because PFAS with longer carbon chain lengths tend to be more hydrophobic, this result confirms that hydrophobic interaction plays a key role on the sorption capacity of PFAS on the zinc hydroxide flocs, while charge interaction may also influence as sulfonate head groups tend to have higher charge density than carboxylates in PFAS. According to the adsorption affinity constant shown in **Table 10** (smaller number indicates greater sorption affinity), the sorption affinity of the 10 PFAS followed the order PFHxS > PFOS > PFNA > PFOA > 6:2 FtS > PFHpA > 8:2 FtS > 4:2 FtS > PFHxA >

PFBS. The order differs somewhat from that for the sorption capacity, with the larger molecules (PFNA, 8:2 FtS) shifted down in the order. It seems that the bulkier molecules may be penalized in terms of sorption affinity, while charge interactions play a key role in the intensity of the sorption interactions.

Table 10. Parameters obtained by fitting Isotherm-Like Sorption Data using Langmuir Equation.

Compound	Q_m (µmol/g)	k_L (L/µmol)
PFNA	40.78	0.07
PFOA	15.11	0.08
PFHpA	1.01	0.20
PFHxA	0.10	1.8
PFOS	55.36	0.04
PFHxS	13.52	0.03
PFBS	0.01	194.38
8:2 FtS	21.71	0.25
6:2 FtS	4.17	0.11
4:2 FtS	1.94	0.35

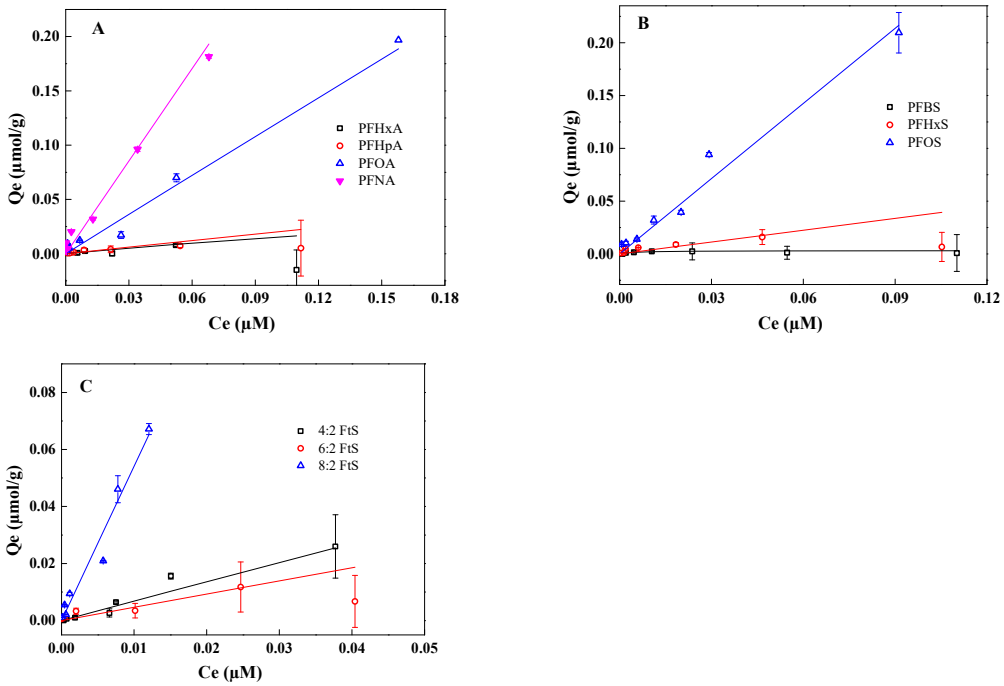

Figure 20. Langmuir sorption isotherm of 10 PFAS on the zinc hydroxide flocs (C0 = 0.001-0.1 µM, current density = 0.3 mA cm^{-2}, 20 mM Na_2SO_4).

4.2 Zinc in the EC Floc

The EC process generates zinc hydroxide floc. Prior to coupling the EC and EO, the floc is proposed to be dissolved using a low volume of acid solution, which releases PFAS back into solution and also dissolves zinc hydroxide. The EO process was tested to directly destroy PFAS in the acidic zinc solution (Section 4.3); however, zinc in the final zinc solution should still be removed and disposed of. An experiment was performed to assess the methods of removing zinc ions in the solution. First, EC was conducted in a 100-mM Na_2SO_4 solution without any PFAS added using 0.3 mA/cm^2 for 120 min or at 5 mA/cm^2 for 60 min. The entire solution, including flocs, was then collected and filtered through a 0.22-µm acetate membrane filter. The EC flocs from both current density conditions were then collected and dissolved in 10 mL of 4.0-M H_2SO_4. Subsequently, Na_2S or Na_2CO_3 was then added to the solution at different dosages to confirm zinc precipitation. Zn^{2+} concentrations in the solution were measured using an ICP-MS (Perkin Elmer Elan 9000 inductively coupled plasma equipped with a mass spectrometer). The zinc data are presented in **Figure 21**. The dissolved zinc concentrations decreased as an increased dosage of Na_2S or Na_2CO_3 was added. This experiment confirmed that most dissolved Zn^{2+} was precipitated out when sufficient salts had been added.

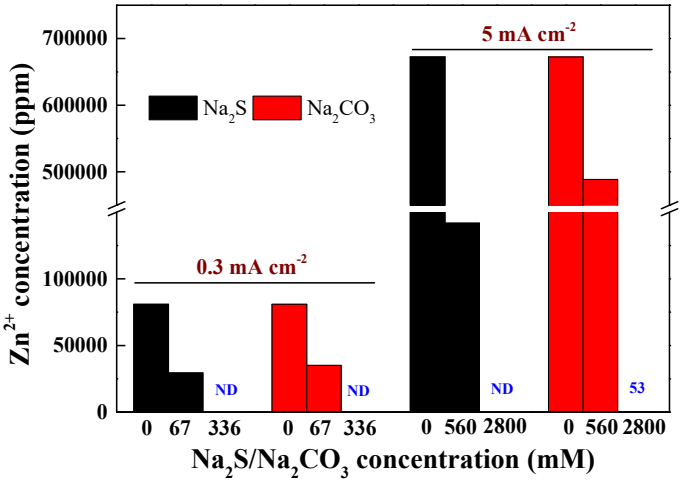

Figure 21. Zinc removal with Na_2S or Na_2CO_3 added at different dosages.

4.3 EO Treatment of PFAS in EC Flocs and Foams

One EC treatment was performed using 0.3 mA cm^{-2} for 120 min containing 20 mM of Na_2SO_4 as the supporting electrolyte and a mixture of 10 PFAS (0.005 µM each). After the EC treatment, the floc slurry was filtered through a 0.22-µm acetate membrane (Sartorius, Germany). The zinc hydroxide flocs were collected and dissolved in 10 mL of 4.0 M H_2SO_4 (Solution 1), which was subject to subsequent EO treatment. Another EC treatment was performed using 5 mA cm^{-2} for 60 min containing 20 mM Na_2SO_4, and a mixture of 10 PFAS (0.5 µM each). Foam was formed during this EC process and was collected using a pipette throughout the EC process. After the EC treatment, the floc slurry was filtered through a 0.22-µm acetate membrane (Sartorius, Germany). The zinc hydroxide flocs were collected and dissolved in 10 mL of 4.0-M H_2SO_4 (Solution 2), which was subject to subsequent EO treatment. After completion of the treatment, a 4.5-M H_2SO_4

solution was added to the collected foam to a final volume of 10 mL and then supplemented with 20 mM Na_2SO_4 (Solution 3).

All three solutions prepared through the EC process as described above were subjected to EO treatment using a Magnéli phase Ti_4O_7 anode at the current density of 10 mA cm^{-2}. The results shown in **Figure 22** indicate that PFAS in all three EC-derived solutions were removed efficiently during EO except for PFBS, PFHxA, and 4:2 FtS. Most PFAS removal occurred in the first 30 min of the EO reaction. This result is generally consistent with the results obtained previously on the electrochemical oxidation of PFAS mixture in spiked solutions (Wang et al., 2020), while the reactor setup, i.e., reaction volume to electrode surface area ratio, as well as the different electrolyte compositions could have impacted the degradation rates. For the EO treatment, Solution 1 and Solution 2 already contained high conductivity because of the presence of zinc and sulfate ions, therefore no supplement of electrolyte addition was needed, while 20 mM Na_2SO_4 was supplemented to Solution 3 (foam solution) for the EO treatment. Data in **Figure 22** shed light that coupling EC and EO is achievable and can be effective on breaking down PFAS.

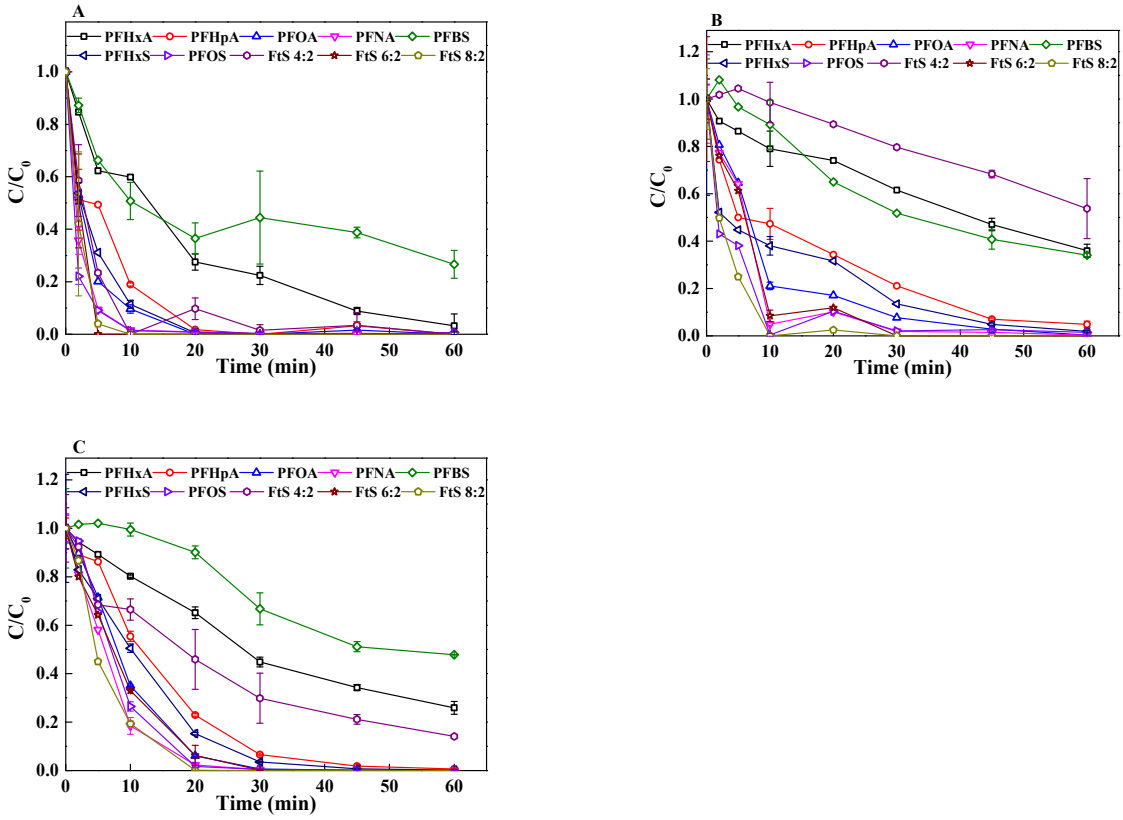

Figure 22. PFAS removal during EO treatment (current density = 10 mA cm^{-2}) of three solutions prepared by EC. (A) Solution 1: acid dissolved solution of the PFAS-laden flocs produced by EC at 0.3 mA cm^{-2}; (B) Solution 2: acid dissolved solution of PFAS-laden flocs produced by EC at 5 mA cm^{-2}; (C) Solution 3: foam solution produced during EC at 5 mA cm^{-2}. Error bars represent standard deviation of triplicate samples.

4.4 Groundwater System

A groundwater sample was collected from WAFB in September 2019. The PFAS concentrations in the collected groundwater were characterized by UGA and are summarized in **Table 11**. The groundwater sample was analyzed for the 10 PFAS compounds monitored in this study. Nine out of 10 PFAS were detected in the WAFB groundwater. The highest concentration detected was 8,162.7 ng/L for PFOS. PFOA was detected above 1,000 ng/L. The lowest concentration detected was 22.3 ng/L for PFNA. 4:2 FTS was below detection limit (3.7 nanograms per liter). The low ng/L range was not tested in the water spike studies (Section 4.1.3), thus the PFAS removal, PFAS recovery, and PFAS distribution among phases (aqueous, floc and foam) were less understood.

Table 11. PFAS concentrations in collected WAFB groundwater sample.

PFAS	PFHxA	PFHpA	PFOA	PFNA	PFBS	PFHxS	PFOS	4:2 FTS*	6:2 FTS	8:2 FTS
Concentration (ng/L)	642.15	190.41	1744.90	22.30	33.32	2367.79	8162.70	< 3.7	963.38	291.74

* Below detection limit

4.4.1 EC Treatment Using Low Current Density

The groundwater sample was treated in the EC reactor at the current density of 0.3 mA cm^{-2} for 120 min, and the results are shown in **Figure 23**. The concentrations of all PFAS in the aqueous phase decreased after a 120-min EC treatment. The removal of PFOS and PFOA was greater than other PFAS. The PFAS removal efficiency generally followed the chain length of the PFAS with better removal for the longer-chain PFAS.

A subsequent experiment was performed to examine the PFAS mass distribution to the zinc hydroxide flocs. At the completion of the EC treatment, the entire solution including flocs was collected and then filtered through a 0.22-μm acetate membrane (Sartorius, Germany). After the zinc hydroxide flocs were collected, 10 mL of 4.0-M H_2SO_4 solution was added to dissolve the EC flocs. PFAS concentrations in the acid solution were measured, accounting for the PFAS mass on the flocs. The PFAS mass distribution in different phases for all 10 PFAS are presented in **Figure 24** and **Table 12**. Comparing to the spiked water systems, the PFAS mass distribution was generally consistent except that PFNA had lower sorption on the floc in the groundwater sample, and PFBS, on the other hand, had higher sorption on floc in the groundwater sample than the spiked water sample. PFNA and PFBS were two compounds with low detection levels and were not in the range of concentrations for the EC studies in the spiked water systems.

The mass recoveries of all PFAS were all around 100% except PFOA. **Appendix A** includes the QA/QC data. The QA/QC data generally meet the requirements except PFBS in floc has an ISR% of 48.39%, lower than 50%. RPD% data were not available for PFAS in floc, because all collected floc was treated as one sample during the sample analysis. The relatively low recovery of PFOA (60%) in the groundwater sample was not seen in the spiked water sample (93%) (**Table 9** and **Figure 17).**

Table 12. PFAS Mass Distribution (%) of 9 PFAS after EC treatment for 120 min (current density = 0.3 mA cm^{-2}, 20 mM Na_2SO_4).

PFAS	PFAS Removal (%)	Aqueous Phase (%)	Flocs (%)	Total Recovery (%)
PFNA	1.28	98.72	39.33	138.05
PFOA	62.91	37.09	22.77	60
PFHpA	3.25	96.75	18.59	115.3
PFHxA	5.95	94.05	6.66	100.72
PFOS	99.12	0.88	109.76	110.64
PFHxS	22.38	77.62	27.79	105.41
PFBS	74.96	25.04	88.33	113.37
8:2 FtS	84.46	15.54	101.91	117.46
6:2 FtS	46.73	53.27	75.15	128.42

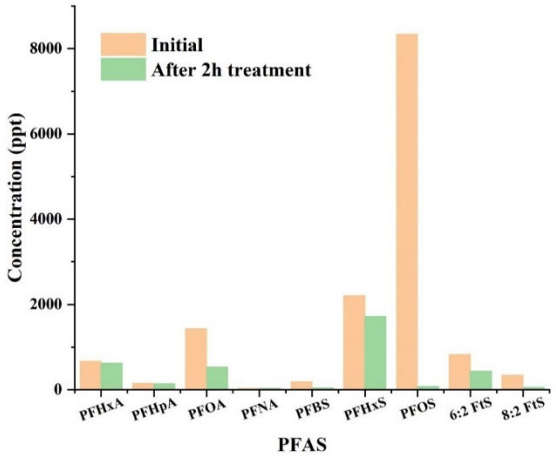

Figure 23. EC treatment of PFAS in WAFB groundwater using current density of 0.3 mA cm^{-2} and 20 mM Na_2SO_4 for 120 min.

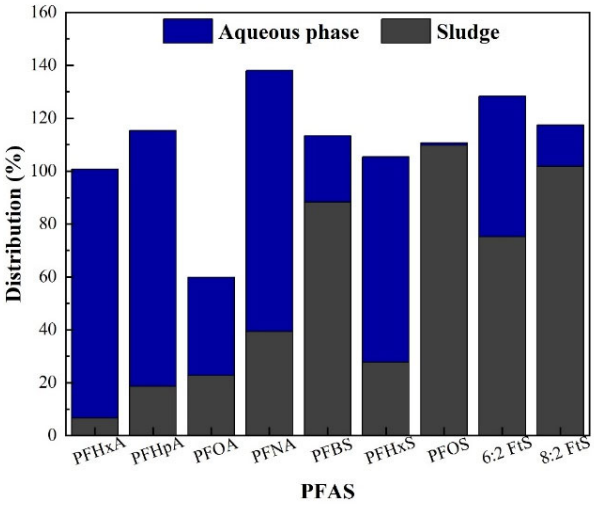

Figure 24. The distribution of 10 PFAS in different phases after EC treatment for 120 min (current density = 0.3 mA cm^{-2}, 20 mM Na_2SO_4).

4.4.2 EC Treatment Using High Current Density

Figure 25 presents the groundwater sample treated with high current density 5 mA cm^{-2} for 60 min. The concentrations of all PFAS in the aqueous phase decreased during the EC treatment except PFBS. The removal efficiencies were significantly greater than the EC treatment using a low current density (**Table 13**). Due to the lower PFAS concentrations in the groundwater sample, there was no foam generated through EC even when the high current density was applied.

PFAS mass distribution to the zinc hydroxide flocs was also evaluated. At the completion of the EC treatment, the entire solution, including flocs, was collected and then filtered through a 0.22-µm acetate membrane (Sartorius, Germany). After the zinc hydroxide flocs were collected, 10 mL of 4.0-M H_2SO_4 solution was added to dissolve the EC flocs. The PFAS concentrations in the acid solution were measured, accounting for the PFAS mass on the flocs. The PFAS mass distribution in different phases for all 10 PFAS are presented in **Figure 26** and **Table 14**. The study shows mass recovery lower than 70% for most PFAS except PFHxA, PFNA, and PFBS. Such data are significantly different when low current density was applied. The total PFBS mass recovery was greater than 300%. Such high mass recovery can be due to the challenges of recovering PFBS at very low concentrations and can also be due to generation of PFBS through oxidation/degradation under a higher current density condition.

Appendix A includes the QA/QC data. The QA/QC data generally meet the requirements except that PFBS in sludge has an ISR% of 45.17% and PFOS in sludge has an ISR% of 39.2%, lower than 50%. The RPD% data were not available for PFAS in sludge samples, because all collected sludge was treated as one sample. The PFAS recovery varied in a larger range than shown in **Figure 25** for low current density. This may reflect the variability associated with the experiments at high current density (with more flocs generated) and low PFAS concentrations, and it may also suggest that some PFAS may have been degraded at the higher current density conditions.

Table 13. Comparing PFAS removal in aqueous phase (%)* using 0.3 mA/cm^2 for 120 min or 5 mA/cm^2 for 60 min.

PFAS	Low Current Density (0.3 mA/cm^2), %	High Current Density (5 mA/cm^2), %
PFNA	1.28	96.7
PFOA	62.91	94.74
PFHpA	3.25	70.08
PFHxA	5.95	18.02
PFOS	99.12	97.81
PFHxS	22.38	92.01
PFBS	74.96	-33.64
8:2 FtS	84.46	98.79
6:2 FtS	46.73	97.14

* Calculated by 1 minus the ratio between the PFAS concentration after and before EC treatment.

Table 14. PFAS Mass Distribution (%) of 9 PFAS after EC treatment for 60 min (current density = 5 mA cm^{-2}, 20 mM Na_2SO_4).

PFAS	Aqueous Phase (%)	Flocs (%)	Total Mass Recovery (%)
PFHxA	81.98	46.95	128.93
PFHpA	29.92	36.65	66.57
PFOA	5.26	66.23	71.49
PFNA	3.30	125.78	129.08
PFBS	133.64	244.11	377.75
PFHxS	7.99	11.69	19.68
PFOS	2.19	50.10	52.29
6:2 FtS	2.86	18.00	20.86
8:2 FtS	1.21	53.45	54.66

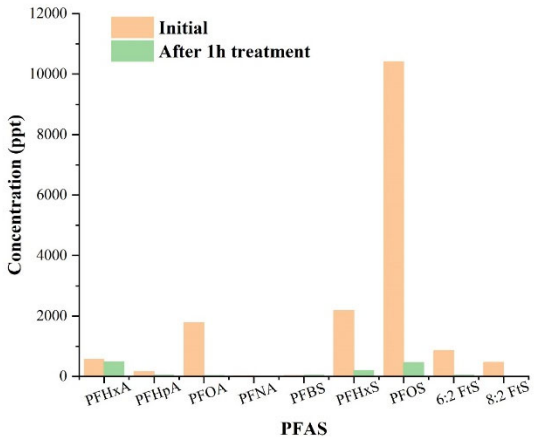

Figure 25. Removal of 9 PFAS in groundwater after EC treatment for 60 min (current density = 5 mA cm^{-2}, 20 mM Na_2SO_4).

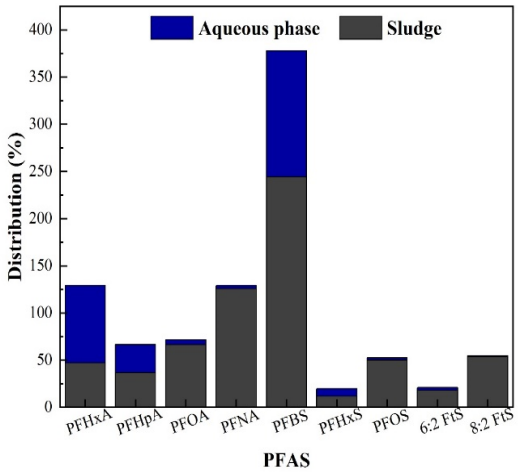

Figure 26. The distribution of 9 PFAS from different phases after EC treatment for 60 min (current density = 5 mA cm^{-2}, 20 mM Na_2SO_4).

4.5 Performance Evaluation

The performance evaluation criteria for each individual objective of this project are provided in **Table 15**.

1. Remove PFAS and co-contaminants by EC

Co-contaminants were not tested in this project. For PFAS, the performance criteria were mostly achieved, particularly for longer-chain PFAS. The EC treatment efficiency was evaluated in a spiked water system. Low and high concentrations and low and high current density were tested. The test results show that removal rate for PFOS in PFOS-spiked water could be as high as 100%. In the PFAS compounds mixture system, the removal rates for most long-chain PFAS compounds (carbon number 6-10), such as PFNA, PFOA, PFOS, PFHxS, 8:2 FtS, 6:2 FtS, and FOSA, were above 90%. Long-chain PFAS compounds tend to have a higher removal rate than short-chain PFAS compounds. Removal rate increases as the current density increases.

2. Dissolve PFAS-floc using small volume of acid

The performance criteria were achieved. The floc could be completely dissolved by a small amount of H_2SO_4. The PFAS mass distribution was determined for the flocs and foam when foam was produced.

3. Re-precipitate zinc without removing PFAS

Zinc precipitation test results show that Zn precipitation increased as more Na2S or Na2CO3 was added, and almost 100% of Zn^{2+} was precipitated when sufficient salts had been added; however, whether PFAS would adsorb on zinc precipitates was not tested. It was anticipated as highly possible to have PFAS adsorbed on precipitate when precipitate is formed. Based on this concern, the project team tested PFAS destruction using EO before the zinc precipitation step.

4. Remove PFAS from groundwater by EC

Under a low current density (0.3 mA/cm^2), the removal rate for PFOS in the groundwater system was above 99%. Removal rates increased as current density increased. Under high current density (5 mA/cm^2), the removal rate for PFOA, PFNA, PFHxS, PFOS, 6:2 FtS, and 8:2 FtS were all above 90%. The removal rate for PFHpA was also above 70%. The only two compounds with poor removal rates were PFHxA and PFBS.

Table 15. Project performance evaluation.

Performance Objectives	Performance Measurements	Performance Criteria	Achieved?
Remove PFAS and co-contaminants by EC	PFAS concentration in initial and final solution Note: Co-contaminant treatment efficiency was not performed	> 90% removal of measurable PFAS	Mostly achieved for long-chain PFAS.
Dissolve PFAS-floc using small volume of acid	PFAS and zinc concentrations in dissolved solution	Complete dissolve zinc floc and ~ 100% recovery of adsorbed PFAS	Achieved.
Re-precipitate zinc without removing PFAS	PFAS concentration before and after re-precipitation Zinc mass balance	< 5% PFAS adsorption on solids > 90% zinc re-precipitation	Partially achieved. <5% PFAS adsorption on zinc precipitates was not examined.
Remove PFAS from groundwater by EC	PFAS concentration in groundwater before and after EC treatment Zinc recovery rate	> 90% removal of measurable PFAS >90% zinc recovery	Mostly achieved for long-chain PFAS.

5. APPLICATIONS FOR FUTURE RESEARCH/IMPLEMENTATION

5.1 Conclusions

The following key points are concluded from the results of Task 1 and preliminary Task 2 tests:

1. The EC experiments were conducted for DI water spiked with individual or combined PFAS compounds (up to 11 compounds) at varying initial concentrations (0.005 to 0.5 μM) and for groundwater collected at WAFB. Varying current densities (0.3 to 5.0 mA cm^{-2}) for different reaction times were applied to generate zinc hydroxide flocs. An acid dissolution method was used for releasing PFAS from the zinc hydroxide flocs back into solution phase to concentrate the PFAS.

2. After adjusting two parameters (current density and reaction time), the removal rates for most long-chain PFAS compounds (carbon number 6-10), such as PFNA, PFOA, PFOS, PFHxS, 8:2 FtS, 6:2 FtS, and FOSA, were above 90%. Long-chain PFAS compounds tend to have a higher removal rate than short-chain PFAS compounds. Removal rates increase as the current density increases.

3. PFAS removal efficiency follows the order of FOSA≈ 8:2 FTS≈PFNA > PFOS > PFOA > 6:2 FTS > PFHxS > PFHpA > PFHxA ≈ PFBS. The effective removal of long-chain PFAS indicate that hydrophobic interaction between PFAS and flocs is critical. The competing effect between PFAS compounds is observed when the floc-generated surface area is limited.

4. EC could effectively remove PFAS compounds from the WAFB groundwater. Under a low current density (0.3 mA/cm^2), the removal rate for PFOS in the groundwater system was above 99%. Removal rates increased as current densities increased. Under a high current density (5 mA/cm^2), the removal for PFOA, PFNA, PFHxS, PFOS, 6:2 FtS, and 8:2 FtS were above 90%. Removal for PFHpA was also above 70%. The only two compounds with poor removal were PFHxA and PFBS.

5. EC-derived foam was generated when a relatively high current density (> 1 mA/cm^2) was applied to a relatively high PFAS concentration (> 0.1 μM) during EC. When low PFAS concentration solutions were treated by EC, no foam appeared to be formed, regardless of a low or high current density being applied.

6. It is anticipated that long-chain PFAS can fractionate into foams, particularly under high PFAS concentration conditions; however, foam fractionation decreased as PFAS carbon chain length got shorter. The poor removal efficiency for shorter-chain PFAS can also be explained by flocs generated. The amount of flocs generated at low current density may not provide enough surface area for physical adsorption of PFAS for high concentrations of PFAS.

7. Significant amounts of removed PFAS were fractionated into foam at EC treatment conditions facilitating foam formation, especially for FOSA, PFNA, PFOA, and PFOS, which have higher PFAS removal efficiency from the aqueous phase. High distribution of PFAS into foam was

not originally expected. Fractionation of long-chain PFAS into foam is apparently governing long-chain PFAS distribution.

8. As current density decreases, the amount of foam formed decreases, too. The less formation of foam may have encouraged more PFAS to interact with the floc phase, particularly for PFNA, PFOA, PFHpA, PFHxA, PFOS, 8:2 FTS, 6:2 FTS, and 4:2 FTS.

9. It should be noted though foam formation was not observed when the PFAS concentration was relatively low (< 0.1 μM), no matter if a high or low current density was applied. Therefore, the foam formation will only be regarded as applicable to high PFAS-concentration wastes, such as ion exchange resin (IXR) regenerants, reverse osmosis retentates.

10. The floc could be completely dissolved by a small amount of H_2SO_4, and the recovery rate was about 100%. A mass distribution was also determined for the floc – foam system when foam is produced under a high current density, and the recovery rates of individual PFAS ranged from 85% to 100%.

11. When removing the floc from the system using a centrifuge, the high force of the centrifugation (15,000 rpm) can desorb PFOS from flocs into supernatant, thus it's not appropriate for preparing samples to track PFAS removal in the aqueous phase. Centrifugation below 7,500 rpm did not result in apparent PFAS releases from the flocs.

12. Isotherm – Like Adsorption study: The adsorption capacity of the 10 PFAS followed the order PFOS > PFNA > 8:2 FtS > PFOA > PFHxS > 6:2 FtS > PFHpA > PFHxA > PFBS. It is in line with the order of the carbon chain length for each category, while for similar carbon chain length, PFSAs > FTSAs > PFCAs. PFAS with a longer carbon chain length tend to be more hydrophobic. This result may indicate that hydrophobic interaction plays a key role on the sorption capacity of PFAS on the zinc hydroxide flocs, while charge interaction may also influence as sulfonate head groups tend to have higher charge density than carboxylates in PFAS. The sorption affinity of the 10 PFAS followed the order PFHxS > PFOS > PFNA > PFOA > 6:2 FtS > PFHpA > 8:2 FtS > 4:2 FtS > PFHxA > PFBS. It seems that the bulkier molecules may be penalized in terms of sorption affinity, while charge interactions play a key role in the intensity of the sorption interactions.

13. Zinc removal by precipitation: It was found that Zn^{2+} precipitation increased as more Na_2S or Na_2CO_3 was added, and almost all Zn^{2+} was precipitated when sufficient salts had been added.

14. Preliminary EO test: PFAS in all three EC-derived solutions were removed efficiently during EO. Except for PFBS, PFHxA, and 4:2 FtS, the concentrations of all other PFAS were removed nearly completely. The test result indicates that zinc ions do not have to be removed before the EO step; they can be removed after the EO step if still remaining in the solution. The presence of zinc and sulfate ions could replace the supplement of electrolytes.

15. The major QA/QC indicators, including RPD and ISR, are generally in an acceptable range for EC tests performed using either spiked solution or groundwater samples, especially after an improved recovery approach was applied. The ISR values of PFOS and PFBS were slightly lower than the QA/QC criteria at 50%, which was likely due to PFAS interactions with other surfaces (such as filter, apparatus of EC reactor).

5.2 Implications for Future Research

This project involves a series of bench tests that demonstrated the feasibility of using electrocoagulation technology to effectively remove and concentrate PFAS from groundwater into a small volume of waste stream, which can be further managed using a destructive PFAS treatment technology such as electrochemical oxidation. Preliminary bench tests completed during this project showed the promise of coupling both electrocoagulation with electrochemical oxidation technologies to achieve PFAS sequestration and destruction on site, therefore avoiding off-site disposal or treatment of PFAS-laden wastes. Future research efforts should focus on streamlining the coupling strategies to combine the individual unit operations into a sequential treatment train and evaluating its performance. Specifically, the operation and treatment performance may be firstly collected from each process and evaluated individually and in series using water samples spiked with PFAS. Then site groundwater should be evaluated to help select treatment conditions with a focus on technology implementability and scale-up feasibility.

The next step of developing this treatment train will be constructing a larger scale continuous-flow EC-EO treatment unit. The larger scale electrocoagulation cell may be comprised of several zinc plate anodes and stainless-steel plate cathodes. The EO unit will be comprised of a flow-through reactor with multiple Ti_4O_7 plate anodes that are arranged in parallel with stainless-steel cathodes. The effects of the operation parameters, including applied current density, PFAS concentrations, and flow rate, on PFAS degradation should be systematically investigated in this phase, and thus the performance-condition relationships will be established to guide pilot-scale demonstrations.

To advance to larger scale reactor tests, it is crucial to build a pilot-scale EC/EO treatment train and demonstrate it in the field to test the scale-up effects and further evaluate the application potential. In the field pilot demonstration phase, the concentrations of PFAS, co-contaminants, TOC, and inorganic ions should be monitored over time to evaluate the impacts of background water quality. Based on the field demonstration results, the energy consumption of the entire treatment train can also be analyzed in relation to the operation conditions. The optimized conditions will be determined based on considerations of performance-condition relationships and the energy consumption to achieve the best cost-effectiveness. Field pilot demonstration provides the correlation between PFAS degradation efficiency and energy consumption in relation to system scales, which will further guide the process design and scale-up optimization of the technology.

6. LITERATURE CITED

Ahrens, L., Bundschuh, M., 2014. Fate and effects of poly- and perfluoroalkyl substances in the aquatic environment: a review. Environ. Toxicol. Chem. 33, 1921-1929.

An, Y.J., Carraway, E.R. and Schlautman, M.A., 2002. Solubilization of polycyclic aromatic hydrocarbons by perfluorinated surfactant micelles. Water research, 36(1), pp.300-308.

Anderko, L. and Pennea, E., 2020. Exposures to per-and polyfluoroalkyl substances (PFAS): Potential risks to reproductive and children's health. Current problems in pediatric and adolescent health care, 50(2), p.100760.

Andersen, M., Butenhoff, J., Chang, S., Farrar, D., Kennedy, G., Lau, C., Olsen, G., Seed, J., Wallace, K., 2008. Perfluoroalkyl acids and related chemistries-toxicokinetics and modes of action. Toxicol. Sci. 102, 3-14.

Arvaniti, O., Stasinakis, A., 2015. Review on the occurrence, fate and removal of perfluorinated compounds during wastewater treatment. Sci. Total Environ. 524, 81-92.

Bentel, M., Yu Y., Xu, L., Li, Z., Wong, B., Men, Y., Liu, J., 2019. Defluorination of per- and polyfluoroalkyl substances (PFAS) with hydrated electrons: Structural dependence and implications to PFAS remediation and management. Environ. Sci. Technol. 53, 3718-3728.

Buck, R., Franklin, J., Berger, U., CondeCousins, J., Voogt, P., Jensen, A., Kannan, K., Mabury, S., Leeuwen, S., 2011. Perfluoroalkyl and polyfluoralkyl substances (PFAS) in the environment: terminology, classification, and origins. Integr. Environ. Assess. Manage. 7, 513.

Carter, K., Farrell, J., 2008. Oxidative destruction of perfluorooctane sulfonate using boron-doped diamond film electrodes. Environ. Sci. Technol. 42, 6111-6115.

Cheng, J., Vecitis, C., Park, H., Mader, B., Hoffmann, M., 2008. Sonochemical degradation of perfluorooctane sulfonate (PFOS) and perfluorooctanoate (PFOA) in landfill groundwater: environmental matrix effects. Environ. Sci. Technol. 42, 8057-8063.

Conder, J., Hoke, R., De Wolf, W., Russell, M., Buck, R., 2008. Are PFCAs bioaccumulative? A critical review and comparison with regulatory criteria and persistent lipophilic compounds. Environ. Sci. Technol. 42, 995-1003.

Corsini, E., Sangiovanni, E., Avogadro, A., Galbiati, V., Viviani, B., Marinovich, M., Galli, C., Dellagli, M., Germolec, D., 2012. In vitro characterization of the immunotoxic potential of several perfluorinated compounds (PFCs). Toxicol. Appl. Pharmacol. 258, 248-255.

Davis, K., Aucoin, M., Larsen, B., Kaiser, M., Hartten, A., 2007. Transport of ammonium perfluorooctanoate in environmental media near a fluoropolymer manufacturing facility. Chemosphere 67, 2011-2019.

Du, Z., Deng, S., Bei, Y., Huang, Q., Wang, B., Huang, J., Yu, G., 2014. Adsorption behavior and mechanism of perfluorinated compounds on various adsorbents--a review. J. Hazard. Mater. 274, 443-454.

Ebersbach, I., Ludwig, S., Constapel, M., Kling, H., 2016. An alternative treatment method for fluorosurfactant-containing wastewater by aerosol-mediated separation. Water Res. 101, 333-340.

Ehresman, D.J., Froehlich, J.W., Olsen, G.W., Chang, S.C. and Butenhoff, J.L., 2007. Comparison of human whole blood, plasma, and serum matrices for the determination of perfluorooctanesulfonate (PFOS), perfluorooctanoate (PFOA), and other fluorochemicals. Environmental research, 103(2), pp.176-184.

Ganiyu, S. O.; Oturan, N.; Raffy, S.; Cretin, M.; Esmilaire, R.; van Hullebusch, E.; Esposito, G.; Oturan, M. A., Sub-stoichiometric titanium oxide (Ti_4O_7) as a suitable ceramic anode for electrooxidation of organic pollutants: a case study of kinetics, mineralization and toxicity assessment of amoxicillin[J]. Water Research, 2016, 106: 171-182.

Garcia-Costa AL, Savall A, Zazo JA, Casas JA, Serrano KG., 2020. On the role of the cathode for the electro-oxidation of perfluorooctanoic acid. Catalysts, 10, 902.

Garcia-Segura, S., Ocon, J.D. and Chong, M.N., 2018. Electrochemical oxidation remediation of real wastewater effluents—a review. Process Safety and Environmental Protection, 113, pp.48-67.

Geng, P.; Su, J.; Miles, C.; Comninellis, C.; Chen, G., Highly-Ordered Magnéli Ti4O7 Nanotube Arrays as Effective Anodic Material for Electro-oxidation[J]. Electrochimica Acta, 2015, 153: 316-324.

Ghisi, R., Vamerali, T., Manzetti, S., 2019. Accumulation of perfluorinated alkyl substances (PFAS) in agricultural plants: A review. Environ. Res. 169, 326-341.

Gomez-Ruiz, B., Gómez-Lavín, S., Diban, N., Boiteux, V., Colin, A., Dauchy, X., Urtiaga, A., 2017. Efficient electrochemical degradation of poly- and perfluoroalkyl substances (PFASs) from the effluents of an industrial wastewater treatment plant. Chem. Eng. J. 322, 196-204.

Gomis, M., Vestergren, R., Borg, D., Cousins, I., 2018. Comparing the toxic potency in vivo of long-chain perfluoroalkyl acids and fluorinated alternatives. Environ. Int. 113, 1-9.

Gonzalez, D., Thompson, K., Quinones, O., Dickenson, E., Bott, C., 2021. Assessment of PFAS fate, transport, and treatment inhibition associated with a simulated AFFF release within a wastewater treatment plant. Chemosphere 262, 127900.

Guelfo, J., Adamson, D., 2018. Evaluation of a national data set for insights into sources, composition, and concentrations of per- and polyfluoroalkyl substances (PFAS) in U.S. drinking water. Environ. Pollut. 236, 505-513.

Hudlicky, M., 1979. Hydrogenolysis of carbon-fluorine bonds in catalytic hydrogenation. J. Fluorine Chem. 14, 189-199.

Hussin, F., Abnisa, F., Issabayeva, G. and Aroua, M.K., 2017. Removal of lead by solar-photovoltaic electrocoagulation using novel perforated zinc electrode. Journal of cleaner production, 147, pp.206-216.

Javed, H., Lyu, C., Sun, R., Zhang, D. and Alvarez, P.J., 2020. Discerning the inefficacy of hydroxyl radicals during perfluorooctanoic acid degradation. Chemosphere, 247, p.125883.

Keech, P. G., and N. J. Bunce. "Electrochemical oxidation of simple indoles at a PbO2 anode." Journal of applied electrochemistry 33.1 (2003): 79-83.

Kissa, E., 2001. Fluorinated surfactants and repellents. Text. Res. J. 71, 750c-750c.

Kreysa, G.; Ota, K.-i.; Savinell, R. F., Pollutants in water-electrochemical remediation using ebonex electrodes[J]. Encyclopedia of applied electrochemistry, 2014: 1629-1633.

Krusic, P., Roe, D., 2004. Gas-phase NMR technique for studying the thermolysis of materials: thermal decomposition of ammonium perfluorooctanoate. Anal. Chem. 76, 3800-3803.

Lampert, D., Frisch, M., Speitel, G., 2007. Removal of perfluorooctanoic acid and perfluorooctane sulfonate from wastewater by ion exchange. Practice Periodical of Hazardous, Toxic, and Radioactive Waste Management 11, 60-68.

Le, T. X. H., Haflich, H., Shah, A. D., Chaplin, B. P., 2019. Energy- efficient electrochemical oxidation of perfluoroalkyl substances using a Ti_4O_7 reactive electrochemical membrane anode. Environ. Sci. Technol. Lett. 6 (8), 504−510.

Li, Xiaoyun, et al. "Efficient photocatalytic decomposition of perfluorooctanoic acid by indium oxide and its mechanism." Environmental science & technology 46.10 (2012): 5528-5534.

Liang, S., Lin, H., Yan, X., Huang, Q., 2018. Electro-oxidation of tetracycline by a magnéli phase Ti_4O_7 porous anode: kinetics, products, and toxicity. Chem. Eng. J. 332, 628-636.

Lin, H., Niu, J., Ding, S., Zhang, L., 2012. Electrochemical degradation of perfluorooctanoic acid (PFOA) by Ti/SnO_2-Sb, Ti/SnO_2-Sb/PbO_2 and Ti/SnO_2-Sb/MnO_2 anodes. Water Res. 46, 2281-2289.

Lin, H., Niu, J., Liang, S., Wang, C., Wang, Y., Jin, F., Luo, Q., Huang, Q., 2018. Development of macroporous magnéli phase Ti_4O_7 ceramic materials: As an efficient anode for mineralization of poly- and perfluoroalkyl substances. Chem. Eng. J. 354, 1058-1067.

Lin, H., Wang, Y., Niu, J., Yue, Z., Huang, Q., 2015. Efficient sorption and removal of perfluoroalkyl acids (PFAAs) from aqueous solution by metal hydroxides generated in situ by electrocoagulation. Environ. Sci. Technol. 49, 10562-10569.

Liu, J., Avendano, S., 2013. Microbial degradation of polyfluoroalkyl chemicals in the environment: A review. Environ. Int. 61, 98-114.

Liu, G., Zhou, H., Teng, J., You S., 2019. Electrochemical degradation of perfluorooctanoic acid by macro-porous titanium suboxide anode in the presence of sulfate. Chem. Eng. J. 371, 7-14.

Luo, Q., Yan, X., Lu, J., Huang, Q., 2018. Perfluorooctanesulfonate degrades in a laccase-mediator system. Environ. Sci. Technol. 52, 10617–10626.

Lutze, Holger, et al. "Treatment options for the removal and degradation of polyfluorinated chemicals." Polyfluorinated Chemicals and Transformation Products. Springer Berlin Heidelberg, 2012. 103-125.

Martinezhuitle, C., Rodrigo, M., Sires, I., Scialdone, O., 2015. Single and coupled electrochemical processes and reactors for the abatement of organic water pollutants: A critical review. Chem. Rev. 115, 13362-13407.

Meng, P., Deng, S., Maimaiti, A., Wang, B., Huang, J., Wang, Y., Cousins, I., Yu, G., 2018. Efficient removal of perfluorooctane sulfonate from aqueous film-forming foam solution by aeration-foam collection. Chemosphere 203, 263-270.

Mollah, M., Morkovsky, P., Gomes, J., Kesmez, M., Parga, J., Cocke, D., 2004. Fundamentals, present and future perspectives of electrocoagulation. J. Hazard. Mater. 114, 199-210.

Moriwaki, H., Takagi, Y., Tanaka, M., Tsuruho, K., Okitsu, K., Maeda, Y., 2005. Sonochemical decomposition of perfluorooctane sulfonate and perfluorooctanoic acid. Environ. Sci. Technol. 39, 3388-3392.

Moussa, D.T., El-Naas, M.H., Nasser, M. and Al-Marri, M.J., 2017. A comprehensive review of electrocoagulation for water treatment: Potentials and challenges. Journal of environmental management, 186, pp.24-41.

Niu, J., Li, Y., Shang, E., Xu, Z., Liu, J., 2016. Electrochemical oxidation of perfluorinated compounds in water. Chemosphere 146, 526-538.

Niu, J., Lin, H., Xu, J., Wu, H., Li, Y., 2012. Electrochemical mineralization of perfluorocarboxylic acids (PFCAs) by Ce-doped modified porous nanocrystalline PbO_2 film electrode. Environ. Sci. Technol. 46, 10191.

Paul, A., Jones, K., Sweetman, A., 2009. A first global production, emission, and environmental inventory for perfluorooctane sulfonate. Environ. Sci. Technol. 43, 386-392.

Pistocchi, A., Loos, R., 2009. A map of European emissions and concentrations of PFOS and PFOA. Environ. Sci. Technol. 43, 9237-9244.

Radjenovic, J., Sedlak, D., 2015. Challenges and opportunities for electrochemical processes as next-generation technologies for the treatment of contaminated water. Environ. Sci. Technol. 49, 11292-11302.

Safwat, S.M., 2020. Treatment of real printing wastewater using electrocoagulation process with titanium and zinc electrodes. Journal of Water Process Engineering, 34, p.101137.

Rahman, M., Peldszus, S., Anderson, W., 2014. Behaviour and fate of perfluoroalkyl and polyfluoroalkyl substances (PFAS) in drinking water treatment: A review. Water Res. 50, 318-340.

Shi, H., Wang, Y., Li, C., Pierce, R., Gao, S., Huang, Q., 2019. Degradation of perfluorooctanesulfonate by reactive electrochemical membrane composed of magnéli phase titanium suboxide. Environ. Sci. Technol. 53, 14528-14537.

Shu, Y., Zheng, N., Zheng, A., Guo, T., Yu, Y., Wang, J., 2019. Intracellular zinc quantification by fluorescence imaging with a FRET System. Anal. Chem. 91, 4157-4163.

Singh, R., Fernando, S., Baygi, S., Multari, N., Thagard, S., Holsen, T., 2019. Breakdown products from perfluorinated alkyl substances (PFAS) degradation in a plasma-based water treatment process. Environ. Sci. Technol. 53, 2731-2738.

Soriano, Á., Gorri, D., Biegler, L., Urtiaga, A., 2019. An optimization model for the treatment of perfluorocarboxylic acids considering membrane preconcentration and BDD electrooxidation. Water Res. 164, 114954.

Sun, Z., Zhang, C., Chen, P., Zhou, Q., Hoffmann, M., 2017. Impact of humic acid on the photoreductive degradation of perfluorooctane sulfonate (PFOS) by UV/Iodide process. Water Res. 127, 50-58.

Torres, F., Ochoaherrera, V., Blowers, P., Sierraalvarez, R., 2009. Ab initio study of the structural, electronic, and thermodynamic properties of linear perfluorooctane sulfonate (PFOS) and its branched isomers. Chemosphere 76, 1143-1149.

Trellu, C., Chaplin, B., Coetsier, C., Esmilaire, R., Cerneaux, S., Causserand, C., Cretin, M., 2018. Electro-oxidation of organic pollutants by reactive electrochemical membranes. Chemosphere 208, 159-175.

USEPA, 2016. Drinking Water Health Advisory for Perfluorooctanoic Acid (PFOA). EPA 822R16005, Environmental Protection Agency, Washington, DC, U.S.

USEPA, 2019. EPA's per- and polyfluoroalkyl substances (PFAS) action plan, Washington, DC.

USEPA, 2020. Per- and Polyfluoroalkyl Substances (PFAS): Incineration to Manage PFAS Waste Streams Technical BRIEF: Innovative Research for a Sustainable Future.

Vecitis, C., Park, H., Cheng, J., Mader, B., Hoffmann, M., 2009. Treatment technologies for aqueous perfluorooctanesulfonate (PFOS) and perfluorooctanoate (PFOA). Front. Environ. Sci. Eng. China 3, 129-151.

Walsh, F., Wills, R., 2010. The continuing development of Magnéli phase titanium sub-oxides and Ebonex electrodes. Electrochim. Acta 55, 6342-6351.

Wang, L., Lu, J., Li, L., Wang, Y., Huang, Q., 2020. Effects of chloride on electrochemical degradation of perfluorooctanesulfonate by magnéli phase Ti_4O_7 and boron doped diamond anodes. Water Res. 170, 115254.

Wang, Y., Lin, H., Jin, F., Niu, J., Zhao, J., Bi, Y., Li, Y., 2016. Electrocoagulation mechanism of perfluorooctanoate (PFOA) on a zinc anode: Influence of cathodes and anions. Sci. Total Environ. 557, 542-550.

Wang, Y., Pierce, R., Shi, H., Li, C., Huang, Q., 2020. Electrochemical degradation of perfluoroalkyl acids by titanium suboxide anodes. Environ. Sci.: Water Res. Technol. 6, 144-152.

Xiao, X., Ulrich, B., Chen, B., Higgins, C., 2017. Sorption of poly- and perfluoroalkyl substances (PFAS) relevant to aqueous film-forming foam (AFFF)-impacted groundwater by biochars and activated carbon. Environ. Sci. Technol. 51, 6342-6351.

Yang, B., Han, Y., Yu, G., Zhuo, Q., Deng, S., Wu, J., Zhang, P., 2016. Efficient removal of perfluoroalkyl acids (PFAAs) from aqueous solution by electrocoagulation using iron electrode. Chem. Eng. J. 303, 384-390.

Yang, B., Wang, J., Jiang, C., Li, J., Yu, G., Deng, S., Lu, S., Zhang, P., Zhu, C., Zhuo, Q., 2017. Electrochemical mineralization of perfluorooctane sulfonate by novel F and Sb co-doped Ti/SnO2 electrode containing Sn-Sb interlayer. Chem. Eng. J. 316, 296-304.

Yasuoka, K., Sasaki, K., Hayashi, R., 2011. An energy-efficient process for decomposing perfluorooctanoic and perfluorooctane sulfonic acids using dc plasmas generated within gas bubbles. Plasma Sources Sci. Technol. 20, 034009.

Zaky, A. M.; Chaplin, B. P., Mechanism of p-substituted phenol oxidation at a Ti4O7 reactive electrochemical membrane[J]. Environmental Science and Technology, 2014, 48 (10): 5857-5867.

Zhang, D., Zhang, W., Liang, Y., 2019. Adsorption of perfluoroalkyl and polyfluoroalkyl substances (PFAS) from aqueous solution - A review. Sci. Total Environ. 694, 133606.

Zhang, K., Huang, J., Yu, G., Zhang, Q., Deng, S., Wang, B., 2013. Destruction of perfluorooctane sulfonate (PFOS) and perfluorooctanoic acid (PFOA) by ball milling. Environ. Sci. Technol. 47, 6471-6477.

Zhi, J., Wang, H., Nakashima, T., Rao, T., Fujishima, A., 2003. Electrochemical incineration of organic pollutants on boron-doped diamond electrode. Evidence for direct electrochemical oxidation pathway. J. Phys. Chem. B. 107, 13389-13395.

Zhuo, Q., Deng, S., Yang, B., Huang, J., Wang, B., Zhang, T., Yu, G., 2012. Degradation of perfluorinated compounds on a boron-doped diamond electrode. Electrochim. Acta 77, 17-22.

7. APPENDICES

A. Supporting Information

Supporting data that are not provided in the *Results and Discussion* section above are included as Appendix A.

B. List of Scientific/Technical Publications

Peer-reviewed journal article

1. Shi, H., Chiang, S.Y.D., Wang, Y., Wang, Y., Liang, S., Zhou, J., Fontanez, R., Gao, S. and Huang, Q., 2021. An electrocoagulation and electrooxidation treatment train to remove and degrade per-and polyfluoroalkyl substances in aqueous solution. *Science of The Total Environment*, p.147723.

Platform presentations at conferences

1. Electrochemical-based Coagulation and Foam Fractionation for PFAS Treatment. International conference on remediation of chlorinated and recalcitrant compounds, May 31 – June 4, 2020, Portland, Oregon.
2. 2019 SERDP & ESTCP Symposium, December 3-5, 2019, Washington D.C.
3. An Electrocoagulation and Electrooxidation Treatment Train to Degrade Perfluoroalkyl Substances in Aqueous Solution, 258th ACS National meeting, San Diego, August 2019.

C. Other Supporting Materials

1. Standard Operation Procedure, Quantification of Per- and Poly-fluoroalkyl Acids, Huang Laboratory, University of Georgia.

Appendix A. Supporting Information

An Electrocoagulation and Electrooxidation Treatment Train to Degrade Perfluoroalkyl Substances and Other Persistent Organic Contaminants in Groundwater

Final Report

Project Number: SERDP ER18-C2-1278

Principal Investigator: Dora Chiang, Ph.D., P.E., Wood

Co-Performers: Qingguo Huang, Ph.D., University of Georgia; Jing Zhou, Ph.D., P.E., Shangtao Liang, Ph.D., AECOM

Table A1. Information on PFASs used in this study.

Analyte Name	Acronym	Chemical Formula	logKow[a]	Internal Standard		
				Analyte Name	Acronym	Chemical Formula
Perfluorononanoic acid	PFNA	$CF_3(CF_2)_7COOH$	5.48	Perfluoro-n-[$^{13}C_9$]nonanoic acid	M9PFNA	$^{13}C_9F_{17}O_2^-$
Perfluorooctanoic acid	PFOA	$CF_3(CF_2)_6COOH$	4.81	Perfluoro-n-[$^{13}C_8$]octanoic acid	M8PFOA	$^{13}C_8F_{15}O_2^-$
Perfluoroheptanoic acid	PFHpA	$CF_3(CF_2)_5COOH$	4.15	Perfluoro-n-[1,2,3,4-$^{13}C_4$]heptanoic acid	M4PFHpA	$^{13}C_4{}^{12}C_3F_{13}O_2^-$
Perfluorohexanoic acid	PFHxA	$CF_3(CF_2)_4COOH$	3.48	Perfluoro-n-[1,2,3,4,6-$^{13}C_5$]hexanoic acid	M5PFHxA	$^{13}C_5{}^{12}C_1F_{11}O_2^-$
Perfluorooctanesulfonic acid	PFOS	$CF_3(CF_2)_7SO_3H$	4.49	perfluoro-[$^{13}C_8$]octanesulfonate	M8PFOS	$^{13}C_8F_{17}SO_3^-$
Perfluorohexanesulfonic acid	PFHxS	$CF_3(CF_2)_5SO_3H$	3.16	Sodium perfluoro-1-[1,2,3-$^{13}C_3$]hexanesulfonate	M3PFHxS	$^{13}C_3{}^{12}C_3F_{13}SO_3^-$
Perfluorobutanesulfonic acid	PFBS	$CF_3(CF_2)_3SO_3H$	1.82	Sodium perfluoro-1-[2,3,4-$^{13}C_3$]	M3PFBS	$^{13}C_3{}^{12}C_1F_9SO_3^-$
Fluorotelomer sulfonic acid 8:2	8:2 FtS	$CF_3(CF_2)_7(CH_2)_2SO_3H$	NA	Sodium 1H,1H,2H,2H-perfluoro-1-[1,2-$^{13}C_2$]decanesulfonate	M2-8:2FtS	$^{13}C_2{}^{12}C_8H_4F_{17}SO_3^-$
Fluorotelomer sulfonic acid 6:2	6:2 FtS	$CF_3(CF_2)_5(CH_2)_2SO_3H$	NA	Sodium 1H,1H,2H,2H-perfluoro-1-[1,2-$^{13}C_2$]octanesulfonate	M2-6:2FtS	$^{13}C_2{}^{12}C_6H_4F_{13}SO_3^-$
Fluorotelomer sulfonic acid 4:2	4:2 FtS	$CF_3(CF_2)_3(CH_2)_2SO_3H$	NA	Sodium 1H,1H,2H,2H-perfluoro-1-[1,2-$^{13}C_2$]hexanesulfonate	M2-4:2FtS	$^{13}C_2{}^{12}C_4H_4F_9SO_3^-$

[a] Data provided by PubChem.

Appendix A. Quality Control Data

Major QC indicators for the data presented in this report are included in this appendix. The major QC indicators are presented in Table A2, and all QC data are compiled in the following tables. Non-conformance is shown in red font.

Table A2. Major QC indicators.

QC Indicators	Full Name	QC Criteria
RPD	Relative percent difference for duplicate	< 30%
ISR	Internal Standard Recovery	50-150%

Table A3. QC Data for **Figure 11**.

Sample	Chemical	Average Conc (µg/L)	RPD (%)	ISR (%)	Conformance
Foam	PFNA	452.05		104.3693	Y
	PFOA	260.86		105.4204	Y
	PFHpA	103.59		115.836	Y
	PFHxA	53.84		123.291	Y
	PFOS	448.53		124.7734	Y
	PFHxS	183.23		121.5516	Y
	PFBS	62.86		107.4139	Y
	8:2FtS	336.24		98.54097	Y
	6:2FtS	294.45		65.01116	Y
	4:2FtS	116.83		69.31174	Y
	FOSA	108.56		109.6894	Y
Aqueous phase	PFNA	2.66	2.91	65.84099	Y
	PFOA	0.75	23.88	76.19611	Y
	PFHpA	35.43	1.35	66.60302	Y
	PFHxA	81.67	0.99	48.86843	N
	PFOS	0.00	0.00	63.08244	Y
	PFHxS	13.12	6.37	69.96902	Y
	PFBS	106.15	5.18	46.91724	N
	8:2FtS	1.50	51.61	20.20202	N
	6:2FtS	0.47	0.00	28.90625	N
	4:2FtS	75.23	4.42	45.77598	N
	FOSA	0.31	52.34	25.82536	N
Sludge	PFNA	0.10		18.95	N
	PFOA	0.66		5.80	N
	PFHpA	0.67		5.58	N
	PFHxA	1.89		2.71	N
	PFOS	1.28		46.81	N
	PFHxS	12.97		14.31	N
	PFBS	42.89		4.10	N
	8:2FtS	1.05		29.18	N

Sample	Chemical	Average Conc (µg/L)	RPD (%)	ISR (%)	Conformance
	6:2FtS	20.74		16.97	N
	4:2FtS	50.81		12.96	N
	FOSA	0.17		45.60	N

Table A4. QC data for **Figure 12**.

Sample	Chemical	Average Conc (µg/L)	RPD (%)	ISR (%)	Conformance
0 min	PFNA	387.23	0.67	58.42	Y
	PFOA	280.28	18.58	48.63	N
	PFHpA	195.93	10.94	62.97	Y
	PFHxA	142.77	4.78	56.86	Y
	PFOS	249.99	1.28	63.52	Y
	PFHxS	214.08	8.72	64.64	Y
	PFBS	203.57	15.76	47.78	N
	8:2FtS	166.22	1.53	104.47	Y
	6:2FtS	136.95	4.37	59.80	Y
	4:2FtS	159.32	48.94	58.01	N
5 min	PFNA	48.82	9.01	126.31	Y
	PFOA	129.20	13.01	118.38	Y
	PFHpA	189.62	8.26	85.03	Y
	PFHxA	145.46	12.87	59.80	Y
	PFOS	15.58	10.90	99.84	Y
	PFHxS	161.58	6.88	102.01	Y
	PFBS	208.78	7.68	54.52	Y
	8:2FtS	3.38	38.33	252.09	Y
	6:2FtS	106.44	0.19	166.70	Y
	4:2FtS	123.82	17.08	90.33	Y
10 min	PFNA	9.62	4.72	119.71	Y
	PFOA	47.74	27.99	198.94	N
	PFHpA	168.00	2.33	95.50	Y
	PFHxA	146.71	3.54	72.57	Y
	PFOS	3.55	39.29	99.11	Y
	PFHxS	127.38	8.58	110.34	Y
	PFBS	197.90	7.15	61.66	Y
	8:2FtS	0.57	41.41	184.24	N
	6:2FtS	68.08	3.84	196.97	N
	4:2FtS	130.10	12.74	87.02	Y
20 min	PFNA	1.82	19.69	121.82	Y
	PFOA	19.52	18.49	118.87	Y
	PFHpA	149.26	8.59	68.60	Y
	PFHxA	145.81	1.84	61.27	Y

Sample	Chemical	Average Conc (µg/L)	RPD (%)	ISR (%)	Conformance
	PFOS	0.65	23.93	102.27	Y
	PFHxS	71.77	10.01	104.73	Y
	PFBS	159.65	23.39	63.04	Y
	8:2FtS	0.42	2.60	88.01	Y
	6:2FtS	15.33	44.66	103.36	N
	4:2FtS	87.51	34.20	93.65	N
30 min	PFNA	0.94	11.70	99.47	Y
	PFOA	15.77	28.47	62.87	Y
	PFHpA	129.77	2.23	66.51	Y
	PFHxA	149.45	6.91	59.06	Y
	PFOS	0.78	56.83	85.14	N
	PFHxS	55.66	2.13	86.92	Y
	PFBS	164.28	19.43	54.32	Y
	8:2FtS	0.22	16.20	56.21	Y
	6:2FtS	3.61	21.08	64.97	Y
	4:2FtS	91.28	5.94	63.81	Y
45 min	PFNA	0.32	66.88	86.62	N
	PFOA	5.52	6.28	67.79	Y
	PFHpA	100.83	5.30	68.04	Y
	PFHxA	143.61	0.94	56.03	Y
	PFOS	0.45	21.65	91.46	Y
	PFHxS	35.29	2.26	89.82	Y
	PFBS	166.74	6.70	51.94	Y
	8:2FtS	0.00	0.00	48.55	Y
	6:2FtS	1.51	8.56	75.90	Y
	4:2FtS	94.43	0.97	47.24	Y
60 min	PFNA	0.17	59.07	120.27	N
	PFOA	2.51	9.72	101.68	Y
	PFHpA	73.65	1.91	80.44	Y
	PFHxA	125.95	1.13	63.10	Y
	PFOS	0.40	34.79	92.31	N
	PFHxS	20.95	8.89	101.13	Y
	PFBS	170.51	6.72	54.32	Y
	8:2FtS	0.00	0.00	91.70	Y
	6:2FtS	3.03	33.33	95.24	N
	4:2FtS	91.46	2.59	67.13	Y

Table A5. QC data for **Figure 13**.

Sample	Chemical	Average Conc (µg/L)	RPD (%)	ISR (%)	Conformance
Foam	PFNA	3324.44	3.78	78.73	Y
	PFOA	3077.92	1.33	117.89	Y

Sample	Chemical	Average Conc (µg/L)	RPD (%)	ISR (%)	Conformance
	PFHpA	1157.50	1.69	89.22	Y
	PFHxA	215.30	6.01	98.47	Y
	PFOS	1653.80	6.09	122.78	Y
	PFHxS	1713.65	3.40	81.57	Y
	PFBS	591.32	33.47	182.79	N
	8:2FtS	1872.43	5.68	110.09	Y
	6:2FtS	1408.55	0.36	71.76	Y
	4:2FtS	728.25	0.26	58.01	Y
Aqueous phase	PFNA	0.17	59.07	120.27	N
	PFOA	2.51	9.72	101.68	Y
	PFHpA	73.65	1.91	80.44	Y
	PFHxA	125.95	1.13	63.10	Y
	PFOS	0.40	34.79	92.31	N
	PFHxS	20.95	8.89	101.13	Y
	PFBS	170.51	6.72	54.32	Y
	8:2FtS	0.00	0.00	91.70	Y
	6:2FtS	3.03	33.33	95.24	N
	4:2FtS	91.46	2.59	67.13	Y
Sludge	PFNA	592.85	19.20	45.14	N
	PFOA	503.11	26.57	73.33	Y
	PFHpA	292.82	11.01	65.43	Y
	PFHxA	0.00	0.00	62.48	Y
	PFOS	0.00	0.00	71.65	Y
	PFHxS	197.10	8.91	67.94	Y
	PFBS	0.00	0.00	70.63	Y
	8:2FtS	0.00	0.00	46.15	N
	6:2FtS	162.62	28.83	38.50	N
	4:2FtS	0.00	0.00	76.74	Y

Table A6. QC data for **Figure 15.**

Sample	Chemical	Average Conc (µg/L)	RPD (%)	ISR (%)	Conformance
Foam	PFNA	1268.58		78.68	Y
	PFOA	640.24		80.01	Y
	PFHpA	217.21		112.86	Y
	PFHxA	124.41		119.26	Y
	PFOS	1472.12		86.68	Y
	PFHxS	400.63		119.91	Y
	PFBS	114.51		100.25	Y
	8:2FtS	1037.68		135.81	Y
	6:2FtS	794.39		87.83	Y
	4:2FtS	249.54		107.7	Y

Sample	Chemical	Average Conc (µg/L)	RPD (%)	ISR (%)	Conformance
	FOSA	344.53		64.55	Y
Aqueous phase	PFNA	9.93	0.86	91.33	Y
	PFOA	51.74	3.99	83.01	Y
	PFHpA	98.46	5.62	75.71	Y
	PFHxA	98.26	5.96	68.76	Y
	PFOS	3.89	20.93	100.35	Y
	PFHxS	90.46	6.3	95.98	Y
	PFBS	104.41	2.2	62.01	Y
	8:2FtS	0.67	2.5	71.53	Y
	6:2FtS	73.27	22.78	68.44	Y
	4:2FtS	205.39	0.53	65.73	Y
	FOSA	1.67	8.98	74.98	Y
Sludge	PFNA	97.50	7.42	93.40	Y
	PFOA	77.91	2.85	83.24	Y
	PFHpA	97.13	2.81	92.42	Y
	PFHxA	99.71	0.64	130.49	Y
	PFOS	39.96	9.43	109.32	Y
	PFHxS	91.76	3.27	109.76	Y
	PFBS	104.93	2.19	126.58	Y
	8:2FtS	123.15	9.31	89.64	Y
	6:2FtS	71.41	27.27	70.16	Y
	4:2FtS	211.31	20.07	90.58	Y
	FOSA	77.22	16.16	65.88	Y

Table A7. QC data for **Figure 17**.

Sample	Chemical	Average Conc (µg/L)	RPD (%)	ISR%	Conformance
0 min	PFNA	292.88		122.46	Y
	PFOA	233.66		98.74	Y
	PFHpA	243.70		91.39	Y
	PFHxA	202.39		80.27	Y
	PFOS	322.25		93.18	Y
	PFHxS	239.58		93.51	Y
	PFBS	201.25		110.09	Y
	8:2FtS	336.83		52.34	Y
	6:2FtS	194.30		82.13	Y
	4:2FtS	172.55		61.65	Y
20 min	PFNA	264.35	3.02	93.97	Y
	PFOA	207.54	11.33	125.95	Y
	PFHpA	233.78	6.00	94.57	Y
	PFHxA	203.92	0.04	92.19	Y
	PFOS	219.27	4.24	92.14	Y

Sample	Chemical	Average Conc (µg/L)	RPD (%)	ISR%	Conformance
	PFHxS	213.93	1.06	101.45	Y
	PFBS	197.22	9.09	113.54	Y
	8:2FtS	177.74	22.10	87.60	Y
	6:2FtS	184.38	4.98	98.89	Y
	4:2FtS	162.22	16.19	57.68	Y
40 min	PFNA	204.58	1.78	63.63	Y
	PFOA	201.19	14.64	62.20	Y
	PFHpA	228.97	14.06	55.29	Y
	PFHxA	193.68	9.26	79.23	Y
	PFOS	149.74	11.08	50.01	Y
	PFHxS	207.39	10.93	55.61	Y
	PFBS	193.55	24.29	46.95	Y
	8:2FtS	94.99	0.15	192.29	N
	6:2FtS	167.14	3.46	82.34	Y
	4:2FtS	158.90	1.98	79.55	Y
60 min	PFNA	142.66	1.66	81.76	Y
	PFOA	166.81	17.39	101.07	Y
	PFHpA	224.07	3.06	95.66	Y
	PFHxA	187.88	7.36	89.05	Y
	PFOS	104.89	20.89	62.67	Y
	PFHxS	194.17	0.18	101.60	Y
	PFBS	193.18	0.87	107.36	Y
	8:2FtS	46.02	25.01	88.15	Y
	6:2FtS	160.33	22.07	82.75	Y
	4:2FtS	142.73	18.03	94.47	Y
90 min	PFNA	74.91	3.14	136.58	Y
	PFOA	126.62	3.47	103.40	Y
	PFHpA	201.23	0.95	106.40	Y
	PFHxA	183.16	2.99	102.64	Y
	PFOS	49.73	5.99	103.35	Y
	PFHxS	146.94	13.07	101.15	Y
	PFBS	186.30	5.30	87.34	Y
	8:2FtS	38.16	13.10	81.54	Y
	6:2FtS	119.17	17.08	116.06	Y
	4:2FtS	137.19	26.80	123.31	Y
120 min	PFNA	34.63	7.89	123.32	Y
	PFOA	89.99	8.14	125.95	Y
	PFHpA	196.60	4.12	92.08	Y
	PFHxA	180.15	4.87	90.62	Y
	PFOS	24.21	11.72	97.95	Y

Sample	Chemical	Average Conc (µg/L)	RPD (%)	ISR%	Conformance
	PFHxS	130.24	3.03	94.73	Y
	PFBS	183.30	0.15	96.62	Y
	8:2FtS	24.97	4.68	109.64	Y
	6:2FtS	81.36	6.32	151.64	Y
	4:2FtS	131.17	6.03	75.57	Y

Table A8. QC data for **Figure 18**.

Sample	Chemical	Average Conc (µg/L)	RPD (%)	ISR (%)	Conformance
Sludge	PFNA	250.27	2.09	93.01	Y
	PFOA	75.94	18.15	98.75	Y
	PFHpA	43.31	9.48	88.22	Y
	PFHxA	43.09	2.67	63.83	Y
	PFOS	302.66	32.81	74.47	N
	PFHxS	95.47	21.06	88.27	Y
	PFBS	42.77	2.15	91.24	Y
	8:2FtS	295.33	10.66	91.13	Y
	6:2FtS	90.61	9.18	103.39	Y
	4:2FtS	25.86	9.80	80.97	Y
Aqueous phase	PFNA	34.63	7.89	123.32	Y
	PFOA	89.99	8.14	125.95	Y
	PFHpA	196.60	4.12	92.08	Y
	PFHxA	180.15	4.87	90.62	Y
	PFOS	24.21	11.72	97.95	Y
	PFHxS	130.24	3.03	94.73	Y
	PFBS	183.30	0.15	96.62	Y
	8:2FtS	24.97	4.68	109.64	Y
	6:2FtS	81.36	6.32	151.64	Y
	4:2FtS	131.17	6.03	75.57	Y

Table A9. QC data for **Figure 22A**.

Sample	Chemical	Average Conc (µg/L)	RPD (%)	ISR%	Conformance
0 min	PFNA	163.36		66.32	Y
	PFOA	60.65		87.43	Y
	PFHpA	15.32		53.14	Y
	PFHxA	15.79		60.62	Y
	PFOS	112.42		54.83	Y
	PFHxS	26.31		87.71	Y
	PFBS	48.26		51.54	Y
	8:2FtS	208.49		34.07	N
	6:2FtS	59.95		65.56	Y
	4:2FtS	23.76		79.56	Y

Sample	Chemical	Average Conc (µg/L)	RPD (%)	ISR%	Conformance
2 min	PFNA	58.39	10.53	66.12	Y
	PFOA	32.08	2.11	87.43	Y
	PFHpA	7.86	15.97	69.57	Y
	PFHxA	13.37	10.35	62.46	Y
	PFOS	24.83	9.97	96.16	Y
	PFHxS	14.13	5.32	129.29	Y
	PFBS	42.08	2.24	56.70	Y
	8:2FtS	87.70	46.10	34.07	N
	6:2FtS	30.45	24.88	67.33	Y
	4:2FtS	13.92	16.52	116.02	Y
5 min	PFNA	15.30		49.84	Y
	PFOA	12.18		67.79	Y
	PFHpA	7.57		63.13	Y
	PFHxA	9.83		54.01	Y
	PFOS	10.24		51.66	Y
	PFHxS	8.19		131.92	Y
	PFBS	31.99		65.03	Y
	8:2FtS	8.27		26.12	N
	6:2FtS	0.00		67.33	Y
	4:2FtS	5.56		135.91	Y
10 min	PFNA	2.46	20.10	58.48	Y
	PFOA	5.82	11.63	78.59	Y
	PFHpA	2.90	2.27	62.16	Y
	PFHxA	9.45	21.37	58.97	Y
	PFOS	1.54	18.64	56.82	Y
	PFHxS	2.99	9.47	100.87	Y
	PFBS	24.50	9.85	76.92	Y
	8:2FtS	0.00	0.00	13.06	N
	6:2FtS	0.00	0.00	66.15	Y
	4:2FtS	0.00	0.00	119.34	Y
20 min	PFNA	1.42	13.63	33.86	N
	PFOA	0.00	0.00	61.40	Y
	PFHpA	0.27	4.98	57.33	Y
	PFHxA	4.34	7.93	65.40	Y
	PFOS	0.88	36.68	65.56	N
	PFHxS	0.29	26.24	105.78	Y
	PFBS	17.63	11.39	87.23	Y
	8:2FtS	0.00	0.00	13.63	N
	6:2FtS	0.00	0.00	74.12	Y
	4:2FtS	2.31	29.95	140.88	Y

Sample	Chemical	Average Conc (µg/L)	RPD (%)	ISR%	Conformance
30 min	PFNA	0.29	21.06	45.47	N
	PFOA	0.00	0.00	78.10	Y
	PFHpA	0.00	0.00	44.29	N
	PFHxA	3.54	10.94	61.73	Y
	PFOS	0.66	0.00	52.85	Y
	PFHxS	0.17	0.00	109.29	Y
	PFBS	21.45	28.18	48.77	N
	8:2FtS	0.00	0.00	5.68	N
	6:2FtS	0.00	0.00	65.85	Y
	4:2FtS	7.13	0.00	69.61	Y
45 min	PFNA	1.10	0.00	30.08	N
	PFOA	0.95	14.29	75.64	Y
	PFHpA	0.49	33.59	55.88	N
	PFHxA	1.39	10.87	50.70	Y
	PFOS	0.00	0.00	48.48	N
	PFHxS	0.00	0.00	116.31	Y
	PFBS	18.70	3.69	49.96	N
	8:2FtS	0.00	0.00	11.36	N
	6:2FtS	0.00	0.00	55.22	Y
	4:2FtS	1.63	0.00	134.25	Y
60 min	PFNA	0.00	0.00	42.39	N
	PFOA	0.00	0.00	72.21	Y
	PFHpA	0.00	0.00	58.94	Y
	PFHxA	1.01	0.00	68.89	Y
	PFOS	1.39	0.00	43.71	N
	PFHxS	0.19	0.00	108.59	Y
	PFBS	12.86	0.14	66.61	Y
	8:2FtS	0.00	0.00	11.92	N
	6:2FtS	0.00	0.00	93.61	Y
	4:2FtS	0.00	0.00	125.97	Y

Table A10. QC data for **Figure 22B**.

Sample	Chemical	Average Conc (µg/L)	RPD (%)	ISR (%)	Conformance
0 min	PFNA	663.39	4.49	72.08	Y
	PFOA	523.80	4.27	68.77	Y
	PFHpA	291.70	6.03	49.60	N
	PFHxA	29.90	0.29	37.84	N
	PFOS	25.55	13.19	64.37	Y
	PFHxS	185.54	28.78	77.54	Y
	PFBS	20.80	12.00	68.20	Y
	8:2FtS	12.43	9.09	91.01	Y

Sample	Chemical	Average Conc (µg/L)	RPD (%)	ISR (%)	Conformance
	6:2FtS	180.71	18.64	60.24	Y
	4:2FtS	25.72	5.97	72.93	Y
2 min	PFNA	512.76		61.16	Y
	PFOA	422.32		121.82	Y
	PFHpA	216.89		48.63	N
	PFHxA	22.15		63.93	Y
	PFOS	9.71		39.74	N
	PFHxS	96.78		50.17	Y
	PFBS	24.56		75.33	Y
	8:2FtS	3.08		56.89	Y
	6:2FtS	110.26		46.07	N
	4:2FtS	34.17		116.02	Y
5 min	PFNA	425.48		47.06	N
	PFOA	338.75		74.66	Y
	PFHpA	145.85		47.99	N
	PFHxA	25.84		23.15	N
	PFOS	10.98		38.94	N
	PFHxS	83.09		47.01	N
	PFBS	24.27		98.33	Y
	8:2FtS	6.16		73.39	Y
	6:2FtS	137.83		54.34	Y
	4:2FtS	26.88		198.90	N
10 min	PFNA	32.73	7.69	47.86	N
	PFOA	110.43	5.41	113.96	Y
	PFHpA	137.99	9.79	29.95	N
	PFHxA	27.12	5.82	54.38	Y
	PFOS	0.11	0.00	28.61	N
	PFHxS	70.58	7.33	30.52	Y
	PFBS	21.16	7.25	99.12	Y
	8:2FtS	0.00	0.00	73.39	Y
	6:2FtS	15.31	20.00	53.75	Y
	4:2FtS	34.36	15.08	135.91	Y
20 min	PFNA	67.14		56.39	Y
	PFOA	89.54		139.50	Y
	PFHpA	99.96		85.35	Y
	PFHxA	23.62		49.60	N
	PFOS	2.65		49.27	N
	PFHxS	58.73		108.76	Y
	PFBS	10.61		98.33	Y
	8:2FtS	0.31		120.37	Y

Sample	Chemical	Average Conc (µg/L)	RPD (%)	ISR (%)	Conformance
	6:2FtS	21.44		67.92	Y
	4:2FtS	32.25		125.97	Y
30 min	PFNA	12.59		50.64	Y
	PFOA	40.29		113.96	Y
	PFHpA	61.61		55.72	Y
	PFHxA	18.41		59.89	Y
	PFOS	0.53		58.01	Y
	PFHxS	25.03		105.61	Y
	PFBS	10.79		42.03	N
	8:2FtS	0.00		91.01	Y
	6:2FtS	0.00		62.02	Y
	4:2FtS	17.66		129.28	Y
45 min	PFNA	9.65	56.52	64.73	N
	PFOA	14.92	40.00	100.20	N
	PFHpA	20.43	4.62	54.43	Y
	PFHxA	14.06	3.95	58.79	Y
	PFOS	0.66	4.00	69.93	Y
	PFHxS	9.01	7.41	89.47	Y
	PFBS	8.48	7.32	36.48	N
	8:2FtS	0.00	0.00	46.97	N
	6:2FtS	0.00	0.00	59.06	Y
	4:2FtS	20.93	13.76	179.01	N
60 min	PFNA	1.68	0.00	58.38	Y
	PFOA	1.49	0.00	131.64	Y
	PFHpA	14.14	20.00	55.40	Y
	PFHxA	10.76	5.43	65.77	Y
	PFOS	0.37	57.14	59.60	N
	PFHxS	3.50	14.29	92.62	Y
	PFBS	7.08	1.72	68.99	Y
	8:2FtS	0.00	0.00	61.65	Y
	6:2FtS	0.00	0.00	62.02	Y
	4:2FtS	13.82	16.67	89.50	Y

Table A11. QC data for **Figure 22C**.

Sample	Chemical	Average Conc (µg/L)	RPD (%)	ISR (%)	Conformance
0 min	PFNA	3324.44	3.78	78.73	Y
	PFOA	3077.92	1.33	117.89	Y
	PFHpA	1157.50	1.69	89.22	Y
	PFHxA	215.30	6.01	98.47	Y
	PFOS	1653.80	6.09	122.78	Y
	PFHxS	1713.65	3.40	81.57	Y

Sample	Chemical	Average Conc (µg/L)	RPD (%)	ISR (%)	Conformance
	PFBS	591.32	33.47	182.79	N
	8:2FtS	1872.43	5.68	110.09	Y
	6:2FtS	1408.55	0.36	71.76	Y
	4:2FtS	728.25	0.26	58.01	Y
2 min	PFNA	2693.80		74.96	Y
	PFOA	2762.18		104.13	Y
	PFHpA	1032.03		113.37	Y
	PFHxA	192.19		116.47	Y
	PFOS	1566.87		132.72	Y
	PFHxS	1419.95		79.47	Y
	PFBS	760.63		181.20	N
	8:2FtS	1622.84		79.27	Y
	6:2FtS	1127.46		80.62	Y
	4:2FtS	484.14		139.23	Y
5 min	PFNA	1930.97		67.91	Y
	PFOA	2198.19		89.40	Y
	PFHpA	998.03		71.02	Y
	PFHxA	203.16		72.01	Y
	PFOS	1085.32		118.41	Y
	PFHxS	1216.84		83.68	Y
	PFBS	713.87		114.98	Y
	8:2FtS	842.75		66.06	Y
	6:2FtS	904.90		64.38	Y
	4:2FtS	672.87		54.70	Y
10 min	PFNA	613.15	13.28	118.05	Y
	PFOA	1076.59	0.50	144.41	Y
	PFHpA	641.13	2.71	106.77	Y
	PFHxA	172.69	0.40	99.20	Y
	PFOS	437.70	5.13	164.90	N
	PFHxS	865.18	2.42	81.22	Y
	PFBS	622.03	1.81	174.06	N
	8:2FtS	361.95	4.48	68.99	Y
	6:2FtS	465.51	0.11	63.49	Y
	4:2FtS	498.50	4.53	64.64	Y
20 min	PFNA	75.27	4.09	93.82	Y
	PFOA	186.12	4.67	106.10	Y
	PFHpA	265.24	1.57	100.49	Y
	PFHxA	140.27	2.65	90.94	Y
	PFOS	27.81	13.19	143.84	Y
	PFHxS	260.72	2.25	88.59	Y

Sample	Chemical	Average Conc (µg/L)	RPD (%)	ISR (%)	Conformance
	PFBS	532.73	2.06	197.46	N
	8:2FtS	1.08	0.00	39.63	Y
	6:2FtS	88.30	46.75	138.21	N
	4:2FtS	334.38	19.02	76.24	Y
30 min	PFNA	10.72	35.63	125.10	N
	PFOA	18.92	8.11	150.31	N
	PFHpA	75.94	2.38	106.77	Y
	PFHxA	96.49	3.15	63.75	Y
	PFOS	7.18	65.96	158.15	N
	PFHxS	60.44	4.67	97.89	Y
	PFBS	394.97	6.99	133.22	Y
	8:2FtS	0.00	0.00	102.75	Y
	6:2FtS	2.09	0.00	179.84	N
	4:2FtS	217.45	24.53	81.22	Y
45 min	PFNA	1.48	16.67	134.03	Y
	PFOA	3.07	50.00	140.48	N
	PFHpA	20.97	22.41	137.53	Y
	PFHxA	73.76	2.52	104.90	Y
	PFOS	1.07	42.86	170.07	N
	PFHxS	11.75	21.15	106.66	Y
	PFBS	302.28	2.89	210.94	N
	8:2FtS	0.00	0.00	102.75	Y
	6:2FtS	0.00	0.00	92.43	Y
	4:2FtS	153.86	6.67	119.34	Y
60 min	PFNA	0.00	0.00	82.01	Y
	PFOA	0.00	0.00	93.33	Y
	PFHpA	7.41	21.95	102.91	Y
	PFHxA	55.74	7.21	105.63	Y
	PFOS	0.46	0.00	153.77	N
	PFHxS	2.82	4.00	104.20	Y
	PFBS	282.56	0.10	170.10	N
	8:2FtS	0.00	0.00	82.20	Y
	6:2FtS	0.00	0.00	105.43	Y
	4:2FtS	102.57	0.00	82.87	Y

Table A12. QC Data for **Figure 23**.

Sample	Chemical	Average Conc (µg/L)	RPD (%)	ISR (%)	Conformance
Initial	PFHxA	0.665	1.29	57.18	Y
	PFHpA	0.148	10.57	71.26	Y
	PFOA	1.428	18.86	77.70	Y
	PFNA	0.030	26.29	66.71	Y

Sample	Chemical	Average Conc (µg/L)	RPD (%)	ISR (%)	Conformance
	PFBS	0.185	18.33	62.10	Y
	PFHxS	2.206	25.05	84.08	Y
	PFOS	8.335	3.21	62.16	Y
	6:2FtS	0.821	40.27	107.91	N
	8:2FtS	0.341	25.35	106.38	Y
After 2h treatment	PFHxA	0.625	6.97	58.25	Y
	PFHpA	0.143	21.50	58.69	Y
	PFOA	0.530	12.42	148.65	Y
	PFNA	0.029	16.01	79.41	Y
	PFBS	0.046	8.29	69.75	Y
	PFHxS	1.713	24.92	77.19	Y
	PFOS	0.074	15.81	69.62	Y
	6:2FtS	0.438	0.53	132.15	Y
	8:2FtS	0.053	1.52	99.07	Y

Table A13. QC Data for **Figure 24**.

Sample	Chemical	Average Conc (µg/L)	RPD (%)	ISR (%)	Conformance
Aqueous phase	PFHxA	0.625	6.97	58.25	Y
	PFHpA	0.143	21.50	58.69	Y
	PFOA	0.530	12.42	148.65	Y
	PFNA	0.029	16.01	79.41	Y
	PFBS	0.046	8.29	69.75	Y
	PFHxS	1.713	24.92	77.19	Y
	PFOS	0.074	15.81	69.62	Y
	6:2FtS	0.438	0.53	132.15	Y
	8:2FtS	0.053	1.52	99.07	Y
Sludge	PFHxA	0.044		52.48	Y
	PFHpA	0.027		64.08	Y
	PFOA	0.325		65.32	Y
	PFNA	0.012		69.23	Y
	PFBS	0.163		48.39	N
	PFHxS	0.613		72.09	Y
	PFOS	9.149		62.90	Y
	6:2FtS	0.617		107.74	Y
	8:2FtS	0.347		81.12	Y

Table A14. QC Data for **Figure 25**.

Sample	Chemical	Average Conc (µg/L)	RPD	ISR	Conformance
Initial	PFHxA	0.642	25.43	73.92	Y
	PFHpA	0.190	6.34	76.90	Y
	PFOA	1.745	30.25	63.25	N

Sample	Chemical	Average Conc (µg/L)	RPD	ISR	Conformance
	PFNA	0.022	7.54	60.56	Y
	PFBS	0.033	26.92	66.99	Y
	PFHxS	2.368	27.62	64.38	Y
	PFOS	8.163	8.57	38.45	Y
	6:2FtS	0.963	4.79	108.10	Y
	8:2FtS	0.292	18.13	114.82	Y
After 1h treatment	PFHxA	0.526	7.03	77.22	Y
	PFHpA	0.057	8.18	95.61	Y
	PFOA	0.092	10.15	134.04	Y
	PFNA	0.001	2.82	107.84	Y
	PFBS	0.045	2.94	80.77	Y
	PFHxS	0.189	2.75	84.69	Y
	PFOS	0.179	25.93	69.72	Y
	6:2FtS	0.028	12.26	122.96	Y
	8:2FtS	0.004	3.82	127.85	Y

Table A15. QC Data for **Figure 26**.

Sample	Chemical	Average Conc (µg/L)	RPD (%)	ISR (%)	Conformance
Aqueous phase	PFHxA	0.526	7.03	77.22	Y
	PFHpA	0.057	8.18	95.61	Y
	PFOA	0.092	10.15	134.04	Y
	PFNA	0.001	2.82	107.84	Y
	PFBS	0.045	2.94	80.77	Y
	PFHxS	0.189	2.75	84.69	Y
	PFOS	0.179	25.93	69.72	Y
	6:2FtS	0.028	12.26	122.96	Y
	8:2FtS	0.004	3.82	127.85	Y
Sludge	PFHxA	0.301		53.28	Y
	PFHpA	0.070		64.66	Y
	PFOA	1.156		60.24	Y
	PFNA	0.028		54.22	Y
	PFBS	0.081		45.17	N
	PFHxS	0.277		59.25	Y
	PFOS	4.090		39.20	N
	6:2FtS	0.173		74.78	Y
	8:2FtS	0.156		68.40	Y

Appendix C: Standard Operation Procedure, Quantification of Per- and Poly-fluoroalkyl Acids, Huang Laboratory, University of Georgia.

Standard Operating Procedure

Quantification of Per- and Polyfluoroalkyl Substances (PFASs)

Huang laboratory, University of Georgia

1. SCOPE AND APPLICATION

1.1 This standard operation procedure (SOP) is applicable to the quantification of 32 per- and polyfluoroalkyl substances (PFAS) in water (Table 1).

1.2 This SOP is developed based on USEPA Method 537.1 and Method 533 with modifications for analysis of PFAS in different sample matrices other than drinking water. The QA/QC follows QSM 5.1.1 Table B-15.

1.3 The SOP may be applicable to drinking water, ground and surface waters, domestic and industrial wastewater and treatment process samples. A solid phase extraction (SPE) process is used for cleanup and/or concentration. SPE will be used for all field samples unless samples are known to contain high PFAS concentration (e.g., AFFF formulations).

Table 1. PFAS and extracted internal standard analytes list

No.	**Target Analytes**	Acronym	CAS No.
1	Perfluorobutanoic acid	PFBA	375-22-4
2	Perfluoropentanoic acid	PFPeA	2706-90-3
3	Perfluorohexanoic acid	PFHxA	307-24-4
4	Perfluoroheptanoic acid	PFHpA	375-85-9
5	Perfluorooctanoic acid	PFOA	335-67-1
6	Perfluorononanoic acid	PFNA	375-95-1
7	Perfluorodecanoic acid	PFDA	335-76-2
8	Perfluoroundecanoic acid	PFUdA	2058-94-8
9	Perfluorododecanoic acid	PFDoA	307-55-1
10	Perfluorotridecanoic acid	PFTrDA	72629-94-8
11	Perfluorotetradecanoic acid	PFTeDA	376-06-7
12	Perfluorobutanesulfonic acid	PFBS	375-73-5
13	Perfluoropentanesulfonic acid	PFPeS	2706-91-4
14	Perfluorohexanesulfonic acid	PFHxS	355-46-4
15	Perfluoroheptanesulfonic acid	PFHpS	375-92-8
16	Perfluorooctanesulfonic acid	PFOS	1763-23-1
17	Perfluorononanesulfonic acid	PFNS	68259-12-1
18	Perfluorodecanesulfonic acid	PFDS	335-77-3
19	Perfluorooctanesulfonamide	FOSA	754-91-6
20	Fluorotelomer sulfonic acid 8:2	8:2 FTS	39108-34-4
21	Fluorotelomer sulfonic acid 6:2	6:2 FTS	27619-97-2
22	Fluorotelomer sulfonic acid 4:2	4:2 FTS	757124-72-4
23	2-(N-Ethylperfluorooctanesulfonamido) acetic acid	N-EtFOSAA	2991-50-6
24	2-(N-Methylperfluorooctanesulfonamido) acetic acid	N-MeFOSAA	2355-31-9
25	2,3,3,3-Tetrafluoro-2-(1,1,2,2,3,3,3-heptafluoropropoxy)-	HFPO-DA	13252-13-6

	propanoic acid		
26	Perfluoro-4-oxapentanoic acid	PF4OPeA	377-73-1
27	Perfluoro-5-oxahexanoic acid	PF5OHxA	863090-89-5
28	Perfluoro-3,6-dioxaheptanoic acid	3,6-OPFHpA	151772-58-6
29	4,8-Dioxa-3H-perfluorononanoic acid	ADONA	958445-44-8
30	11-Chloroeicosafluoro-3-oxaundecane-1-sulfonic acid	11Cl-PF3OUdS	83329-89-9
31	9-Chlorohexadecafluoro-3-oxanonane-1-sulfonic acid	9Cl-PF3ONS	73606-19-6
32	Perfluoro(2-ethoxyethane) sulfonic acid	PFEESA	117205-07-9
	Extracted Internal Standards		
33	Perfluoro-n-[$^{13}C_4$]butanoic acid	MPFBA	N/A
34	Perfluoro-n-[$^{13}C_5$]pentanoic acid	M5PFPeA	N/A
35	Perfluoro-n-[1,2,3,4,6-$^{13}C_5$]hexanoic acid	M5PFHxA	N/A
36	Perfluoro-n-[1,2,3,4-$^{13}C_4$]heptanoic acid	M4PFHpA	N/A
37	Perfluoro-n-[$^{13}C_8$]octanoic acid	M8PFOA	N/A
38	Perfluoro-n-[$^{13}C_9$]nonanoic acid	M9PFNA	N/A
39	Perfluoro-n-[1,2,3,4,5,6-$^{13}C_6$]decanoic acid	M6PFDA	N/A
40	Perfluoro-n-[1,2,3,4,5,6,7-$^{13}C_7$]undecanoic acid	M7PFUdA	N/A
41	Perfluoro-n-[1,2-$^{13}C_2$]dodecanoic acid	MPFDoA	N/A
42	Perfluoro-n-[1,2-$^{13}C_2$]tetradecanoic acid	M2PFTeDA	N/A
43	Perfluoro-1-[$^{13}C_8$]octanesulfonamide	M8FOSA	N/A
44	N-methyl-d_3-perfluoro-1-octanesulfonamidoacetic acid	d_3-N-MeFOSAA	N/A
45	N-ethyl-d_5-perfluoro-1-octanesulfonamidoacetic acid	d_5-N-EtFOSAA	N/A
46	Sodium perfluoro-1-[2,3,4-$^{13}C_3$]butanesulfonate	M3PFBS	N/A
47	Sodium perfluoro-1-[1,2,3-$^{13}C_3$]hexanesulfonate	M3PFHxS	N/A
48	Perfluoro-[$^{13}C_8$]octanesulfonate	M8PFOS	N/A
49	Sodium 1H,1H,2H,2H-perfluoro-1-[1,2-$^{13}C_2$]hexanesulfonate	M2-4:2FTS	N/A
50	Sodium 1H,1H,2H,2H-perfluoro-1-[1,2-$^{13}C_2$]octanesulfonate	M2-6:2FTS	N/A
51	Sodium 1H,1H,2H,2H-perfluoro-1-[1,2-$^{13}C_2$]decanesulfonate	M2-8:2FTS	N/A
52	2,3,3,3-Tetrafluoro-2-2(1,1,2,2,3,3,3-heptafluoropropoxy)-$^{13}C_3$-propanoic acid	M3HFPO-DA	N/A
	Injection Internal Standards		
53	Perfluoro-n-[2,3,4-$^{13}C_3$]butanoic acid	$^{13}C_3$-PFBA	N/A
54	Perfluoro-[1,2-$^{13}C_2$]octanoic acid	$^{13}C_2$-PFOA	N/A
55	Perfluoro-1-[1,2,3,4-$^{13}C_4$]octanesulfonic acid	$^{13}C_4$-PFOS	N/A

2. CHEMICALS

2.1 All standard and reagent preparation, documentation and labeling must follow the requirements of SOP.

2.2 A total of 32 PFAS analyte standards are used, as listed in Table 1.[1]

2.3 Extracted internal standards used in this method are also shown in Table 1.[2]

2.4 Injection internal standards are included in Table 1 as well.[3]

2.5 UPLC grade methanol from Fisher Scientific, UPLC grade acetonitrile from Sigma Aldrich, or equivalents.

[1] Two PFAS analyte standard mixtures from Wellington Laboratory Inc., (PFAC-24PAR and EPA-533PAR), include all target analytes.

[2] Two extracted internal standard mixtures from Wellington Laboratory Inc., MPFAC-24ES and EPA-533ES, include all these standards.

[3] Injection internal standard from Wellington Laboratory Inc., EPA-533IS, include these standards.

2.6 Ammonium acetate from J.T.Baker, or equivalent.

2.7 Concentrated ammonium hydroxide reagent from Fisher Scientific, or equivalent.

2.8 Sodium phosphate dibasic and sodium phosphate monobasic from Sigma Aldrich, or equivalent.

2.9 DI water produced by Barnstead Nanopure system (≥ 18.2 MΩ cm^{-1} at 20 ºC).

3. APPARATUS

3.1 SPE cartridge[1]

3.2 Solid phase extraction manifold

3.3 Polypropylene bottles with polypropylene screw caps (250 mL and 500 mL)

3.4 Analytical balance

3.5 pH meter

3.6 Extract concentration system (extracts are concentrated by evaporation with high purity nitrogen using a water bath set no higher than 60 °C)

3.7 Laboratory vacuum system (sufficient capacity to maintain a vacuum of at least 10 inches of mercury of extraction cartridges)

3.8 Falcon round-bottom polypropylene tubes

3.9 HPLC autosampler vials (9-425) with 250 µl insert

3.10 Polypropylene centrifuge tubes (2 mL)

4. INSTRUMENT

4.1 An ultra-performance liquid chromatography coupled with a triple-stage quadrupole mass spectrometer (ACQUITY UPLC-MS/MS, Xevo TQD, Waters Corp., USA) equipped with an Acquity UPLC BEH C18 column (2.1 mm × 50 mm, 1.7 µm). The column oven was kept at 40 °C.

4.2 VWR high speed microcentrifuge

5. QUALITY CONTROL

5.1 Batch

5.1.1 A sample batch is a group of environmental samples, which are prepared together using the same process and same lot(s) of reagents. Each batch is analyzed utilizing the same process, lots of reagents and personnel.

5.1.2 Instrument conditions must be the same for all standards, samples and QC

[1] Different SPE cartridges have different performance for different analytes. Polymeric Weak Anion cartridges are suggested. This SOP is described for Phenomenex Strata™-X-AW 33 µm, or equivalents.

samples.

5.1.3 For this analysis, batch QC consists of an Instrument Blank, a Method Blank, a Laboratory Control Sample (LCS) and Sample Replicate (SR).

5.2 Instrument Blank

5.2.1 An instrument blank is a blank matrix sample that running immediately after the highest standard analyzed and daily prior to sample analysis.

5.2.2 An instrument blank must be prepared with every sample batch, which is comprised of DI water.

5.3 Method Blank

5.3.1 A method blank is a blank matrix processed simultaneously with, and under the same conditions as, samples through all steps of procedure.

5.3.2 A method blank must be prepared with every sample batch, which is comprised of DI water.

5.4 Laboratory Control Sample (LCS)

5.4.1 A LCS is a blank matrix spiked with a known amount of all analyte(s) at a concentration above limit of quantification (LOQ) and below the mid-level calibration concentration.

5.4.2 A LCS must be prepared with every sample batch, which is comprised of DI water.

5.5 Sample Replicate (SR)

5.5.1 A sample replicate is an additional aliquot of a sample taken through the entire analytical process to demonstrate precision with every sample batch.

5.6 Instrument Blank

5.6.1 An instrument blank is comprised of DI water.

5.6.2 An instrument blank must be analyzed immediately following the highest standard and daily prior to sample analysis.

5.7 Procedural Variations/ Nonconformance

5.7.1 Any variation shall be completely documented using a Nonconformance Memo and approved by the Supervisor and QA Manager.

5.7.2 Any deviations from QC procedures must be documented as a nonconformance, with applicable cause and corrective action approved by the Supervisor and QA Manager.

5.8 QC Criteria and Corrective Action

5.8.1 For the instrument blank, the concentration of each analyte must be fall

below 1/2 the LOQ.

5.8.2 For the method blank, the results must fall below 1/2 the LOQ or below 1/10 the amount measured in any sample or 1/10 the regulatory limit, whichever is greater.

5.8.3 The LCS results must fall within 10% of the true value for that solution, and the relative standard deviation of triplicate is within 5%.

5.8.4 For SR, relative percent difference (RPD) must be within 30%.

5.8.5 The instrument blank must be ≤ 1/2 the LOQ the for each analyte.

5.8.6 The extracted internal standard recovery in all samples must be within 50-150% of the true value.

5.8.7 The peak areas of injection internal standards must be within 50-150% of the area measured in the Initial Calibration (ICAL) midpoint standard. If the ICAL is not performed, the peak areas must be within 50-150% of the peak area measured in daily initial Continuing Calibration Verification (CCV).

5.8.8 When QC criteria are not met, problem will be corrected and then reanalyze the QC samples and associated sample batch.

6. CALIBRATION AND STANDARDIZATION

6.1 Internal standard calibration is used.

6.1.1 Internal standard calibration is used. If a labeled analog is not commercially available, the Extracted Internal Standard analyte with the closest retention time to the analyte must be used. Each calibration standard is analyzed for each compound calculated using the ratio of the compound/internal standard against the concentration for each compound.

6.2 Initial calibration (ICAL)

6.2.1 The initial calibration contains a minimum of 5 points. The low-level standard must be at LOQ. The other standards define the working range of the detector, with the highest-level standard establishing the linear range of the instrument.

6.2.2 A new calibration curve must be generated after major changes to the system. Major changes include new columns, any significant changes in instrument operating parameters, and major instrument maintenance.

6.2.3 Except in specific instances, it is NOT acceptable to remove points from a calibration curve for the purpose of meeting criteria.

6.2.4 The concentration of each compound is calculated by the ratio of each

compound/internal standard against the standard curve based on the ratio of the standards/internal standard.

6.2.5 A signal-to-noise (S/N) Ratio must be ≥ 10:1 for all ion for quantification; for analytes having a promulgated standard, the qualitative transition ion must have an S/N Ratio ≥ 3:1; the %RSD of the RFs for all analytes must be < 20%.

6.2.6 Linear calibrations must have an $r^2 \geq 0.99$ for each analyte; and analytes must be within ±30% of their true value for each calibration standard.

6.2.7 When ICAL fails, correct problem and repeat ICAL.

6.3 Initial calibration verification (ICV)

6.3.1 A second source standard prior to sample analysis must be analyzed to verify the initial calibration once after each initial calibration analysis, and analyte concentrations must be within ± 30% of their true values.

6.3.2 When ICV fails, correct problem, rerun ICV. If problem persists, repeat ICAL.

6.4 Continuing Calibration Verification (CCV)

6.4.1 CCV will be conducted prior to sample analysis and after every 10 field samples, and at the end of analytical sequence. Concentration of analytes must range from the LOQ to mid-level calibration concentration. Analyte concentration must be within 30% of their true value.

6.4.2 When CCV fails, recalibrate and reanalyze all associated samples since the last acceptable CCV.

6.5 Instrument Sensitivity Check (ISC)

6.5.1 ISC will be performed prior to analysis and at least once every 12 hours. ISC samples will be prepared with analyte concentrations at LOQ. The concentrations must be measured within ±30% of their true values.

6.5.2 When ISC fails, correct problem, and rerun ISC. If problem persists, repeat ICAL.

6.6 Calibration Standard Preparation

6.6.1 Prepare analyte Primary Dilution Standard (PDS) by diluting PFAS analytes stock standard in a methanol/water mixture (99:1, v:v).

6.6.2 Prepare extracted internal standard PDS by diluting extracted internal standard stock standards in a methanol/water mixture (99:1, v:v).

6.6.3 Prepare injection internal standard PDS by diluting injection internal standard

stock standard in a methanol/water mixture (99:1, v:v).

6.6.4 Prepare a PFAS and injection internal standard mix by diluting the analyte PDS to different concentrations and injection internal standard PDS in a methanol/water mixture (80:20, v:v), in which the concentration of $^{13}C_3$-PFBA, $^{13}C_2$-PFOA and $^{13}C_4$-PFOS are 40 ppb, 40 ppb and 120 ppb, respectively.

6.6.5 Dilute extracted internal standard PDS in a methanol/water mixture (80:20, v:v), in which the concentration of M2PFTeDA, M8FOSA, d3-N-MeFOSAA, d5-N-EtFOSAA, M3HFPO-DA are 80 ppb, the concentration of M2-4:2FTS, M2-4:2FTS, M2-4:2FTS are 400 ppb, the concentration of other extracted internal standard analytes are 160 ppb.

6.6.6 Prepare calibration standard by mixing an equal volume (e.g. 500 µL) of the isotope-labeled EIS mix (prepared in 6.6.5) with the diluted analyte PDS (prepared in 6.6.4).

7. PROCEDURE

Solid phase extraction (SPE) must be used unless samples are known to contain high PFASs concentration, which can be prepared by serial dilution instead of SPE.

7.1 Solid Phase Extraction (SPE)[1]

7.1.1 Prepare 0.1 M phosphate buffer (pH=7.0) by mixing 500 mL 0.1 M dibasic sodium phosphate and 275 mL 0.1 M monobasic sodium phosphate.

7.1.2 Prepare 2% ammonium hydroxide in methanol by diluting 2.0 mL of concentrated ammonium hydroxide (56.6% w/w) in 100 mL methanol. This solution should be made fresh on the day of extraction.

7.1.3 Prepare 1.0 g/L ammonium acetate in reagent water by adding 1.0 g ammonium acetate to 1.0 L of reagent water.

7.1.4 Prepare the reconstitute solution by diluting injection internal standard in a methanol/water mixture (80:20, v:v). The concentration of $^{13}C_3$-PFBA, $^{13}C_2$-PFOA and $^{13}C_4$-PFOS in the reconstitute solution are 20 ppb, 20 ppb and 60 ppb, respectively.

7.1.5 Measure the volume of water samples and adjust the pH to 6.0-8.0[2]. An indirect measurement may be done in one of two ways: by marking the level of the sample on the bottle or by weighing the sample and bottle to the nearest 0.1 gram.

[1] The SPE procedure described in this SOP is for Strata™-X-AW (100 mg sorbent) SPE cartridge.

[2] No more than 50 mL sample is used for 100 mg sorbent SPE cartridge, or by the same ratio.

7.1.6 Add an aliquot of extracted internal standard PDS to each sample and mix to serve as isotope dilution standards, which quantities are so that the final concentration (in the reconstitutes after SPE, assuming 100% recovery) of M2PFTeDA, M8FOSA, d3-N-MeFOSAA, d5-N-EtFOSAA and M3HFPO-DA are 40 ppb, the concentration of M2-4:2FTS, M2-4:2FTS, M2-4:2FTS are 200 ppb, and the concentration of the other extracted internal standard analytes are 80 ppb. EIS is added before any sample transfer is performed.

7.1.7 Rinse each cartridge with 10 mL of methanol. Next, rinse each cartridge with 10 mL of aqueous 0.1 M phosphate buffer (pH=7), without allowing the water to drop below the top edge of the packing. Close the valve and add 2–3 mL of phosphate buffer to the cartridge reservoir and fill the remaining volume with reagent water (never let the cartridge dry).

7.1.8 Adjust the vacuum to approximately 5 inches Hg. Begin adding sample to the cartridge. Do not allow the cartridge to go dry before all the sample has passed through.

7.1.9 After the entire sample has passed through the cartridge, rinse the sample bottle with a 10 mL aliquot of 1 g/L ammonium acetate in reagent water. Draw the rinsate through the sample transfer tubes and the cartridges. Add 1.0 mL of methanol to the sample bottle and draw through the transfer tube and SPE cartridge.

7.1.10 Apply maximum vacuum (15-20 inches Hg) to the SPE system for 10 mins till the cartridges are completely dry.

7.1.11 Release the vacuum on the extraction manifold and place a collection tube under each sample position. Rinse the sample bottles with 5 mL of the elution solvent, methanol with 2% ammonium hydroxide (v/v), then elute the analytes from the cartridges by pulling the elution solvent through the sample transfer tubes and the cartridges. Use a low vacuum such that the solvent exits the cartridge in a dropwise fashion. Repeat sample bottle rinse and cartridge elution with a second 5 mL aliquot of elution solvent.

7.1.12 At the end of elution, apply vacuum to the system for another 10 mins.

7.1.13 Concentrate the extract to dryness under a gentle stream of nitrogen in a heated water bath (55–60 °C). Reconstitute the extract with 0.2 mL reconstitute solution for sample analysis. Note that the reconstitute solution contains IIS as described in 7.1.4.

7.2 Sample dilution

7.2.1 When sample dilution is necessary, the volume of water samples is measured by an indirect measurement in one of two ways: by marking the level of the sample on the bottle or by weighing the sample and bottle to the nearest 0.1 gram.

7.2.2 Add an aliquot of extracted internal standard PDS to each sample and mix to serve as isotope dilution standards, which quantities are so that the final concentration (in the final solution if serial dilution is performed) ssuming 100% recovery) of M2PFTeDA, M8FOSA, d3-N-MeFOSAA, d5-N-EtFOSAA and M3HFPO-DA are 40 ppb, the concentration of M2-4:2FTS, M2-4:2FTS, M2-4:2FTS are 200 ppb, and the concentration of the other extracted internal standard analytes are 80 ppb. EIS is added before any sample transfer is performed.

7.2.3 The water sample mixed with EIS is then mixed with appropriate volumes of reagent water and methanol to achieve the desired dilution ratio in methanol/water mixture (80:20, v:v).

7.2.4 Add an aliquot of injection internal standard PDS so that the final concentration of $^{13}C_3$-PFBA, $^{13}C_2$-PFOA and $^{13}C_4$-PFOS in the reconstitute solution are 20 ppb, 20 ppb and 60 ppb, respectively. Note that IIS is added at the final step if serial dilution is performed.

7.3 Sample analysis

7.3.1 Place sample vials in UPLC-MS/MS sample manager in designated order.

7.3.2 Build a sample list with the following methods selected:

7.3.2.1 Inlet method: Method 1 (Table 1 in Appendix)

7.3.2.2 MS method: MS-1 (Table 2 in Appendix)

7.3.2.3 MS tune file: MS tune 1 (Appendix)

7.3.2.4 Injection volume: 5 µL

7.3.3 Make sure the mobile phase are as follows:

7.3.3.1 Solvent A: 5 mM ammonium acetate in HPLC water

7.3.3.2 Solvent B: 5 mM ammonium acetate in a methanol/acetonitrile mixture (80:20, v:v)

7.3.3.3 Weak wash solvent: 10% methanol and 90% HPLC water

7.3.3.4 Strong wash solvent: 100% methanol

7.3.4 Make sure nitrogen gas is enough for the entire run (500 psi ~ 2.5 hours, 10 minutes per sample)

7.3.5 Turn on the inlet flow on inlet method panel, DO NOT start the queue before the pump delta pressure drops to below 30 psi.

7.3.6 On MS tune panel, set ion mode at negative (-) and turn on capillary gas and collision gas, and finally click the operate button.

7.3.7 When the instrument is ready, select samples to be analyzed on sample list and click 'start' to begin the analysis.

7.4 After instrument analysis, record the ion intensity values of all PFAS analytes, the extracted internal standard and injection internal standard.

7.5 The ion transitions used for quantification and confirmation for each PFAS are listed in Appendix Table 2. The EIS and IIS used for each PFAS are listed in Appendix Table 3.

7.6 The Method Detection Limits (MDL) and Limits of Quantification (LoQ) of the method are listed in Appendix Table 4 along with the methods used for the evaluation. When an analyte is detected at a concentration below its LoQ and above its MDL, the concentration will be reported with an annotation.

Appendix 1

Inlet method: Method 1

Table 1. The flow rate and the gradient condition of UPLC program.

Time (min)	Flow rate (mL min^{-1})	%A	%B	Curve
Initial	0.3	95	5	Initial
0.50	0.3	95	5	6
1.50	0.3	60	40	6
10.00	0.3	20	80	6
11.00	0.3	5	95	6
14.00	0.3	95	5	6
16.00	0.3	95	5	6

MS method: MS-1

Table 2. The analysis was carried out in multiple reaction monitoring (MRM) mode. Electrospray ionization (ESI) was operated in a negative mode.

	Compound Name	Parent (m/z)	Daughter (m/z)	Confirmation (m/z)	Dwell (s)	Cone (V)	Collision (V)
1	PFBA	213.00	169.00		0.005	15	10
2	PFPeA	263.00	219.00		0.005	15	9
3	PFHxA	313.00	269.00	119.00	0.005	14	10
4	PFHpA	363.00	319.00	169.00	0.005	15	7
5	PFOA	412.86	368.80	169.00	0.005	14	10
6	PFNA	463.00	418.90	219.00	0.005	20	10
7	PFDA	513.00	468.90	219.00	0.005	20	10
8	PFUdA	563.00	518.90	269.00	0.005	18	10
9	PFDoA	613.00	568.90	169.00	0.005	22	10
10	PFTrDA	663.00	618.90	169.00	0.005	22	15
11	PFTeDA	713.00	668.90	169.00	0.005	15	14
12	PFBS	298.90	80.10	99.10	0.005	56	26
13	PFPeS	349.00	80.10	99.10	0.005	45	25
14	PFHxS	399.00	80.00	99.10	0.005	52	30
15	PFHpS	449.00	80.20	99.10	0.005	60	35
16	PFOS	498.78	80.00	99.10	0.005	60	35
17	PFNS	549.00	80.20	99.20	0.005	65	45
18	PFDS	599.00	80.20	99.10	0.005	70	50
19	FOSA	498.00	77.90	99.10	0.005	40	30
20	8:2FtS	527.00	506.80	444.60/81.20	0.005	53	28
21	6:2FtS	427.00	407.00	344.90/81.00	0.005	47	22
22	4:2FtS	326.86	306.86	81.10	0.005	42	22
23	NEtFOSAA	584.00	418.80	525.90	0.005	30	20
24	NMeFOSAA	570.00	418.90	219.10	0.005	30	20

25	HFPO-DA	285.00	169.00	0.005	12	8
26	PF4OPeA	228.88	84.89	0.005	18	10
27	PF5OHxA	278.88	84.89	0.005	20	12
28	ANODA	377.00	251.00	0.005	14	12
29	3,6-OPFHpA	294.94	200.90	0.005	12	6
30	PFEESA	315.00	135.00	0.005	44	20
31	11Cl-PF3OUdS	631.00	451.00	0.005	60	30
32	9Cl-PF3ONS	531.00	351.00	0.005	55	25
33	MPFBA	217.00	172.00	0.005	22	10
34	M5PFPeA	268.00	223.00	0.005	20	8
35	M5PFHxA	318.00	273.00	0.005	15	8
36	M4PFHpA	367.00	322.00	0.005	15	8
37	M8PFOA	420.60	375.80	0.005	18	10
38	M9PFNA	472.00	427.00	0.005	17	10
39	M6PFDA	519.00	474.00	0.005	22	10
40	M7PFUdA	570.00	525.00	0.005	24	10
41	MPFDoA	615.00	570.00	0.005	22	10
42	M2PFTeDA	715.00	670.00	0.005	15	14
43	M8FOSA	506.00	78.00	0.005	40	30
44	d_3-N-MeFOSAA	573.00	419.00	0.005	32	20
45	d_5-N-EtFOSAA	589.00	419.00	0.005	32	20
46	M3PFBS	302.00	80.00	0.005	45	30
47	M3PFHxS	402.00	80.00	0.005	45	40
48	M8PFOS	506.78	80.00	0.005	45	45
49	M2-4:2FTS	329.00	309.00	0.005	40	18
50	M2-6:2FTS	429.00	409.00	0.005	47	22
51	M2-8:2FTS	216.00	172.00	0.005	22	10
52	M3HFPO-	287.00	169.00	0.005	15	5

	DA					
53	$^{13}C_3$-PFBA	216.00	172.00	0.005	22	10
54	$^{13}C_2$-PFOA	415.00	370.00	0.005	18	10
55	$^{13}C_4$-PFOS	503.00	80.00	0.005	45	45

Table 3. PFAS analytes and suggested EIS and IIS

	PFAS analytes	EIS	IIS
1	PFBA	MPFBA	$^{13}C_3$-PFBA
2	PFPeA	M5PFPeA	$^{13}C_3$-PFBA
3	PFHxA	M5PFHxA	$^{13}C_2$-PFOA
4	PFHpA	M4PFHpA	$^{13}C_2$-PFOA
5	PFOA	M8PFOA	$^{13}C_2$-PFOA
6	PFNA	M9PFNA	$^{13}C_2$-PFOA
7	PFDA	M6PFDA	$^{13}C_2$-PFOA
8	PFUnA	M7PFUnA	$^{13}C_2$-PFOA
9	PFDoA	MPFDoA	$^{13}C_2$-PFOA
10	PFTrDA	M2PFTeDA	$^{13}C_2$-PFOA
11	PFTeDA	M2PFTeDA	$^{13}C_2$-PFOA
12	PFBS	M3PFBS	$^{13}C_4$-PFOS
13	PFPeS	M3PFHxS	$^{13}C_4$-PFOS
14	PFHxS	M3PFHxS	$^{13}C_4$-PFOS
15	PFHpS	M8PFOS	$^{13}C_4$-PFOS
16	PFOS	M8PFOS	$^{13}C_4$-PFOS
17	PFNS	M8PFOS	$^{13}C_4$-PFOS
18	PFDS	M8PFOS	$^{13}C_4$-PFOS
19	FOSA	M8FOSA	$^{13}C_4$-PFOS
20	8:2FTS	M2-8:2FTS	$^{13}C_4$-PFOS
21	6:2FTS	M2-6:2FTS	$^{13}C_4$-PFOS
22	4:2FTS	M2-4:2FTS	$^{13}C_4$-PFOS
23	NEtFOSAA	d_5-N-EtFOSAA	$^{13}C_4$-PFOS
24	NMeFOSAA	d_3-N-MeFOSAA	$^{13}C_4$-PFOS
25	HFPO-DA	M3HFPO-DA	$^{13}C_2$-PFOA
26	PFMPA	MPFBA	$^{13}C_3$-PFBA
27	PFMBA	M5PFPeA	$^{13}C_3$-PFBA
28	ANODA	M4PFHpA	$^{13}C_2$-PFOA
29	NFDHA	M5PFHxA	$^{13}C_2$-PFOA
30	PFEESA	M3PFBS	$^{13}C_4$-PFOS
31	11Cl-PF3OUdS	M8PFOS	$^{13}C_4$-PFOS
32	9Cl-PF3ONS	M8PFOS	$^{13}C_4$-PFOS

MS tune files: MS tune 1

The mass spectrometer was operated as following: capillary voltage 2.7 kV, cone voltage 60 V, desolvation temperature 350 °C, cone gas flow 40 L/Hr, desolvation gas flow 800 L/Hr, and collision energy 35 V.

Table 4. Method detection limits (MDL) and limits of quantitation (LoQ)

	In-vial[b]		SPE[c]	
Analyte	MDL[a] (µg/L)	LoQ[a] (µg/L)	MDL[a] (ng/L)	LoQ[a] (ng/L)
PFBA	1.3	4.1	6.4	20.2
PFPeA	0.8	2.5	3.5	11.2
PFHxA	1.2	3.8	3.8	12.2
PFHpA	0.6	1.9	6.6	21.0
PFOA	0.7	2.4	4.8	15.3
PFNA	0.4	1.3	6.7	21.3
PFDA	0.5	1.7	1.6	5.1
PFUnA	0.6	1.8	5.5	17.7
PFDoA	0.8	2.4	5.9	18.6
PFTrDA	0.8	2.6	17.6	55.9
PFTeDA	1.7	5.4	12.2	39.0
PFBS	0.5	1.6	10.6	33.7
PFPeS	0.7	2.3	7.3	23.1
PFHxS	1.2	3.7	6.8	21.8
PFHpS	0.8	2.6	4.7	15.0
PFOS	0.5	1.6	4.9	15.6
PFNS	1.5	4.8	10.2	32.4
PFDS	0.9	2.7	7.2	22.8
FOSA	0.4	1.3	18.7	59.4
8:2FTS	0.8	2.7	8.7	27.8
6:2FTS	1.4	4.4	8.8	28.0
4:2FTS	1.1	3.6	5.4	17.2
N-EtFOSAA	0.7	2.1	8.5	27.1

N-MeFOSAA	0.5	1.7	4.9	15.5
HFPO-DA	1.2	3.7	9.8	31.1
PF4OPeA	1.0	3.0	8.4	26.7
PF5OHxA	0.5	1.6	10.2	32.3
ANODA	0.9	2.9	6.4	20.3
3,6-OPFHpA	1.0	3.2	4.9	15.6
PFEESA	0.3	1.1	4.6	14.7
11Cl-PF3OUdS	0.5	1.6	6.8	21.6
9Cl-PF3ONS	0.6	1.9	4.2	13.3

[a.] Method Detection Limits (MDL) and Limits of Quantitation (LoQ) were evaluated according to methods in *Statistical Protocol for the Determination of the Single-Laboratory Lowest Concentration Minimum Reporting Level (LCMRL) and Validation of Laboratory Performance at or Below the Minimum Reporting Level (MRL)* by United States Environmental Protection Agency (US EPA).

[b.] Evaluated by spiking analytes in DI water and going through the analysis in 7.3.

[c.] Evaluated by spiking analytes in DI water and going through the sample preparation in 7.1 using Strata™-X-AW (100 mg sorbent) SPE cartridge with 50 mL sample extracted in 0.20 mL reconstitute solution and then analysis in 7.3.